

NUREG/CR-4147
SAND85-0209
RV

Printed May 1985

The Effect of Environmental Stress on Sylgard® 170 Silicone Elastomer

*When printing a copy of any digitized SAND
Report, you are required to update the
markings to current standards.*

W. H. Buckalew, F. J. Wyant

Prepared by
Sandia National Laboratories
Albuquerque, New Mexico 87185 and Livermore, California 94550
for the United States Department of Energy
under Contract DE-AC04-76DP00789



Prepared for
U. S. NUCLEAR REGULATORY COMMISSION

SF2900Q(8-81)

NOTICE

This report was prepared as an account of work sponsored by an agency of the United States Government. Neither the United States Government nor any agency thereof, or any of their employees, makes any warranty, expressed or implied, or assumes any legal liability or responsibility for any third party's use, or the results of such use, of any information, apparatus product or process disclosed in this report, or represents that its use by such third party would not infringe privately owned rights.

Available from
GPO Sales Program
Division of Technical Information and Document Control
U.S. Nuclear Regulatory Commission
Washington, D.C. 20555
and
National Technical Information Service
Springfield, Virginia 22161

NUREG/CR-4147
SAND85-0209
RV

THE EFFECT OF ENVIRONMENTAL STRESS
ON SYLGARD® 170 SILICONE ELASTOMER

W. H. Buckalew and F. J. Wyant

May 1985

Sandia National Laboratories
Albuquerque, New Mexico 87185
Operated by
Sandia Corporation
for the
U. S. Department of Energy

Prepared for
Electrical Engineering Instrumentation and Control Branch
Division of Engineering Technology
Office of Nuclear Regulatory Research
U.S. Nuclear Regulatory Commission
Washington, DC 20555
Under Memorandum of Understanding 40-550-75
NRC FIN No. A-1051

ABSTRACT

Dow Corning Sylgard® 170 Silicone Elastomer has been investigated to characterize its response to accelerated thermal aging, radiation exposure, and its behavior under applied compressive forces.

Sylgard® 170 response to accelerated thermal aging suggests the material properties are not particularly age dependent. Radiation exposures, however, produce significant, monotonic changes in both elongation and hardness with increasing absorbed radiation dose.

Elastomer response to an applied compressive force was strongly dependent on environment temperature and degree of material confinement. Variations in temperature produced large changes in compressive forces applied to confined samples. Attempts to mitigate force fluctuations by means of pressure relief paths resulted in total loss of the applied compressive force. Thus, seal applications employing this elastomer in Class 1E equipment required to function during or following an accident should consider the potential loss of compressive force from long-term aging and potential LOCA-temperature transient conditions.

TABLE OF CONTENTS

	<u>Page</u>
I. Introduction.	3
II. Elastomer Thermal Aging Studies	6
A. Apparatus and Procedures	6
B. Results.	8
III. Radiation Aging Studies.	19
A. Apparatus and Procedures	19
B. Results.	19
IV. Stress Relief Studies	31
A. Apparatus and Procedures	31
B. Results.	41
C. Specimen Weight Loss	55
V. Conclusions	66
References.	74

LIST OF FIGURES

	<u>Page</u>
1. D. G. O'Brien Type "K" Connector: Sectioned View.	4
2. Effects of Elastomer Extrusion on Cable Insulation-Penetration Test.	5
3. Sandia Normalized Elongation vs. Aging Time at 150°C	9
4. Sandia Normalized Elongation vs. Aging Time at 140°C	10
5. Sandia Normalized Elongation vs. Aging Time at 125°C	11
6. Sandia Normalized Elongation vs. Aging Time at 110°C	12
7. Comparison of Sandia Normalized Elongation Data.	13
8. Dow Corning Normalized Elongation vs. Aging Time at 177°C.	14
9. Dow Corning Normalized Elongation vs. Aging Time at 190°C.	15
10. Dow Corning Normalized Elongation vs. Aging Time at 210°C.	16
11. Comparison of Dow Corning Normalized Data.	17
12. Comparison of Sandia and Dow Corning Elongation Data	18
13. Sandia Normalized Hardness vs. Aging Time at 150°C	20
14. Sandia Normalized Hardness vs. Aging Time at 140°C	21
15. Sandia Normalized Hardness vs. Aging Time at 125°C	22
16. Comparison of Sandia Normalized Hardness Data.	23
17. Dow Corning Normalized Hardness vs. Aging Time at 177°C.	24
18. Dow Corning Normalized Hardness vs. Aging Time at 190°C.	25
19. Dow Corning Normalized Hardness vs. Aging Time at 210°C.	26
20. Comparison of Dow Corning Normalized Hardness Data	27

LIST OF FIGURES

	<u>Page</u>
21-A. Comparison of Sandia and Dow Corning Hardness Data . . .	28
21-B. Combined Initial Hardness Data	29
22. Radiation Aging Data - Normalized Elongation and Hardness	30
23. Elastomer Compression Fixture.	32
24. Elastomer Compression Assembly with Installed Load Cell.	33
25. Exploded View: Elastomer Confinement Geometry	34
26. Zero Hole Confinement Plate.	36
27. 12-Hole Confinement Plate Geometry	37
28. 3-Hole Confinement Plate Configuration	38
29. Stress vs. Strain - Unconfined Specimen.	42
30. Stress vs. Strain - 12 Hole Fixture.	43
31. Stress vs. Strain - Zero Hole Fixture.	44
32. Stress vs. Strain - Composite Data	45
33. Elastomer Response - Steady State Temperatures	46
34. Elastomer Response - 150°C Aging Temperature	48
35. Elastomer Response - 43°C Aging Temperature.	49
36. Elastomer Response - Ambient Aging Temperature	50
37. Elastomer Response - Composite Data.	51
38. Elastomer Response - LOCA Temperature Profile.	53
39. Elastomer Response - LOCA Temperature Profile.	54
40. Effects of Extrusion on Cable Insulation-Disc Test . .	56
41. Elastomer Response - LOCA Temperature Profile.	59

LIST OF FIGURES

	<u>Page</u>
42. Elastomer Response - Force vs. Material Temperature. . .	61
43. Elastomer Response - Force vs. Material Temperature. . .	63
44. Flow Parameter vs. Temperature	67
45. 3-Hole, 3-Wire Fixture in Aging Oven-Preexposure	69
46. 3-Hole, 3-Wire Fixture in Aging Oven-Midexposure	70
47. Sectioned Elastomer Showing Damaged Conductor.	71
48. Damaged Conductor Specimens.	72

LIST OF TABLES

	<u>Page</u>
I. Specimen Aging Time Schedule.	7
II. Compression Studies Outline	39
III. Weight Loss Analysis.	55

ACKNOWLEDGEMENTS

The authors would like to thank S. M. Luker for his valuable technical assistance during all phases of this project, and E. A. Salazar for providing the benefit of his expertise in elastomeric material behavior.

EXECUTIVE SUMMARY

This document reports the results of an experimental program designed to characterize the behavior of Dow Corning Sylgard® 170 silicone elastomer exposed to accelerated aging and extended-time compressive loading environments. The program was prompted by the results obtained during an NRC-sponsored qualification test of a D. G. O'Brien electrical penetration assembly. Cable grommets, fabricated from Sylgard 170 elastomer, proved to be sensitive to both the degree of confinement and environment temperature. During the qualification test the cable grommets underwent major dimensional change as the result of the combined elevated temperature and loading stress, causing damage to interfacing electrical conductor insulation and loss of the assembly sealing integrity. Damaged grommet-cable insulation conditions were manifested by degradation in insulation resistance measurements and, in some cases, short circuiting of the conductors.

Following the qualification test, Sandia was requested to study further the response of the Sylgard 170 elastomer to compressive loading and elevated temperature stresses. Test specimens were fabricated to the specific test requirements, but simulated actual penetration components

The experimental program was designed to investigate the effects of accelerated thermal and radiation aging, and extended compressive-time loading. Accelerated aging was considered first, followed by studies of the effect of compressive stress.

The accelerated thermal aging studies indicated that the Sylgard elastomer is not particularly susceptible to accelerated thermal aging. Plots of thermal degradation as a function of accelerated aging time indicate that several processes may be contributing to the observed elastomer degradation.

Radiation induced degradation, on the other hand, followed a pattern characteristic of many other materials in that material degradation increased with increasing absorbed dose. Comparison of these Sandia data with data obtained from Dow Corning shows that they are in agreement.

Compressive stress studies considered elastomer response as a function of degree of elastomer confinement, environment temperature, and available relief path. In addition, the effects of elastomer extrusion on electrical conductor insulation was considered using a mock-up of the D. G. O'Brien grommet-electrical wiring interface. The compression stress experiments demonstrated that behavior of Sylgard, subjected to compressive stress in close confinement, is complex. We noted that stress relief may proceed by three methods--relaxation, material flow,

and material extrusion. In addition it was observed that (1) total relief of any applied compressive stress will occur when any relief path is present, and (2) the compressive relief rate increases, from the ambient value, with increasing environment temperature. Finally it was demonstrated that insulated electrical conductors in intimate contact with the highly confined elastomer at an elevated temperature, in a simulated electrical penetration-grommet seal, will undergo catastrophic damage (stripping) to the insulation material.

Based on our aging and compressive response studies of the Dow Corning Sylgard 170, we have reached the following conclusions:

- A. The elastomer is relatively insensitive to accelerated thermal aging.
- B. A threshold for the onset of material flow was not observed. Material confined under compressive stress will, if provided a flow path, undergo stress relief at a rate proportional to the environment temperature.
- C. Stress relief of the confined elastomer can be complex depending on compressive stress, available relief path, and environment temperature. Relief was observed to proceed via extrusion, material flow, and stress relaxation.
- D. Under certain conditions, in application designs interfacing the insulated electrical conductors with the confined elastomer, damage to the insulation may occur.

Stress relaxation and elastomer extrusion should be considered in developing seal designs which require long-term maintenance of compressive forces. Also the potential for damaging insulation on wires passing through the elastomeric seal should be considered if the material may possibly experience an elevated (LOCA) temperature transient.

I. INTRODUCTION

This report discusses the behavior of Sylgard® 170 silicone elastomer material to various single environment tests. These tests were performed as part of the Qualification Testing Evaluation (QTE) Program¹, conducted by Sandia National Laboratories on behalf of the Office of Nuclear Regulatory Research, United States Nuclear Regulatory Commission (USNRC). The purpose of these studies was to determine the response of Sylgard® 170 silicone elastomer to several environments that may be associated with their use in seals in nuclear power plant applications.

These studies were motivated by experiences with the material as an integral part of some existing components designated as Class 1E (safety related) equipment. The unexpected behavior of the elastomer during the testing² of a D. G. O'Brien Electrical Penetration Assembly at Sandia suggested that additional examination of the elastomer was in order. Evidence of this behavior is shown in Figure 1, which demonstrates the elastomer response to close confinement coupled with an elevated material temperature. A sectioned connector from the D. G. O'Brien penetration assembly after being subjected to nuclear qualification tests is shown in Figure 1. It may be observed that the elastomer, indicated by the arrows, extruded through the openings in the metal sleeve provided for cable access and, during the extrusion process, stripped insulation from the cables. In Figure 2 the effects of elastomer extrusion on the cable insulation are depicted in greater detail. It is estimated that the initial compressive loading on the penetration assembly silicone grommets was about 2000 pounds (lbf). We surmise that the preponderance of the observed extrusion occurred during accelerated thermal aging of the penetration assembly at an elevated temperature. During the thermal aging cycle, the environment temperature was maintained at 150°C for 168 hours.

Sylgard® 170 is a commercially available silicone elastomer material. Dow Corning supplies that material in kit form consisting of two liquid components. When compounded, the material cures to a flexible elastomer. The company's product information bulletin³ indicates that the material mixing ratio is not critical for constituent variations of ten percent or less. Other pertinent information, obtained from the bulletin, suggests that a major use of this material is in the area of electrical/electronic potting and encapsulating applications. Of particular significance is the manufacturer's caution concerning material applications that are highly confined, in that specific allowance must be made to accommodate temperature-induced volume expansion of the confined material. The

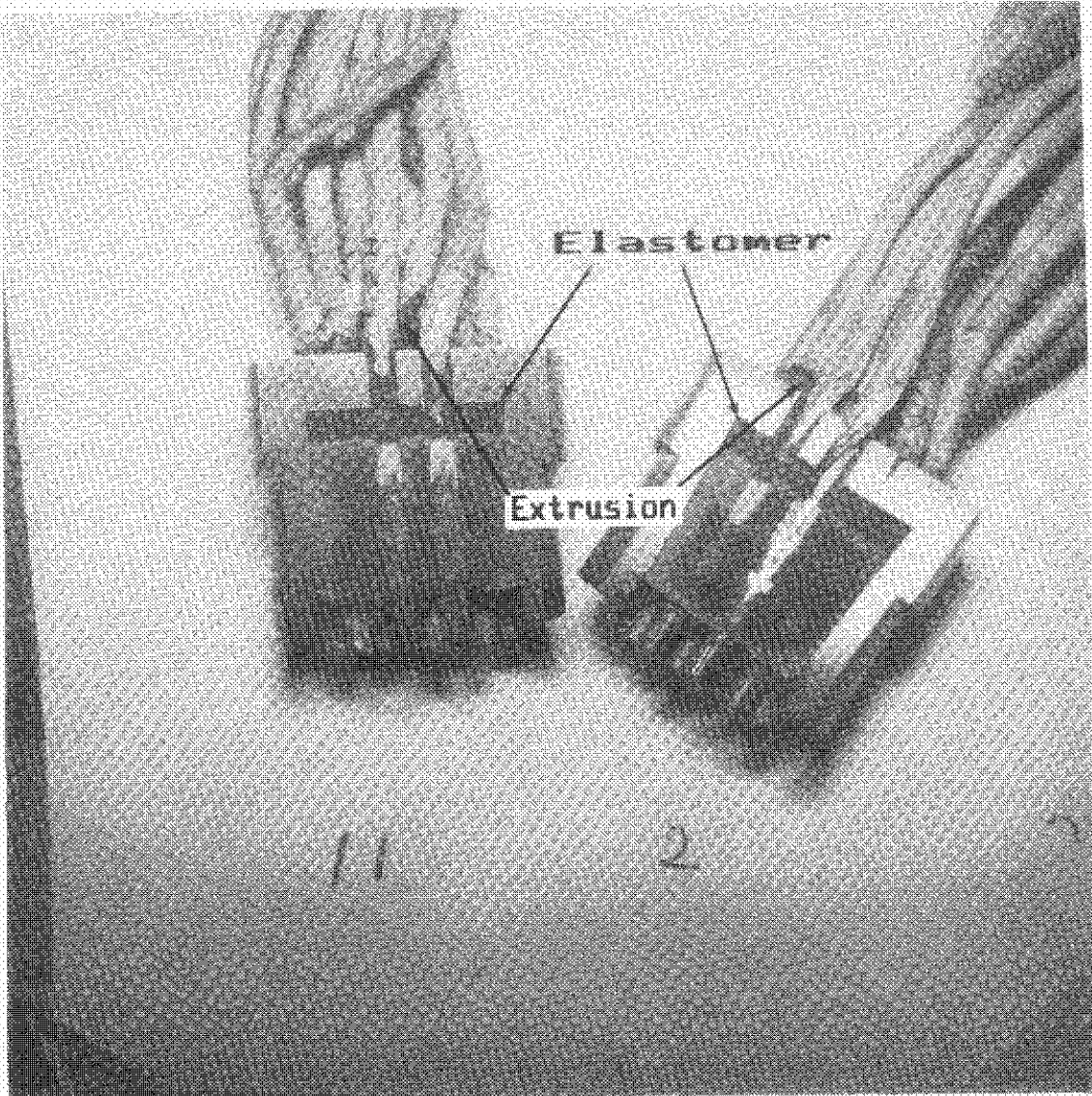


Figure 1. D. G. O'Brien Type "K" Connector: Sectioned View.
(Reference 2)

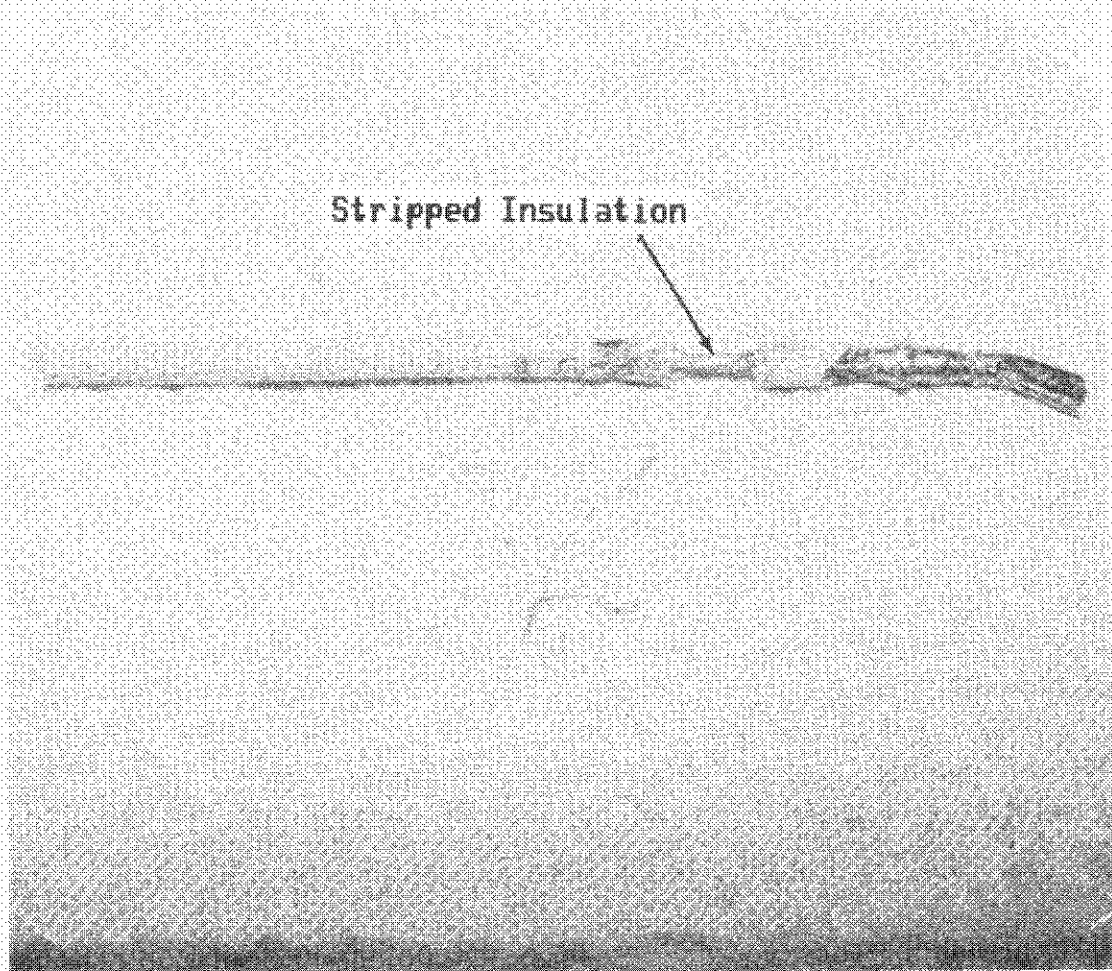


Figure 2. Effects of Elastomer Extrusion on Cable Insulation Penetration Test. (Reference 2)

coefficient of volume expansion is quoted, by the manufacturer, to be

$$8 \times 10^{-4} \text{ cm}^3/\text{cm}^3/^\circ\text{C}.$$

Our concern centered on the material's response to long-term compressive loads, applied to both aged and unaged elastomer specimens. Of particular interest was the response of the strained specimens to both steady state and transient temperature environments. Temperatures considered were those representative of reactor plant (in-containment) ambient conditions and those suggested for qualification tests; i.e., accelerated aging and loss of coolant accident (LOCA) temperature approximations.

Accelerated aging methods were employed to examine material response to aging. Degradation of elastomer mechanical properties was considered a measure of material age. The Arrhenius method was used to estimate times and temperatures required to achieve the desired state of aging.

For completeness, we exposed some Sylgard specimens to Cobalt-60 radiation, at approximately one megarad per hour, to total doses in the range of 0 - 200 Mrad. The data from these exposures were used to determine the effects of radiation aging on the elastomer's response to compressive loading and elevated temperatures.

Material response to applied strain (stress) was studied by observing the stress relief in instrumented test specimens. Stress relief was observed as a function of elapsed time from applied load, thermal environment, and the "degree" of specimen confinement.

We will first discuss the thermal aging experiments and results; next, radiation effects are considered; and finally the elastomer's response to combined compressive loading and (elevated) temperature environments is discussed.

II. ELASTOMER THERMAL AGING STUDIES

A. Apparatus and Procedures

Elastomer samples were fabricated in the form of strips and discs for the comparison mechanical properties studies. The strips were used to monitor elongation and tensile strength as a function of age. The discs were, in the main, used during the stress relief studies and for hardness checks. Strip dimensions were 0.64 cm wide, 0.16 cm thick, and 15 cm long. Disc dimensions were 3.1 cm in diameter by 1.3 cm thick.

Samples were aged in thermostatically controlled ovens, and a constant air flow was maintained across the elastomer specimens. Air flow rate was such that a complete change of air occurred hourly.

Aging times at temperature required to simulate any given age were estimated using the Arrhenius relationship equating simulated age and temperature to actual aging time and temperature on the basis of a known (or assumed) activation energy. In the equation,

$$t_a = t_s \times \exp \left\{ \frac{E}{k} \times \left(\frac{1}{T_a} - \frac{1}{T_s} \right) \right\}$$

where:

t_s is the simulated age, at simulated temperature T_s ,

t_a is the accelerated aging time at aging temperature T_a ,

E is the activation energy, and

k is the Boltzmann Constant.

For purposes of estimating aging time at temperature, we assumed an activation energy of 0.87* eV. On that basis, discs and strips were aged according to the schedule appearing in Table I.

Table I.
Specimen Aging Time Schedule

Aging Time, in Hours at Temperature**

Aging Temperature (°C)	Accelerated Age (yr)				
	5	10	20	40	104
150	8.2	16.3	32.6	65.3	170.0
140	14.6	29.3	58.6	117.0	303.0
125	36.5	73.0	146.0	292.0	760.0
110	98.6	197.3	395.0	--	--

** Based on an assumed activation energy of 0.87 eV at an ambient temperature of 43°C.

* Private communication with K. Gillen, SNL

Three each, disc and strip (tensile), specimens were aged according to the specification of each element appearing in the aging matrix (Table 1).

Each specimen was subjected to the following measurements:

- thickness (strips and discs)
- surface dimensions (strips and discs)
- weight (discs)
- hardness (discs)
- elongation (strips)
- tensile strength (strips)

Sample dimensions were determined with high precision vernier and micrometer calipers while specimen weights were determined with an automatic, self-scaling Mettler balance. Disc hardness measurements were obtained using a Shore A-2 durometer, and tensile (elongation and ultimate strength) measurements were obtained with an Instron 1130 Universal test machine using a continuous tape extensometer graduated in 0.10 inch increments.

B. Results

We include, with the Sandia results, data reported⁴ by Dow-Corning on the same elastomer material. Sandia elongation data are presented in Figures 3 through 7. The data show normalized material elongation, at break, as a function of aging time. Figures 3 through 6 present the data for individual aging temperatures and Figure 7 is a composite of data for all aging temperatures. As may be observed, no clear cut degradation trend is apparent. In fact, for short aging times anomalies are present in that loss of elongation is not a monotonic decreasing function with increasing aging time, and in some instances, degradation appears to be inversely proportional to aging temperature.

The Dow Corning data appear in Figures 8 through 11. While the Sandia data were in the range of 110 to 150°C, we note that the Dow Corning data are in the temperature range between 177 and 210°C.

Figures 8 through 10 present individual (temperature) aging data, and the composite of all data are given in Figure 11. Dow-Corning tensile data are in reasonable agreement with the Sandia results. We note from the composite presentation, Figure 11, that no strong aging trend is apparent. Similarity between the Sandia and Dow Corning results may be noted by comparison of the composite aging curves (from Figures 7 and 11) combined in Figure 12. Examination of the combined plot shows that the Sandia and Dow Corning elongation data are in good agreement.

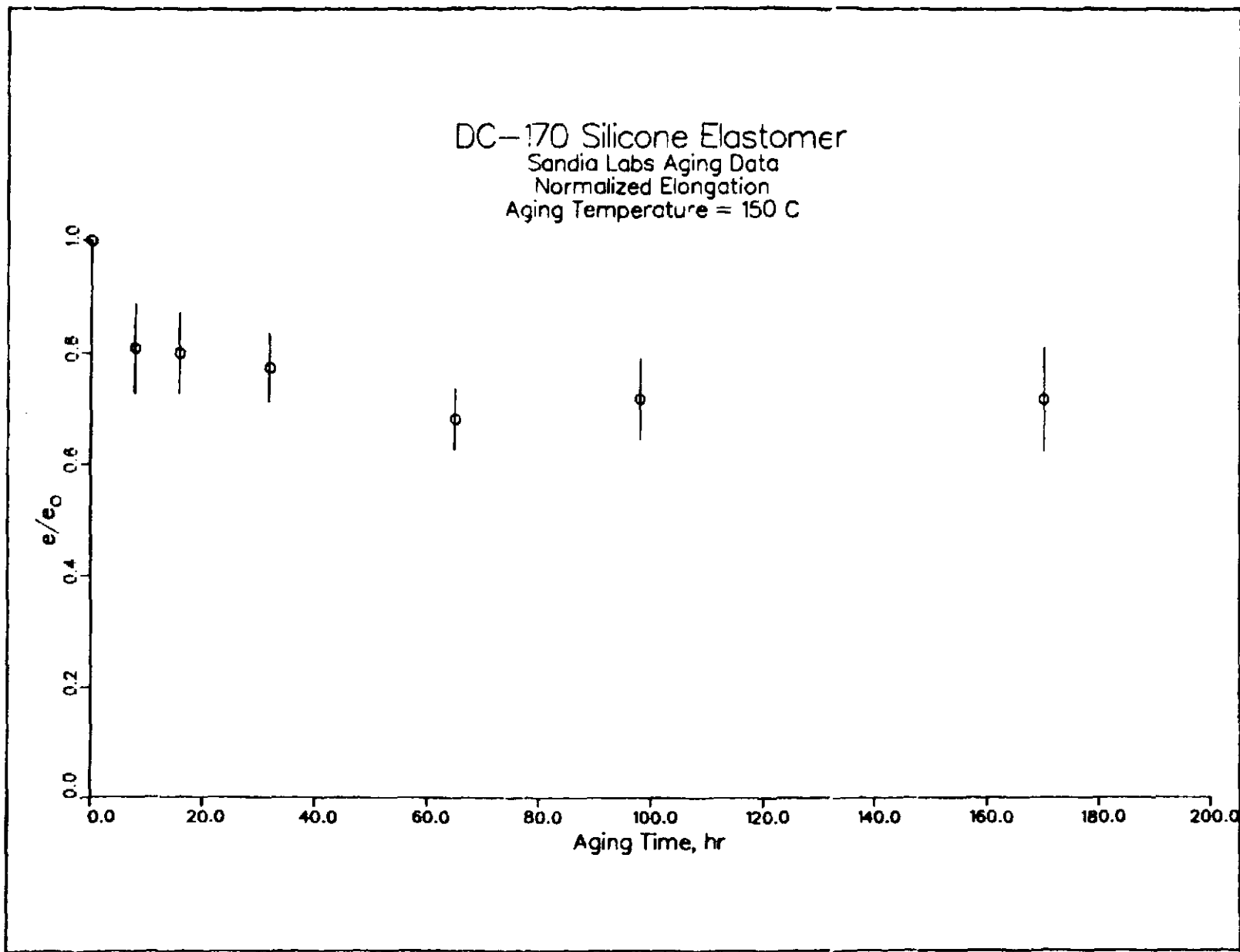


Figure 3. Sandia Normalized Elongation vs. Aging Time at 150°C.

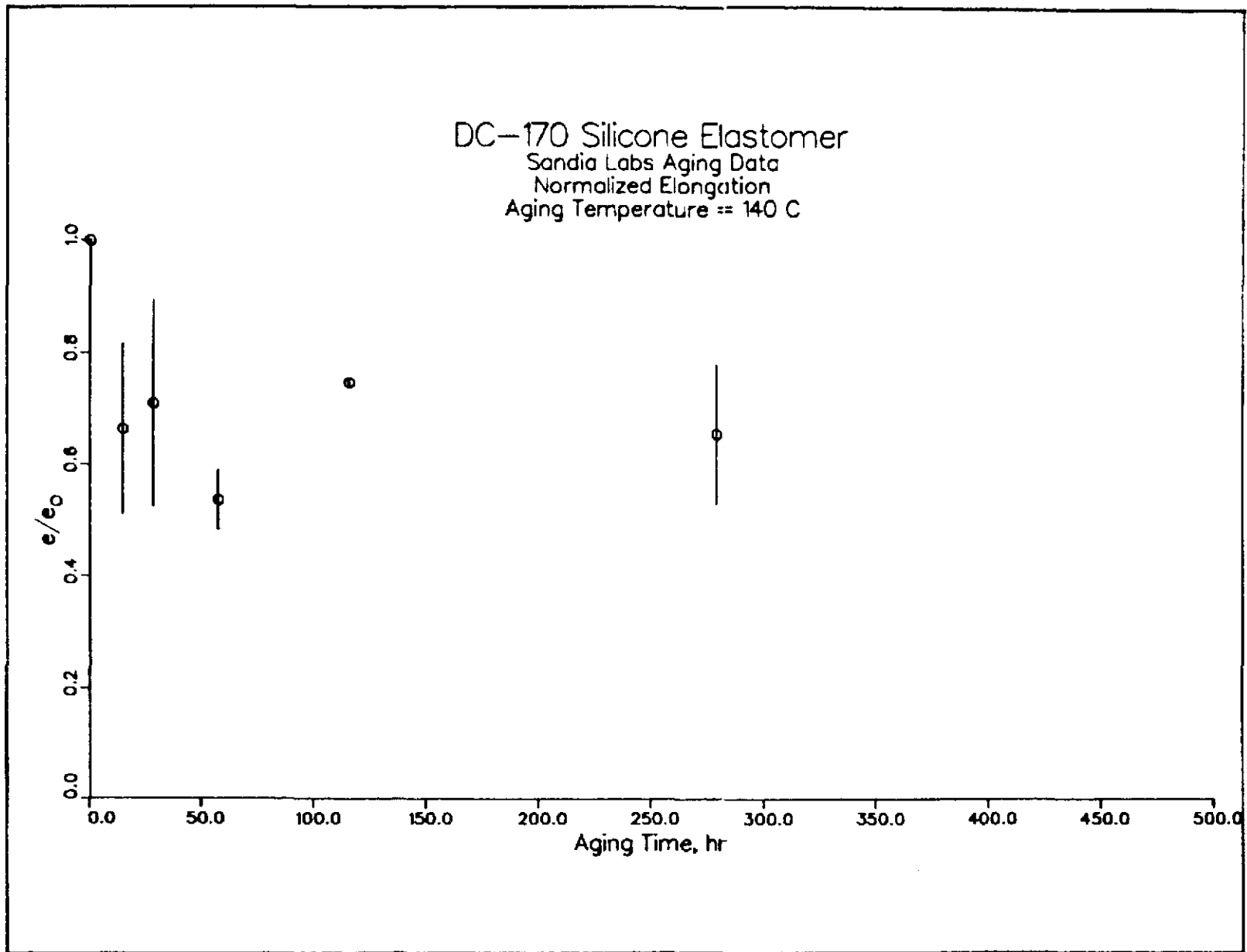


Figure 4. Sandia Normalized Elongation vs. Aging Time at 140°C.

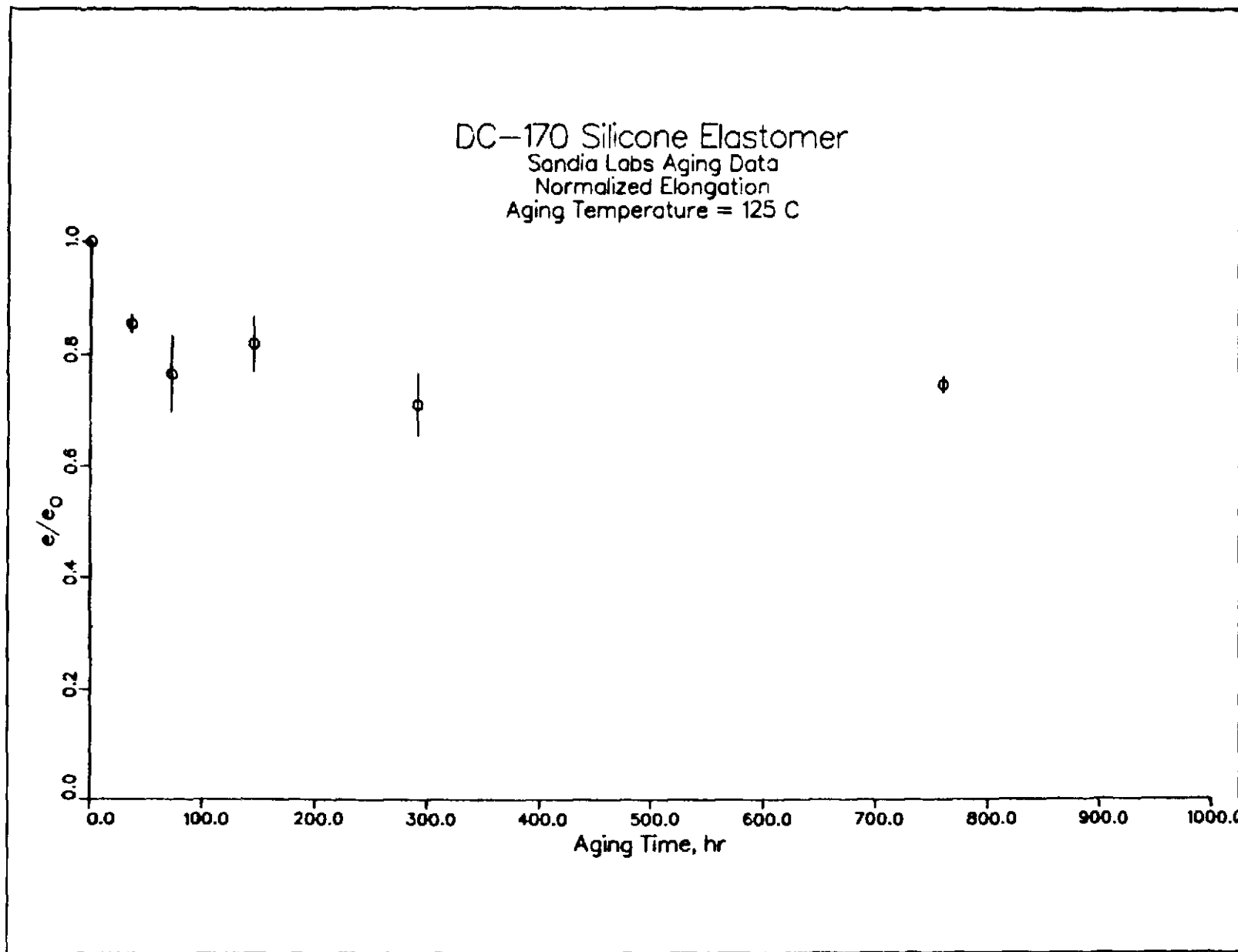


Figure 5. Sandia Normalized Elongation vs. Aging Time at 125°C.

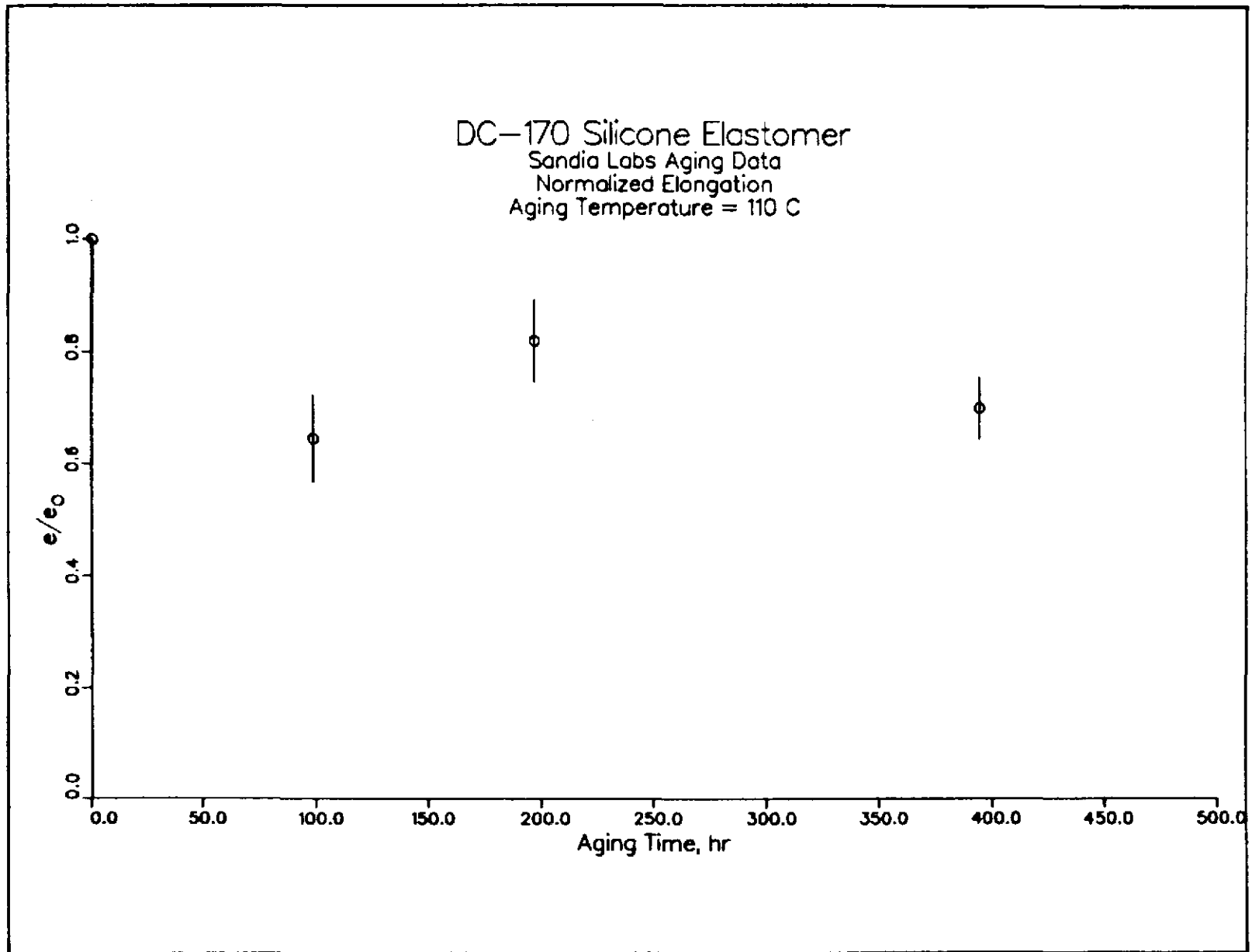


Figure 6. Sandia Normalized Elongation vs. Aging Time at 110°C.

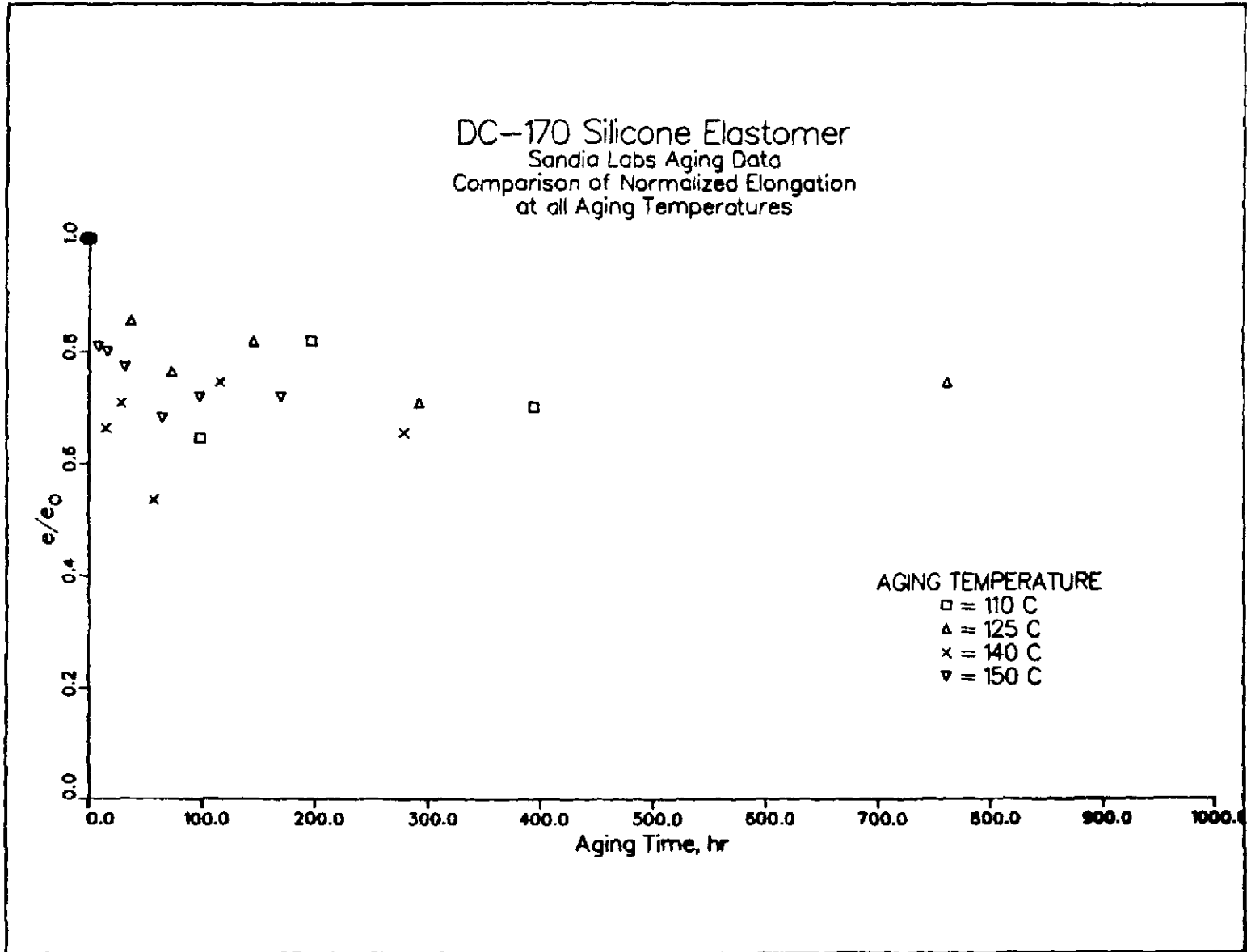


Figure 7. Comparison of Sandia Normalized Elongation Data.

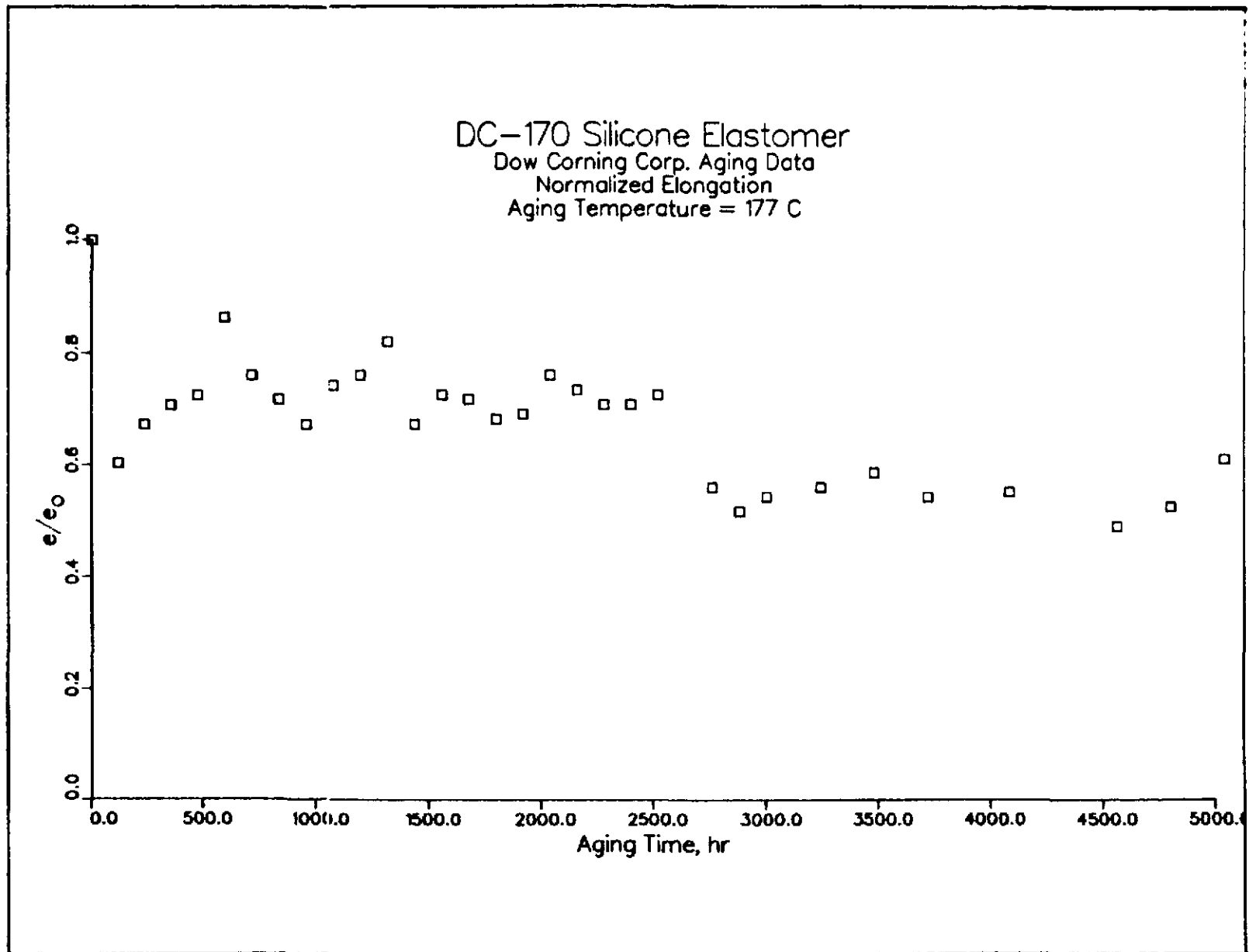


Figure 8. Dow Corning Normalized Elongation vs. Aging Time at 177°C.

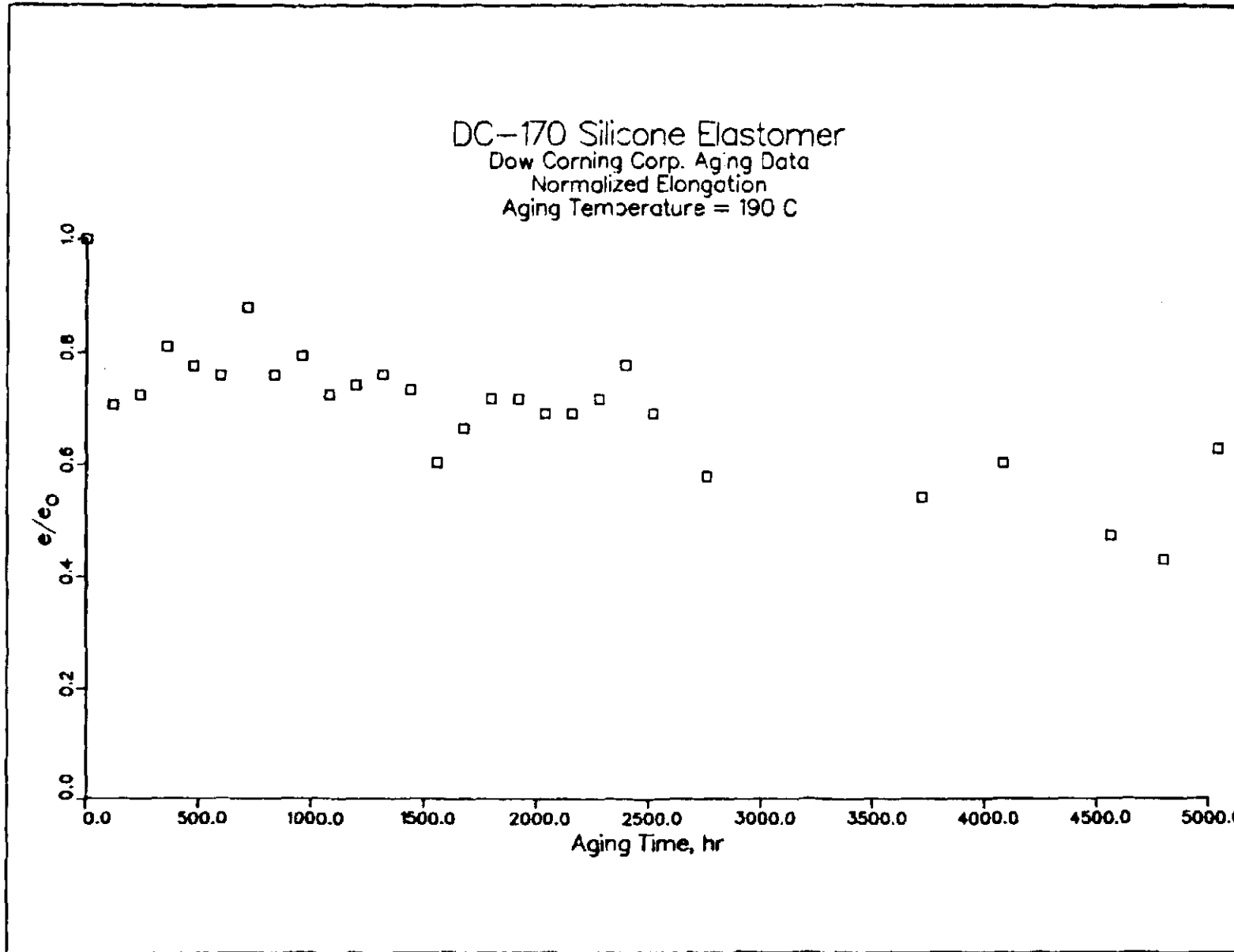


Figure 9. Dow Corning Normalized Elongation vs. Aging Time at 190°C.

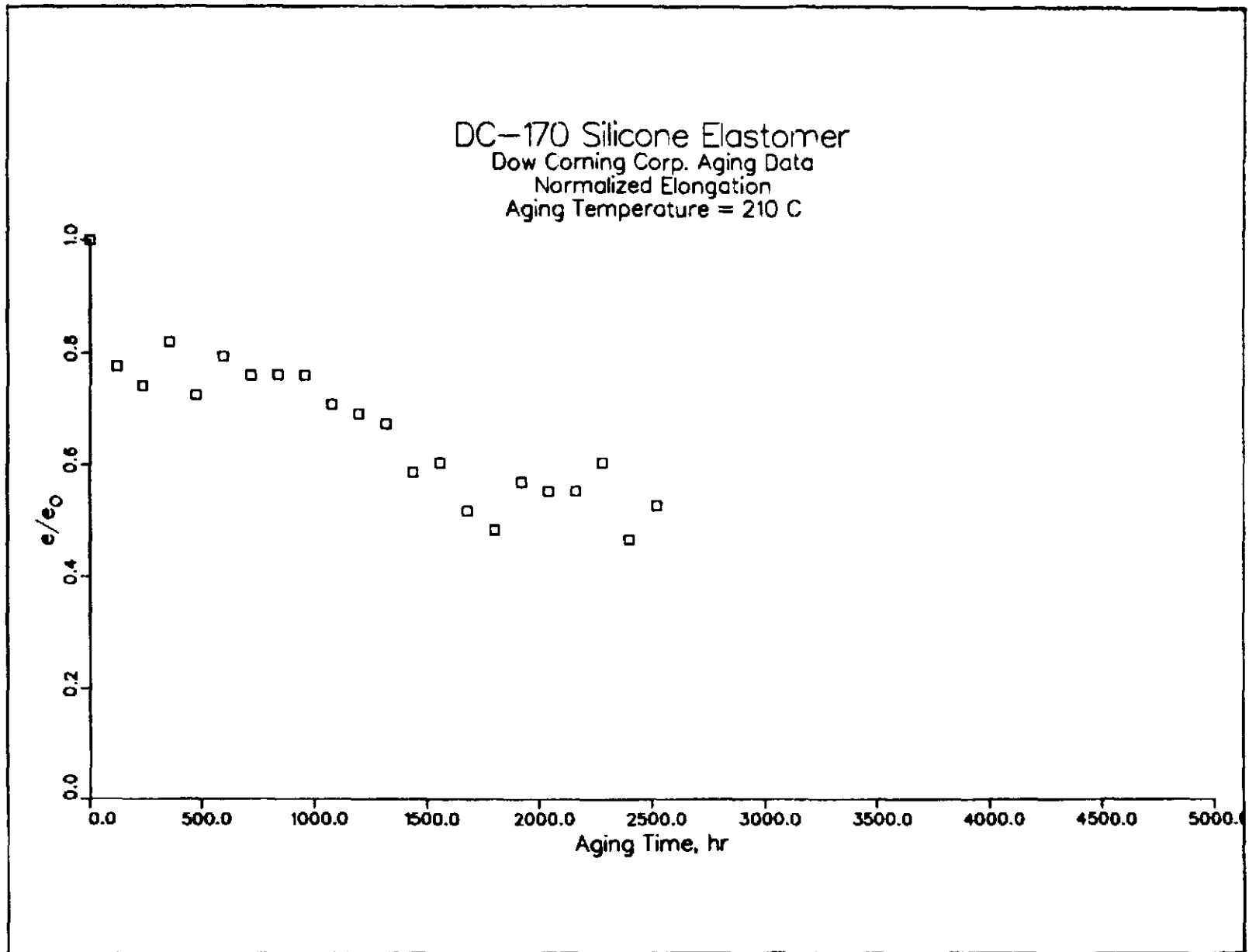


Figure 10. Dow Corning Normalized Elongation vs. Aging Time at 210°C.

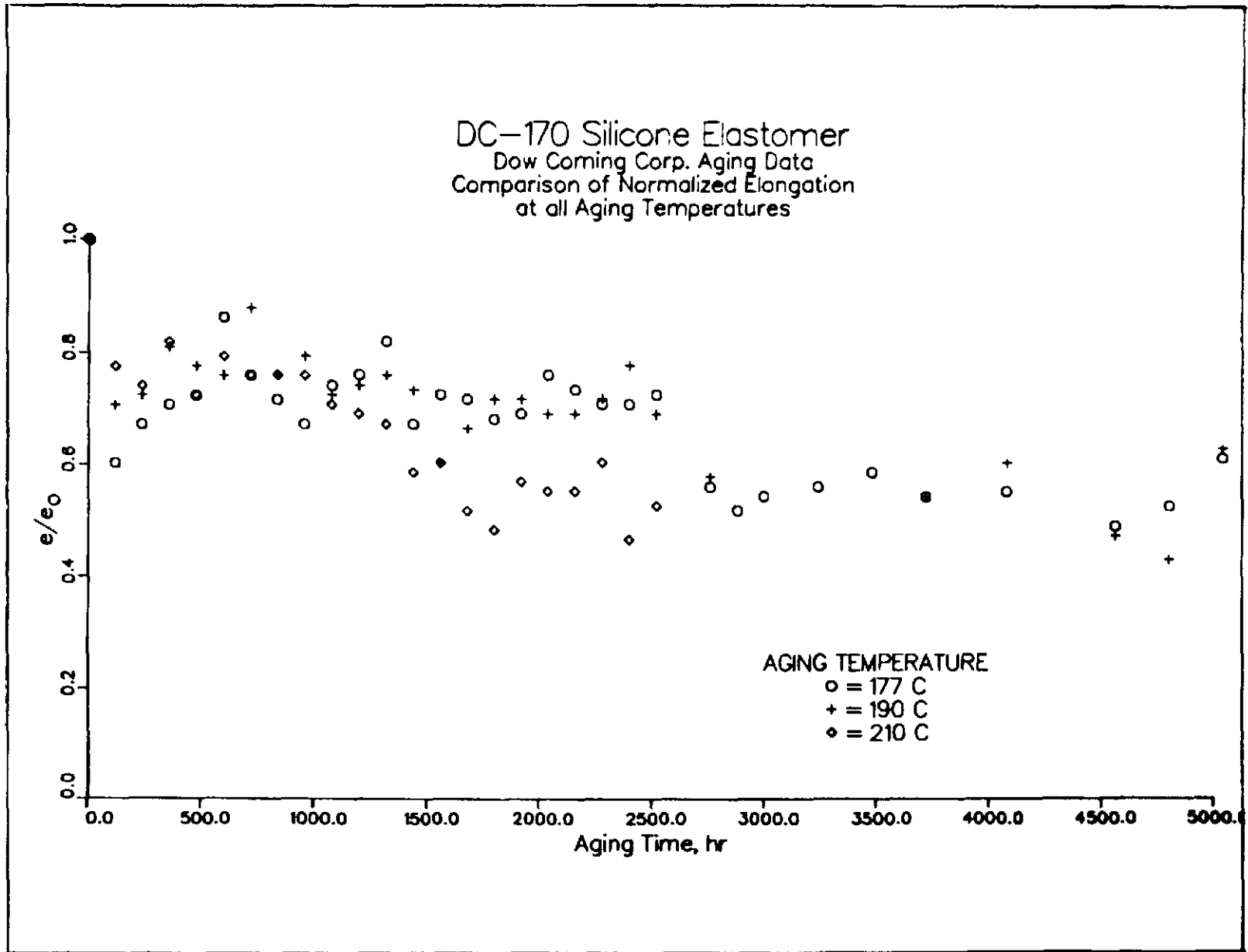


Figure 11. Comparison of Dow Corning Normalized Data.

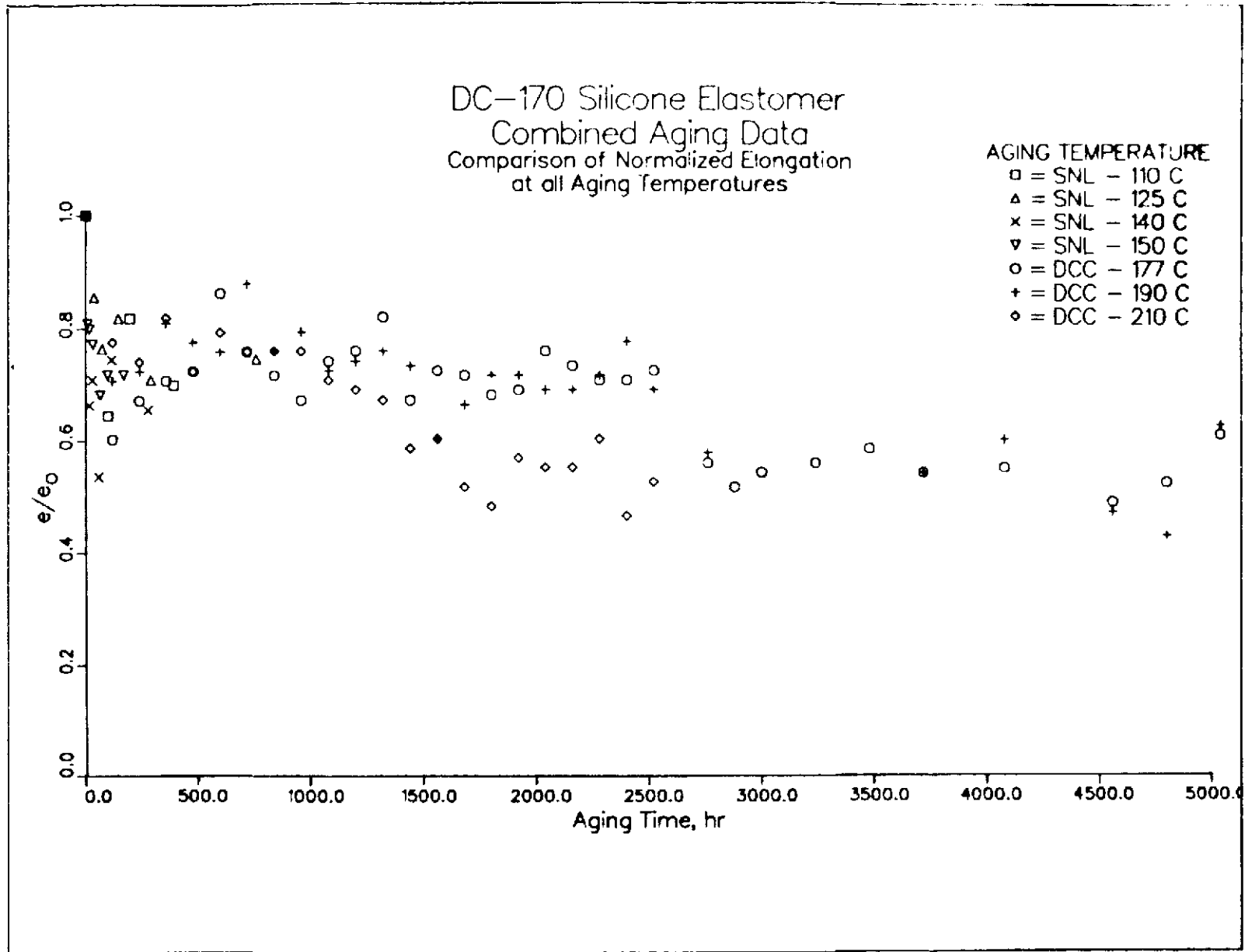


Figure 12. Comparison of Sandia and Dow Corning Elongation Data.

Sandia material hardness data appear in Figures 13 through 16. Data presented are normalized material hardness as a function of aging time. Aging data for 150, 140, and 125°C appear in Figures 13, 14, and 15, respectively. A composite of all data appears in Figure 16. Of interest in these plots is the nearly step-wise increase in material hardness occurring on the order of hours (at the first data point shown) into the aging exposure followed by a long plateau. Of particular interest is the fact that both the step-wise and ultimate material hardness are inverse functions of the aging temperature. The composite data plot, Figure 16, clearly demonstrates this unexpected behavior.

Dow Corning hardness data are given in Figure 17 through 20. Aging temperatures considered were 177, 190, and 210°C. The Dow Corning data are consistent with those obtained by Sandia--a step-wise increase in hardness at early aging times followed by a long plateau and an inverse dependence of ultimate hardness with aging temperature. A comparison of the Sandia and Dow Corning hardness data is given in Figure 21-A. We offer no explanation for either the initial "jump" in material hardness nor its inverse temperature dependence. When the initial change in specimen hardness data are analyzed, we observe correlation between the Sandia and Dow Corning measurements. In Figure 21-B the initial stepwise change in hardness is plotted as a function of aging temperature. In the figure, Sandia data are denoted by triangles and Dow Corning data by circles.

III. RADIATION AGING STUDIES

A. Apparatus and Procedures

Radiation aging studies were carried out using the Sandia low intensity cobalt array (LICA). Disc and tensile strips were exposed to integrated doses of 50, 100, and 200 Mrads (Air). Dose rate during exposure was approximately 0.44 Mrad (Air)/hr. Prior to specimen exposure, radiation dose and/or dose rates in the irradiator were determined using an integrating air ionization chamber. (Previous to the dose/dose rate measurements, the ionization chamber was calibrated on an N.B.S. traceable Cobalt-60 radiation range.)

B. Results

Results of these radiation exposures are summarized in Figure 22. Plotted are normalized elongation (strip data) and normalized hardness (disc data) as a function of integrated radiation exposures. As may be observed in Figure 22, specimen hardness increases (essentially) linearly with increasing radiation exposure and, elongation exhibits a characteristic (exponential) decrease with increasing radiation exposure. It is interesting to note that the normalized elongation and

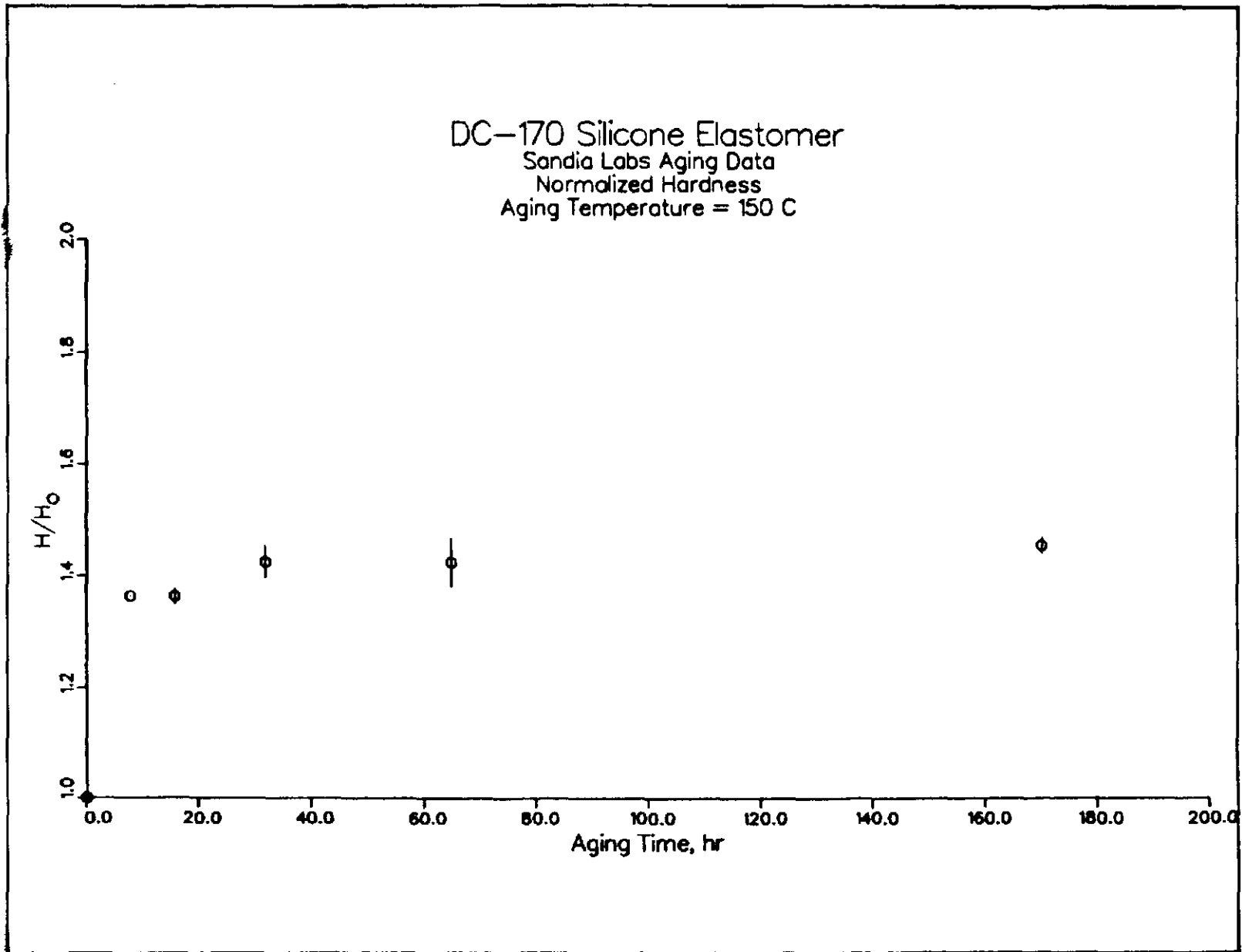


Figure 13. Sandia Normalized Hardness vs. Aging Time at 150°C.

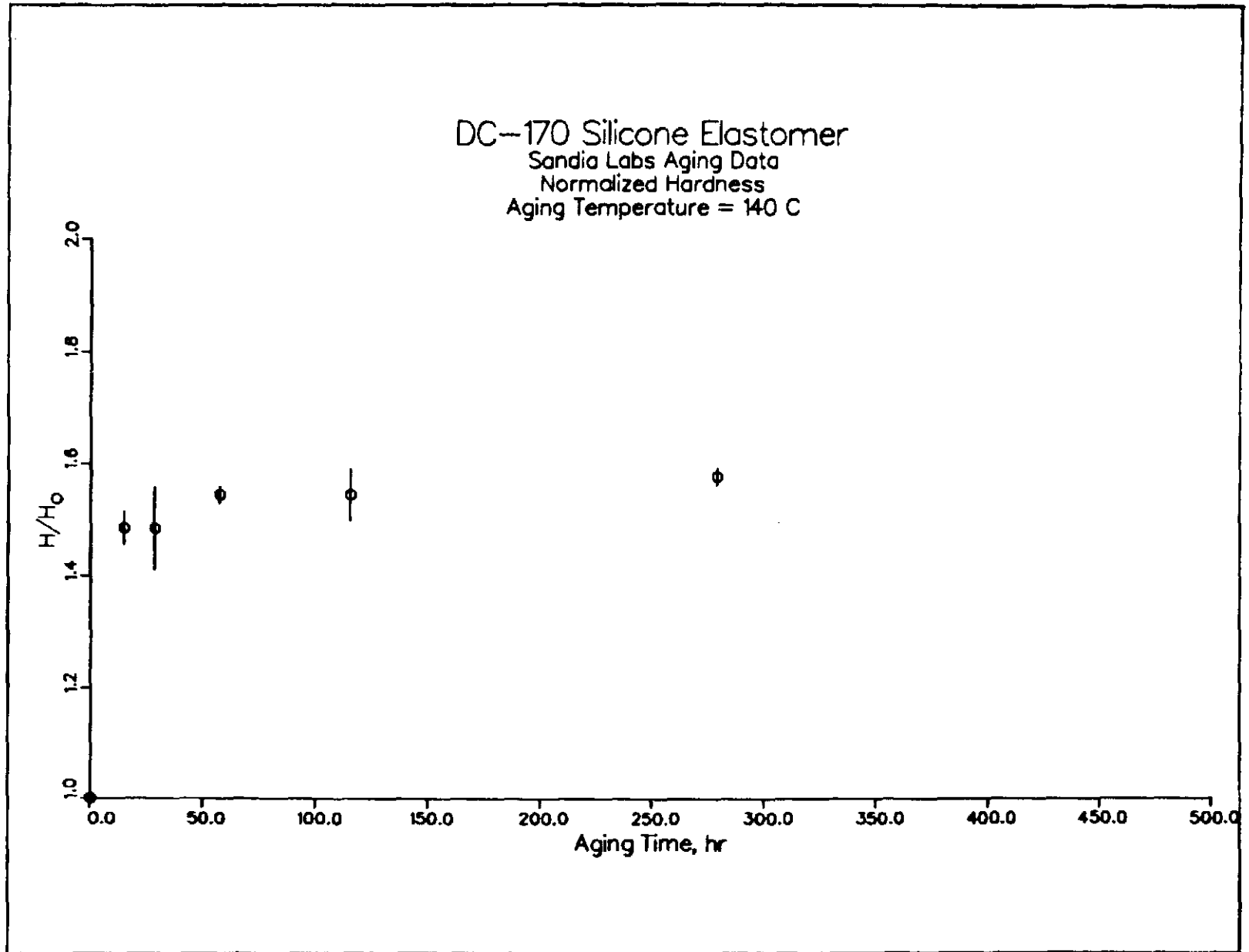


Figure 14. Sandia Normalized Hardness vs. Aging Time at 140°C.

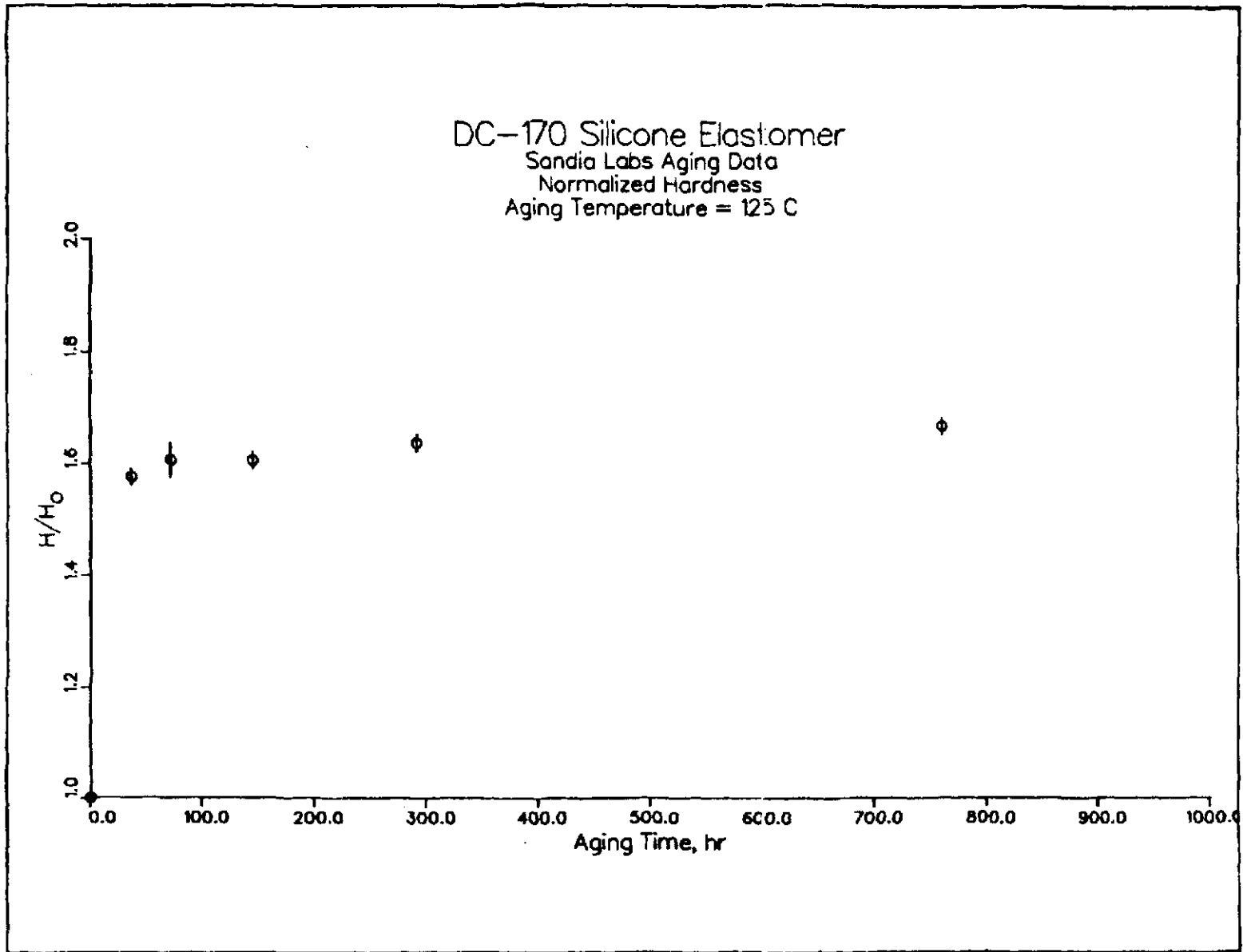


Figure 15. Sandia Normalized Hardness vs. Aging Time at 125°C.

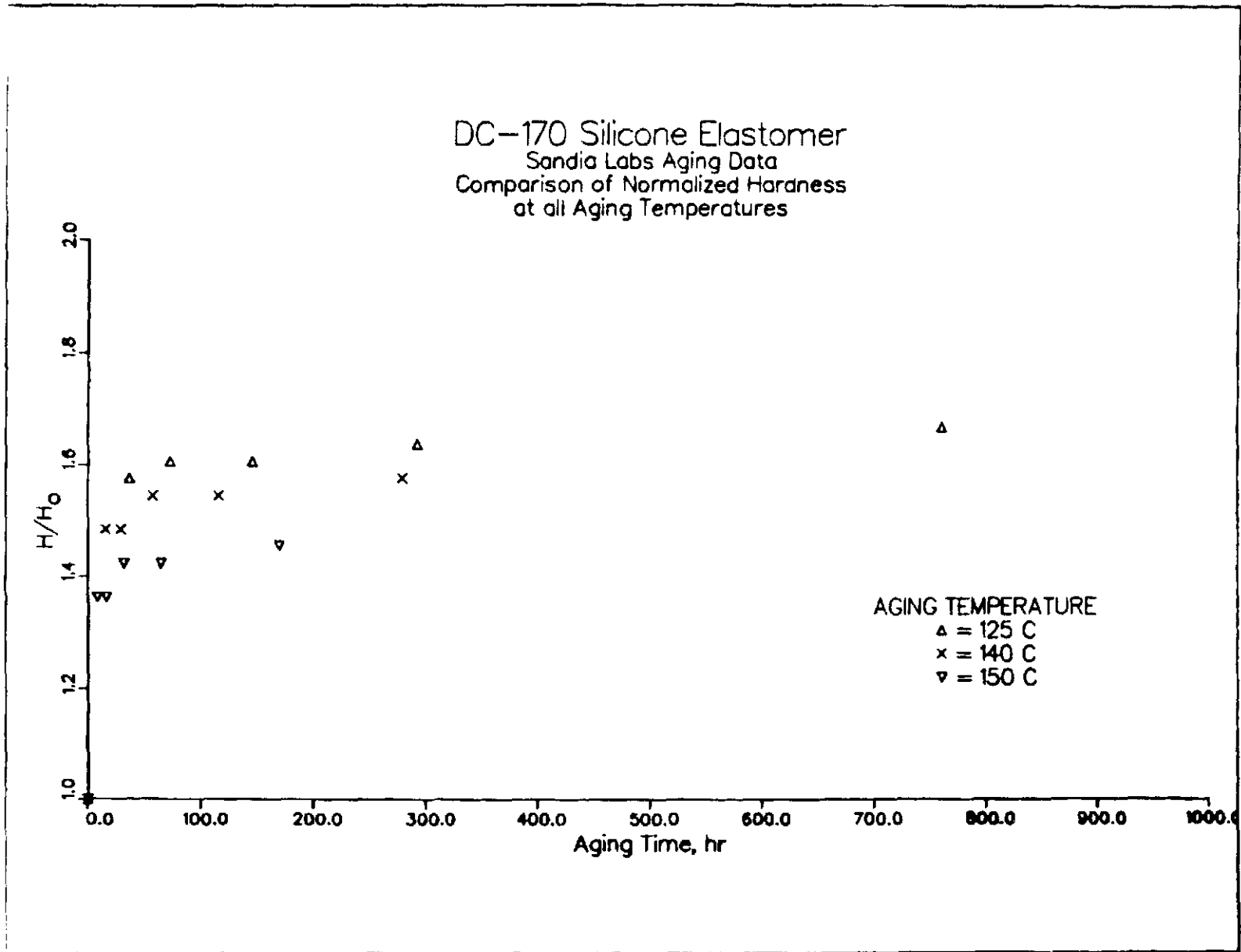


Figure 16. Comparison of Sandia Normalized Hardness Data.

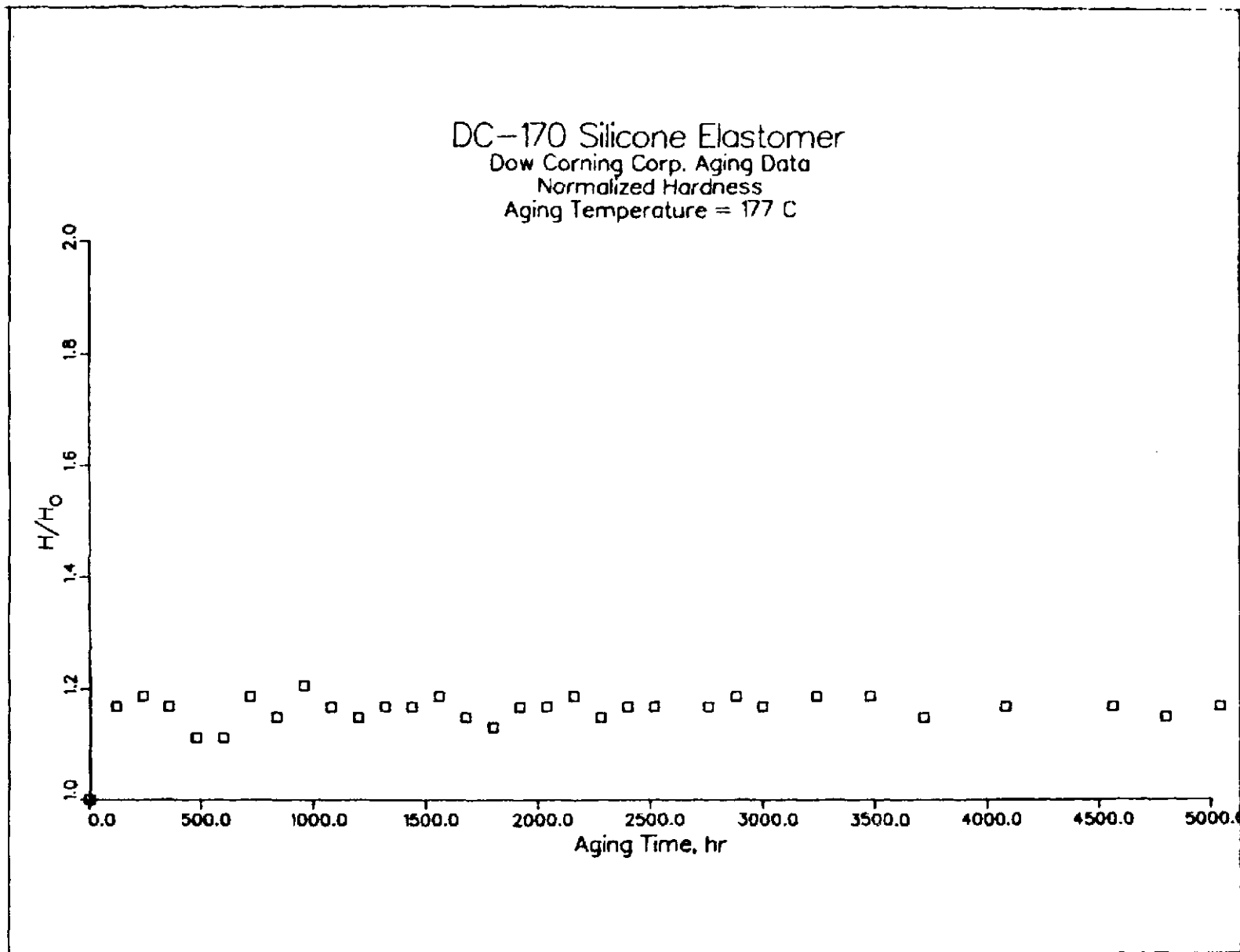


Figure 17. Dow Corning Normalized Hardness vs. Aging Time at 177°C.

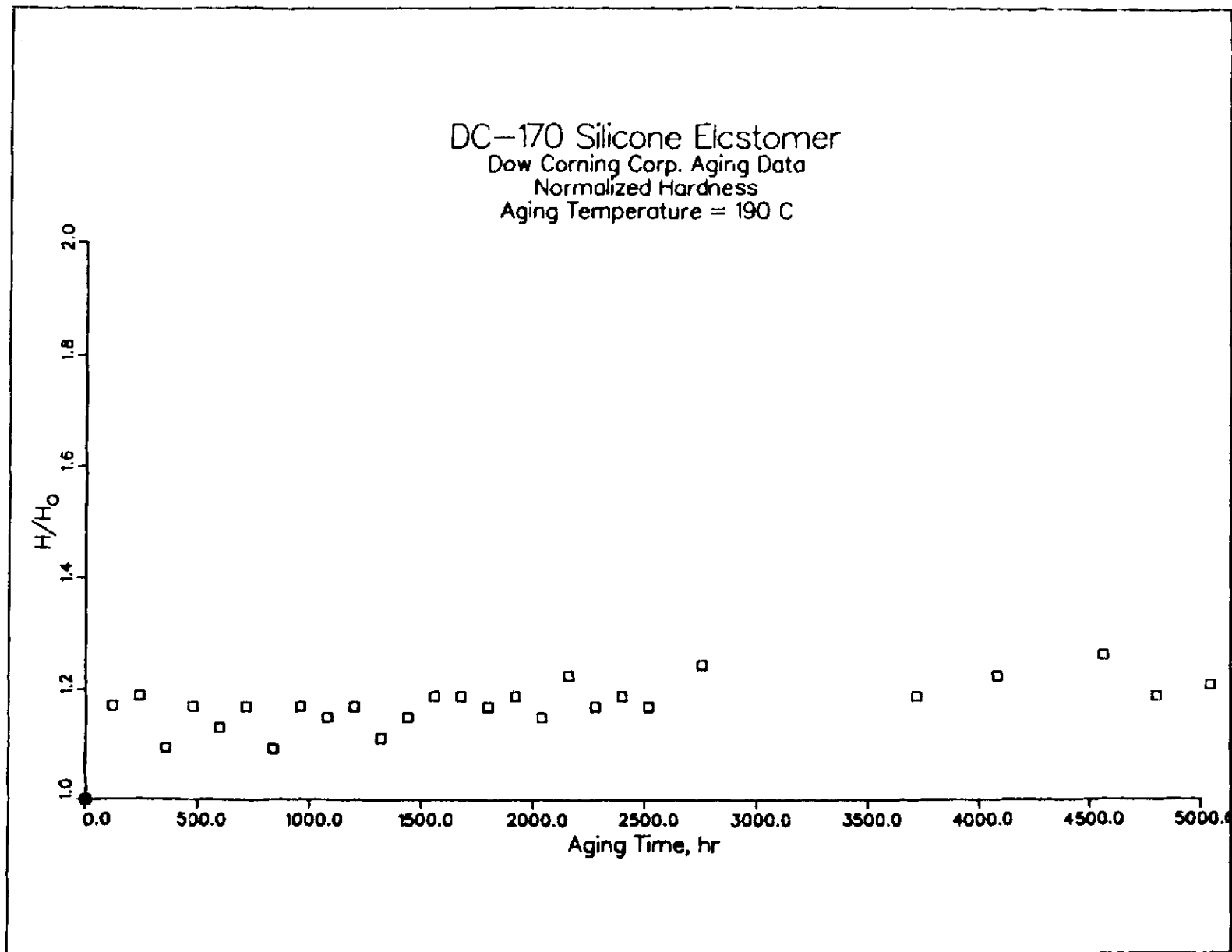


Figure 18. Dow Corning Normalized Hardness vs. Aging Time at 190°C.

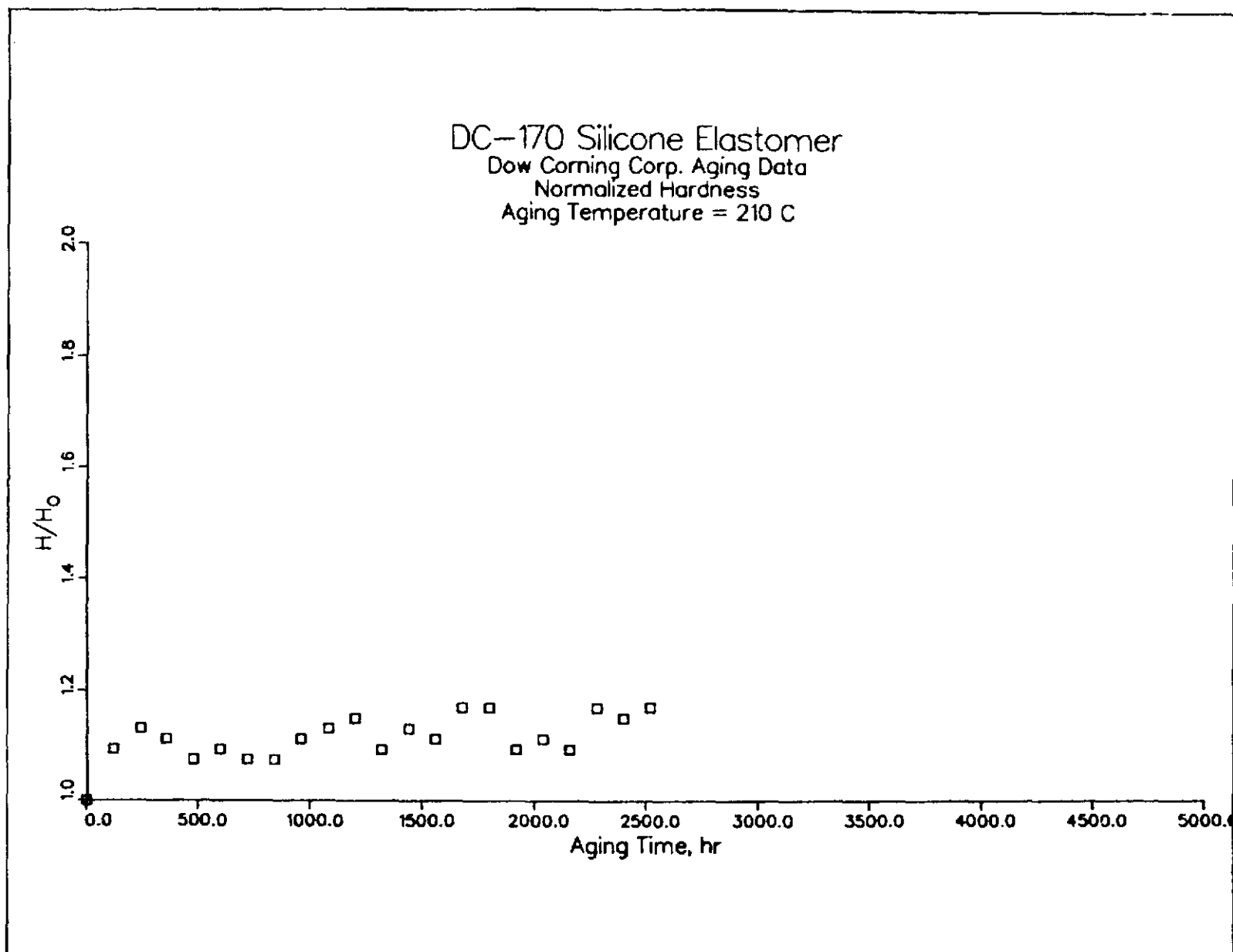


Figure 19. Dow Corning Normalized Hardness vs. Aging Time at 210°C.

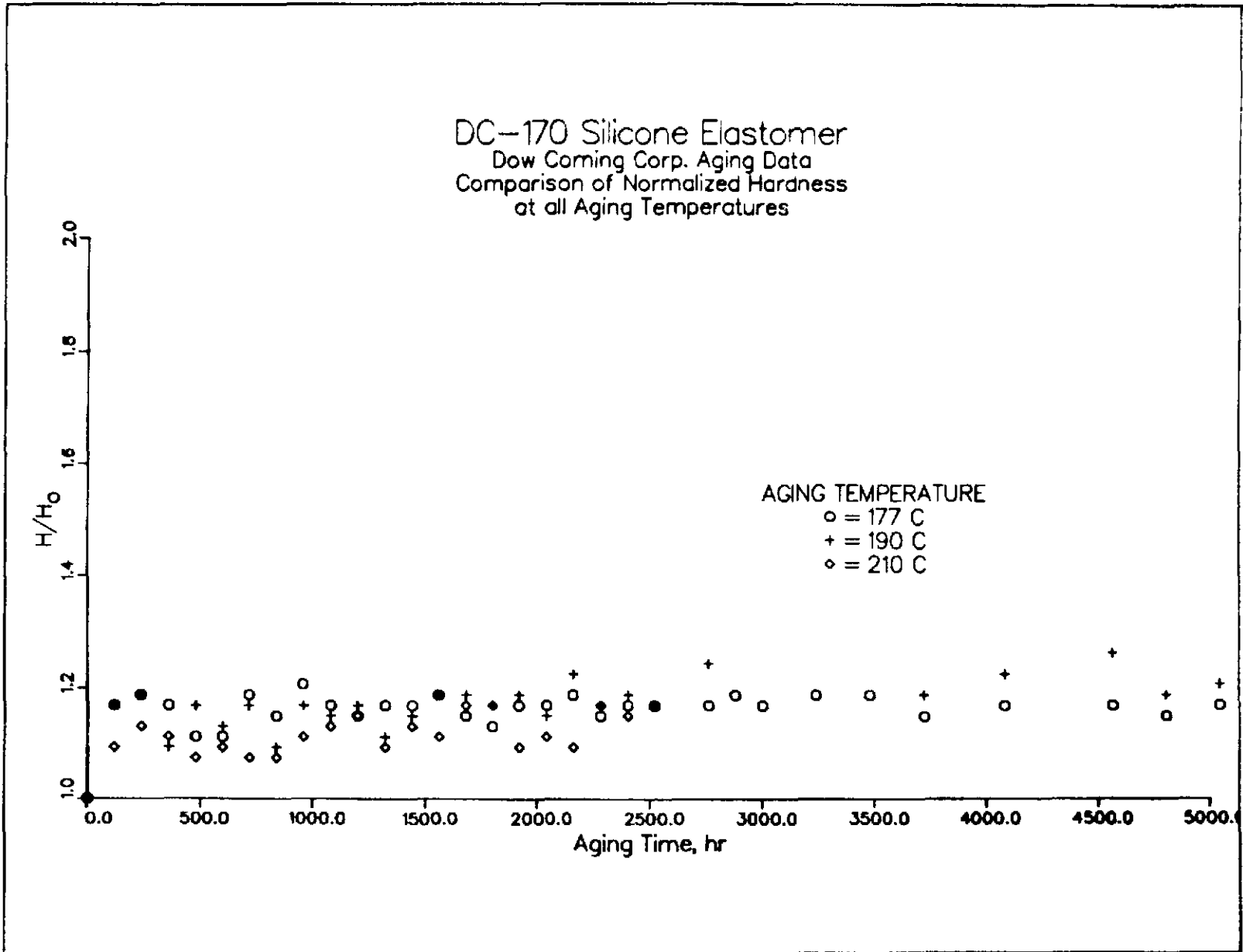
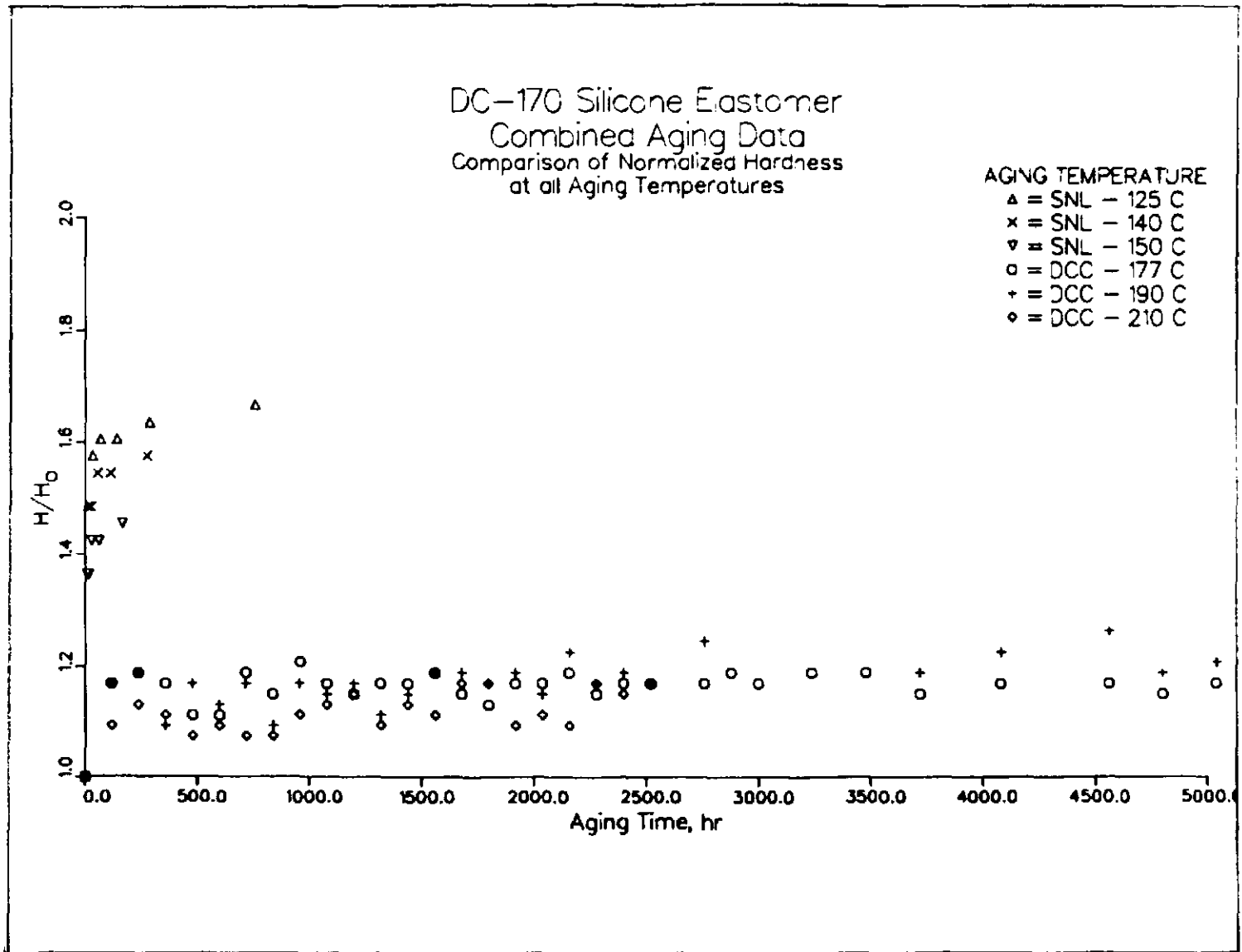


Figure 20. Comparison of Dow Corning Normalized Hardness Data.



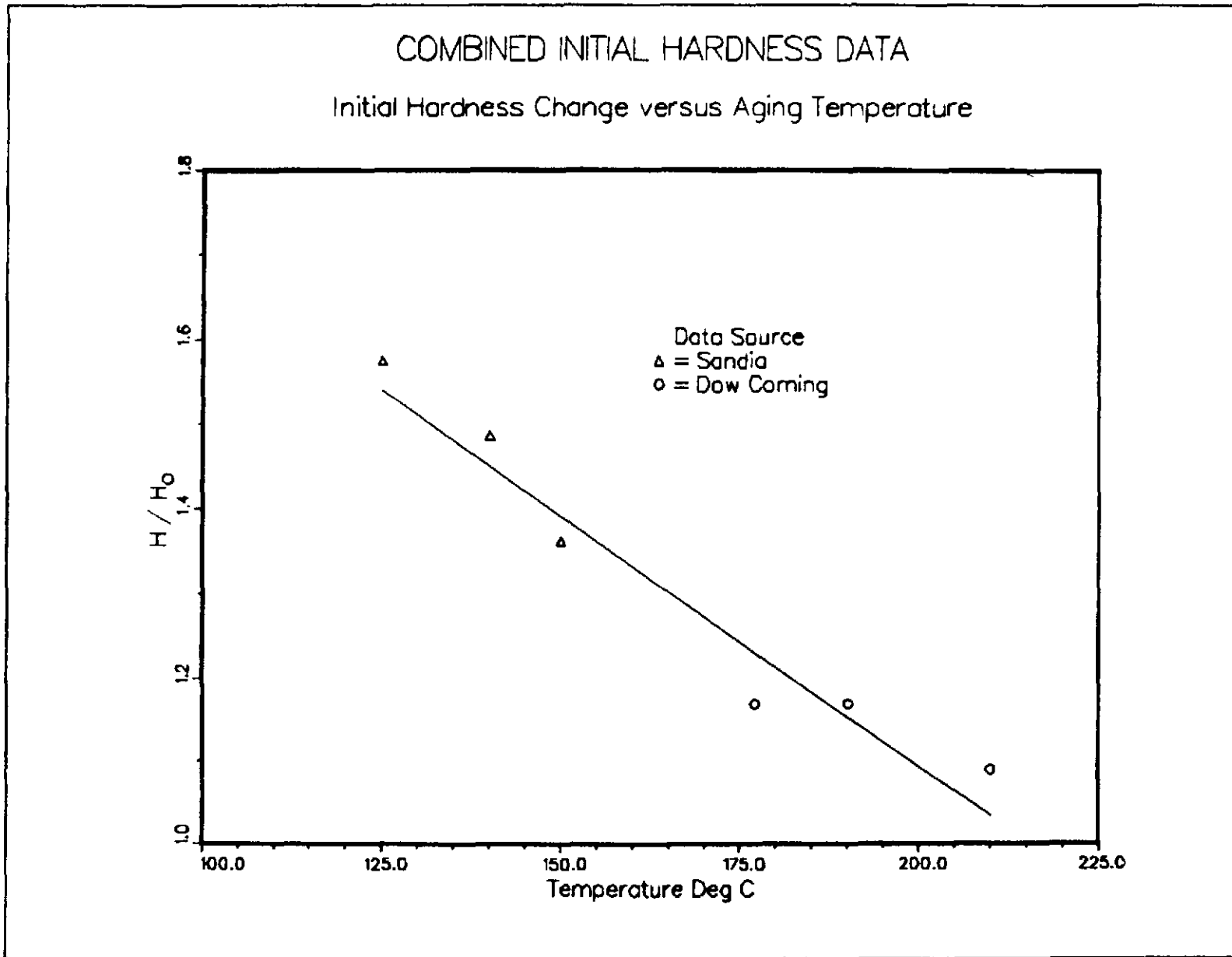


Figure 21-B. Combined Initial Hardness Data.

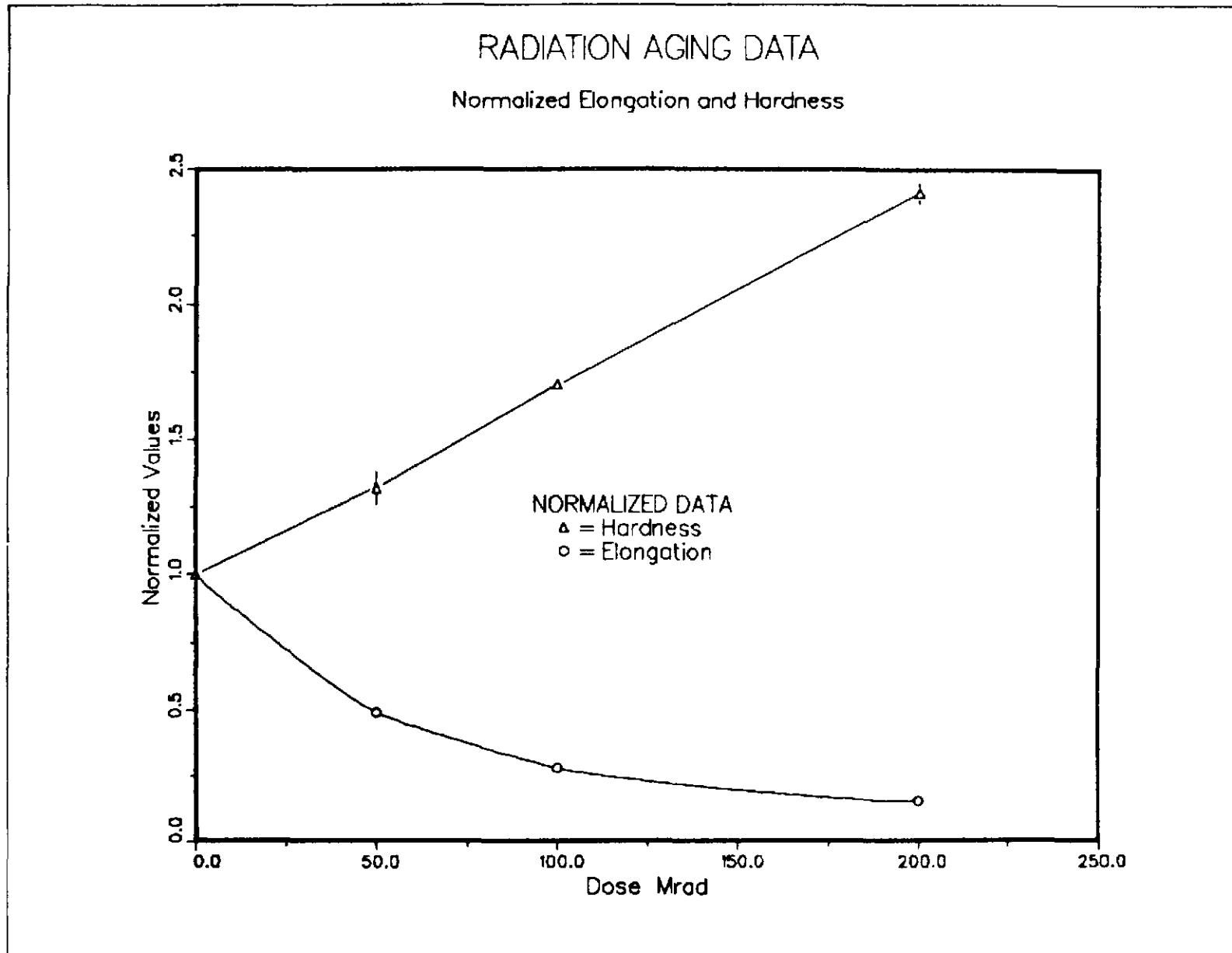


Figure 22. Radiation Aging Data - Normalized Elongation and Hardness.

hardness values at 50 Mrad (a typical radiation aging dose) compare reasonably well with the normalized elongation (Figure 12) and hardness (Figure 21) values obtained for thermal aging times of 2000 hours and longer. However, it should also be noted that as the radiation dose is increased, significant change occurs in the normalized elongation and hardness, whereas this is not the case for thermal aging; i.e., the material's response to increased time-at-temperature or to increased temperature is not changed so significantly.

IV. STRESS RELIEF STUDIES

A. Apparatus and Procedures

The intent of these studies was to observe Sylgard 170 elastomer behavior as a function of applied stress. Accordingly stressed discs were exposed to several thermal environments and stress relief was measured as a function of time at strain and available relief path. Since the tests were concerned with the effect of long-term compressive loads, it was decided to restrict our attention to samples in disc geometry. This geometry approximates that of actual elastomeric insulating/ barrier components (e.g., the D. G. O'Brien connector grommet pictured in Figure 1). In addition the disc geometry is of the configuration recommended by the ASTM for elastomeric compression tests.⁵ Disc geometry used in these studies is identical to that used in the thermal/radiation aging investigations, discussed in earlier report sections.

Specimens were placed under strain using the fixture shown in Figures 23 and 24. By applying torque to the loading ring, the fixture allowed the application of a known compressive force to the confined specimen. Since the compressive force was applied to the test specimen by means of a screw motion, the strain associated with the initial compressive force could be determined on the basis of total screw rotation. The loading force was transmitted through a calibrated load cell and uniformly applied to the test specimen back surface through a rigid compression plate. Stress (compression) relief was then controlled by the plate retaining the specimen front surface. This control was by means of orifices penetrating the retaining plate. Thus in addition to material relaxation, compressive relief was possible through material flow and extrusion through the retaining plate orifices.

In Figure 25 the details of the specimen confinement geometry are shown. Depicted from the left are the fixture housing, compression plate, test specimen, confining ring, and retaining plate. Just visible in the Figure are the retaining plate orifices. Three orifice geometries were selected--blank (zero hole), 12-hole, and 3-hole. The zero hole configuration,

COMPRESSION FIXTURE

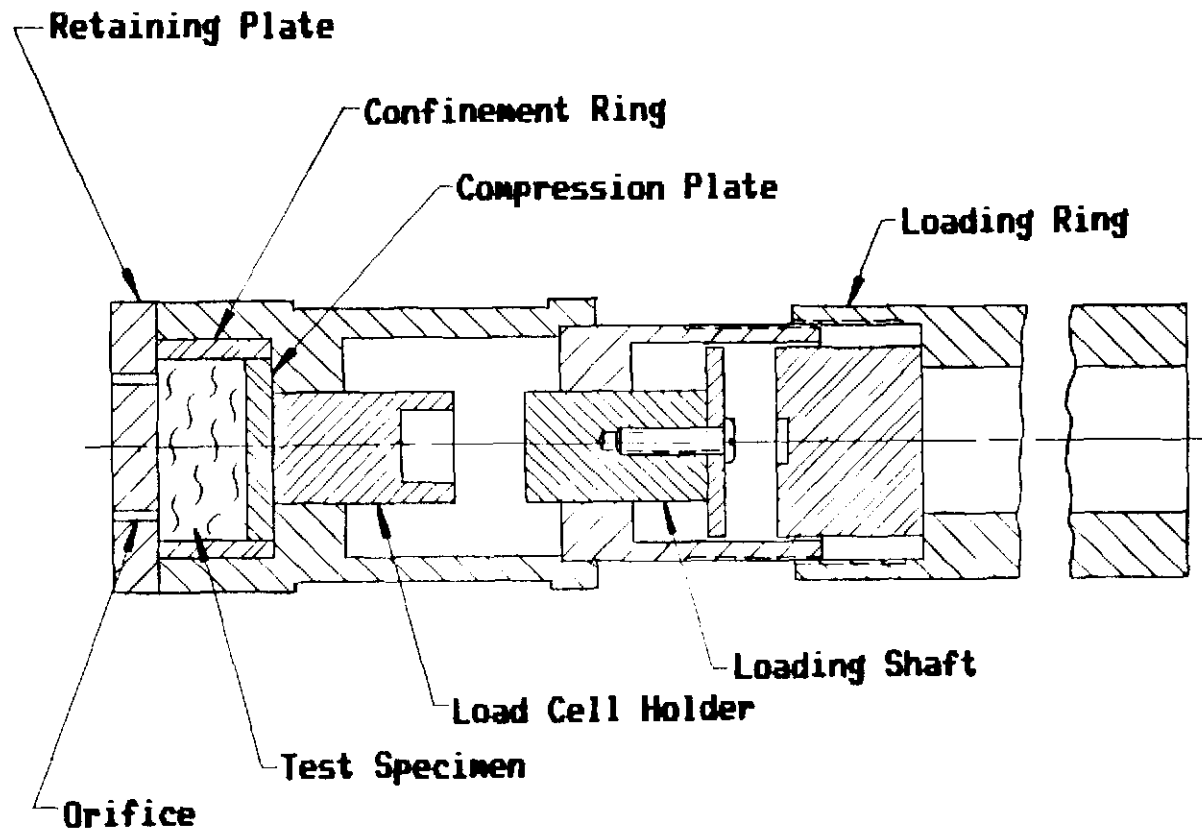


Figure 23. Elastomer Compression Fixture.

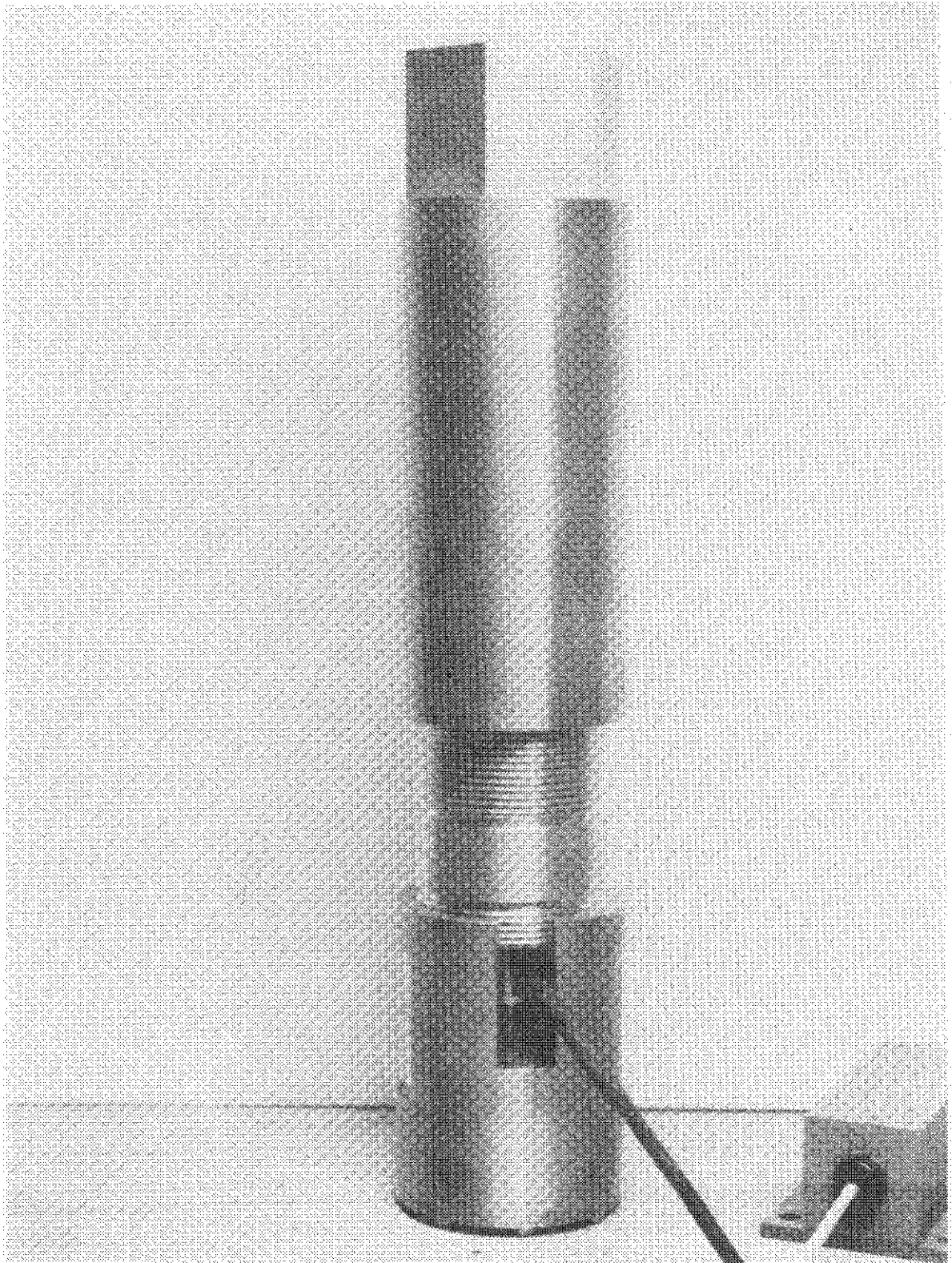


Figure 24. Elastomer Compression Assembly with Installed Load Cell

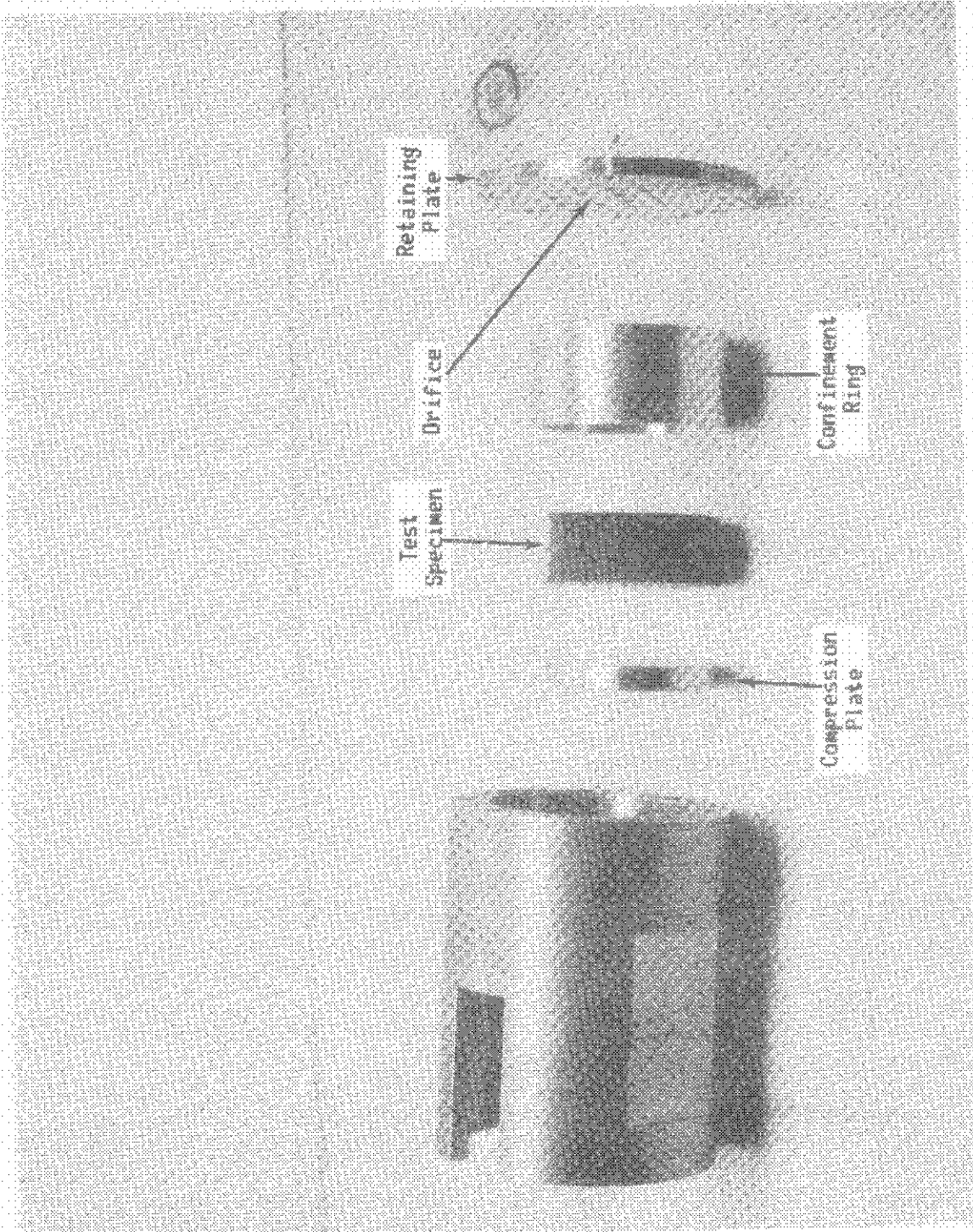


Figure 25. Exploded View: Elastomer Confinement Geometry.

Figure 26. was used to obtain material stress-strain data for total specimen confinement. The 12-hole geometry is presented in Figure 27. Hole diameter for this configuration is .096 inches. Total relief area provided was calculated to be .087 in.² This is the area estimated to be available in the D. G. O'Brien Type "K" connector when it is fully assembled with the specified conductors. The 3-hole configuration dimensions were also based on the Type "K" connector. The diameter of each hole is 0.157 inches, identical to that provided in the Type "K" connector. The 3-hole configuration is shown in Figure 28 in a partially assembled condition. In the Figure, from the left, we note the fixture housing, test specimen positioned in the confining ring and with three insulated conductors penetrating the specimen, and the 3-hole retaining plate. The insulated conductors are identical to those used with the Type "K" connectors. The conductor-insulation diameter is .122 inches. Since hole diameter in the 3-hole retaining plate is 0.157 inches the total relief area available for this configuration, with conductors in place, is 0.023 square inches. Thus available relief area for the configuration is one fourth that available in the 12-hole configuration.

Applied compressive force was continuously monitored with the calibrated load cell. Load cell resistance changes were detected by a resistance bridge, and at specified intervals load cell/resistance bridge output was recorded and converted to compressive force. The converted output was then stored on magnetic tape as a function of time.

Environment temperature - both steady state and transient--was maintained by means of high stability circulating air environmental ovens. Environment and material temperatures were sampled and recorded with each load cell output acquisition.

An outline of the principle experimental parameters is presented in Table II.

From Table II we note that the initial response investigations were concerned with determining the elastomer stress-strain characteristics. We investigated specimen stress-strain characteristics as a function of sample containment and hardness. Unconfined sample data were obtained using the Instron 1000 Tensile-Elongation Test machine in the compression mode. In this mode, test discs were free to deform under the application of a compressive load. In the compressive mode, the Instron machine yields dimensional reduction as a function of applied force. These data were then converted to compressive stress as a function of specimen strain. Data were obtained for samples with hardnesses of 50 and 27, Shore A.

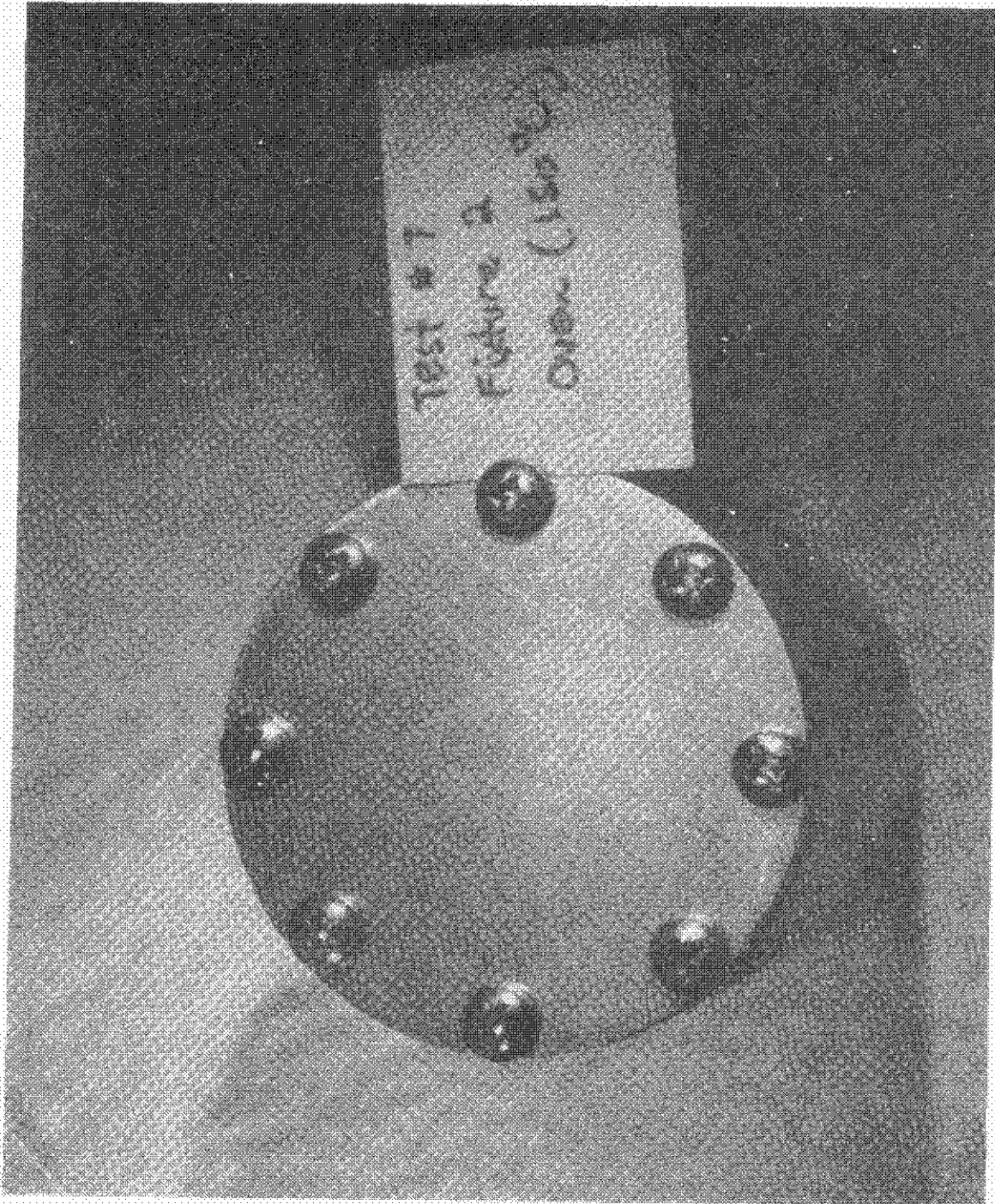


Figure 26. Zero Hole Confinement Plate.

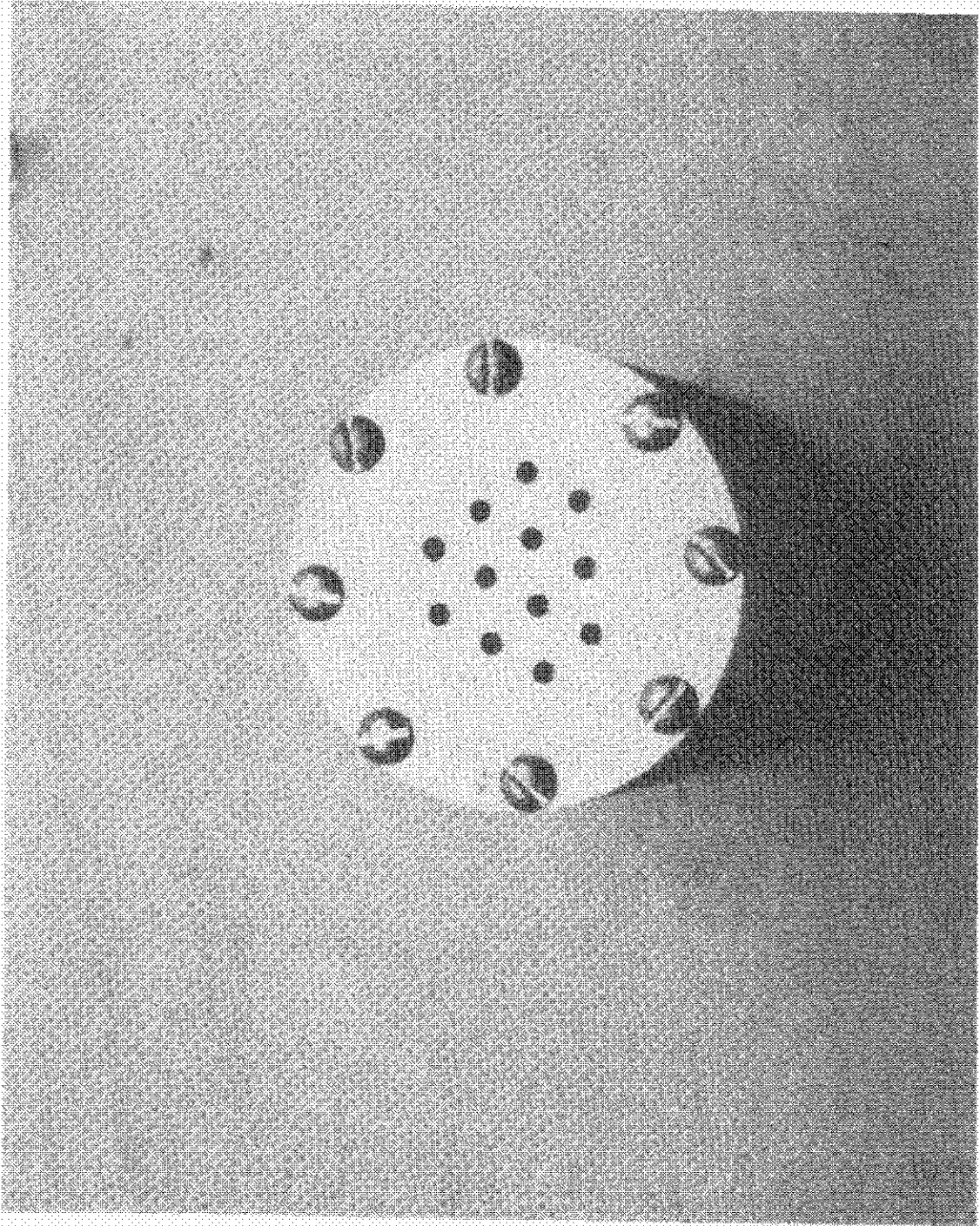


Figure 27. 12-Hole Confinement Plate Geometry.

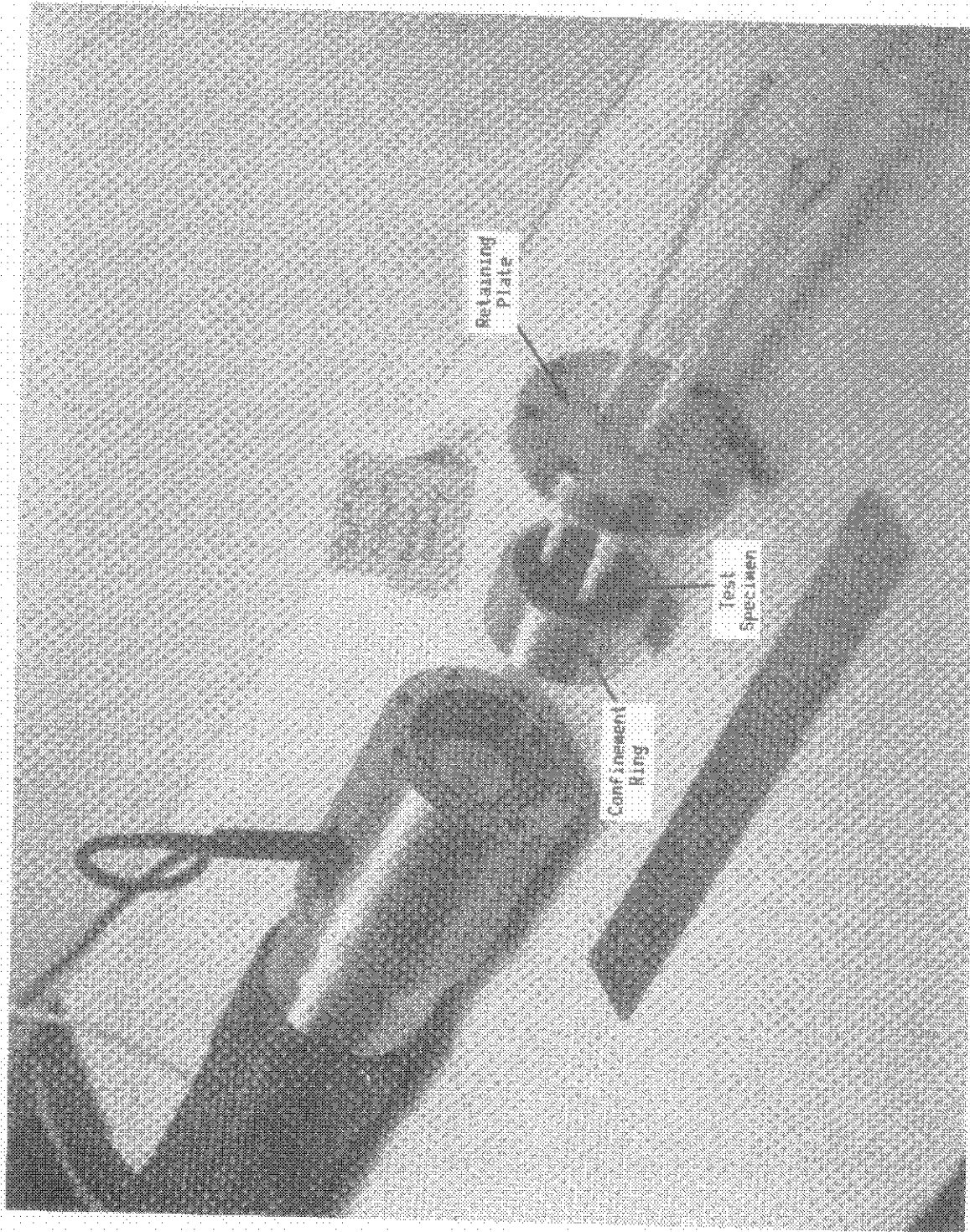


Figure 28. 3-Hole Confinement Plate Configuration.

TABLE II

Compression Studies Outline

1. Stress-Strain Determinations
 - a. Unconfined Sample
 - Sample hardness = 27 Shore A
 - Sample hardness = 50 Shore A
 - b. Zero Compression Fixture
 - Sample hardness = 27 Shore A
 - Sample Hardness = 46 Shore A
 - c. 12-Hole Compression Fixture
 - Sample hardness = 26 Shore A
 - Sample hardness = 47 Shore A

2. Stress Relief
 - a. 12-hole Fixture - 150°C environment
 - b. 12-hole Fixture - 43°C environment
 - c. 3-hole Fixture with conductors - room temperature

3. Specimen Response - LOCA Temperature Profile Simulation
 - a. 12-hole Fixture - sample aged at 150°C
 - b. 12-hole Fixture - sample aged at 43°C
 - c. 12-hole Fixture - sample unaged
 - d. 3-hole Fixture + conductors - sample aged at room temperature
 - e. 3-hole Fixture + conductors - sample unaged

Additional stress/strain data were obtained with test specimens confined in the zero and 12-hole fixture configurations. The technique employed was the same for both fixtures. Specimens were positioned in the fixture and systematically subjected to step-wise increases in material strain. Applied strain was determined on the basis of the loading ring rotation and known screw pitch. For each increase in applied strain, the change in resulting compressive force was monitored with the inline load cell. Again load cell and loading ring data were converted to stress and strain data respectively.

The stress relief studies were performed to determine the elastomer response under steady state environmental conditions and for several different stress-strain relief configurations. Configurations selected and used in these studies were the 3- and 12-hole retaining plate geometries.

For each of the steady state stress relief experiments, the specimen was "torqued" so that an initial compressive force of 2000 pounds (lbf) was uniformly applied to sample back surface. After loading, the instrumented fixture and sample were allowed to age in a steady state temperature environment; these steady state temperature environments consisted of ambient (room temperature), 43°C and 150°C. Ambient exposures provided baseline data for some experiments, and 43°C is more or less a typical plant (in-containment) ambient temperature environment. Since the D. G. O'Brien connector assemblies were exposed to a 150°C environment for thermal aging,² we also studied the elastomer stress response at this temperature. Throughout the aging sequence, the compressive force was periodically monitored. Duration of each experiment was determined by the sample stress relaxation history. Generally, the experiment was terminated when the applied force decayed to a background value or sufficient data were obtained so that an extrapolation to background compressive force could be estimated with confidence. For the 150°C and 43°C exposures, the stress relief path was provided by the 12-hole retaining plate. Ambient exposures were made with the 3-hole fixture, where insulated conductors were penetrating both the relief orifices and elastomer test specimen.

The stress relief studies continued for times on the order of 130 to 180 days.

Following termination of the steady state exposure, the fixture and samples were transferred to ovens for exposure to a typical LOCA qualification temperature profile. During the LOCA temperature excursion, the environment temperature, specimen temperature, compressive force, and elapsed time were recorded. At the conclusion of the LOCA temperature profile, the test

fixtures were disassembled and the test samples weighed for evidence of material loss.

B. Results

Material stress-strain data are presented in Figures 29, 30 and 31 for unconfined, partially confined, and totally confined specimens. Plotted are material stress (force per unit area) as a function of specimen strain (change in length per unit length). From the data in these figures, we note that the stress induced strain is strongly dependent on the degree of specimen confinement. In Figure 32 a composite of the harder disc data is plotted. From this plot it is noted that for a given stress, the unconfined sample is strained about an order of magnitude greater than that observed for confined specimens. Based on the data presented, it is apparent that material response is dependent on its state of confinement, so care must be exercised in use of available stress-strain data.

As stated earlier, specimens were aged in fixtures with 12-hole and 3-hole relief paths. In Figure 33 are presented the elastomer response data for both the 150° and 43° aging temperatures and the 12-hole retaining plate. Plotted are percent of initial compressive load (2000 lbf) as a function of aging time. Oven temperatures are represented by the dashed and chain-dashed curves, and the load versus time curve by the solid (150°C) and dotted (43°C) curve. We applied the compressive loading in two steps of approximately 1000 pounds force (lbf) per step. The initial step appears in the Figure as a two minute pause at about 0.5 of the initial loading. Note that the behavior presented here is for the short-term; total time displayed is on the order of 1.3 hours.

During this phase, samples at both temperatures showed evidences of copious material extrusion. We use the term extrusion to describe rapid material flow coupled with sudden (on the order of hours) decrease in applied stress. Flow, on the other hand, is used to describe slow, steady material loss occurring over a period of many weeks. Note particularly the force-time trace for the 150°C exposure. As the sample absorbed energy from its surroundings, the compressive force increased because of temperature induced expansion. The sudden drop in compressive force then occurred because of extrusion (loss of material). The cyclic nature of this process results in the sawtooth force build-up and decay pattern observed in Figure 33. Behavior of the sample maintained at 43°C is much less pronounced. We note a gradual increase in loading followed by a slow relief in the compressive force. During this time period, it appears that the initial loading placed the material sample near the threshold for extrusion and that the energy transfer from the environment was sufficient to generate appreciable stress in the test

COMPRESSIVE STRESS versus STRAIN

Unconfined Specimen

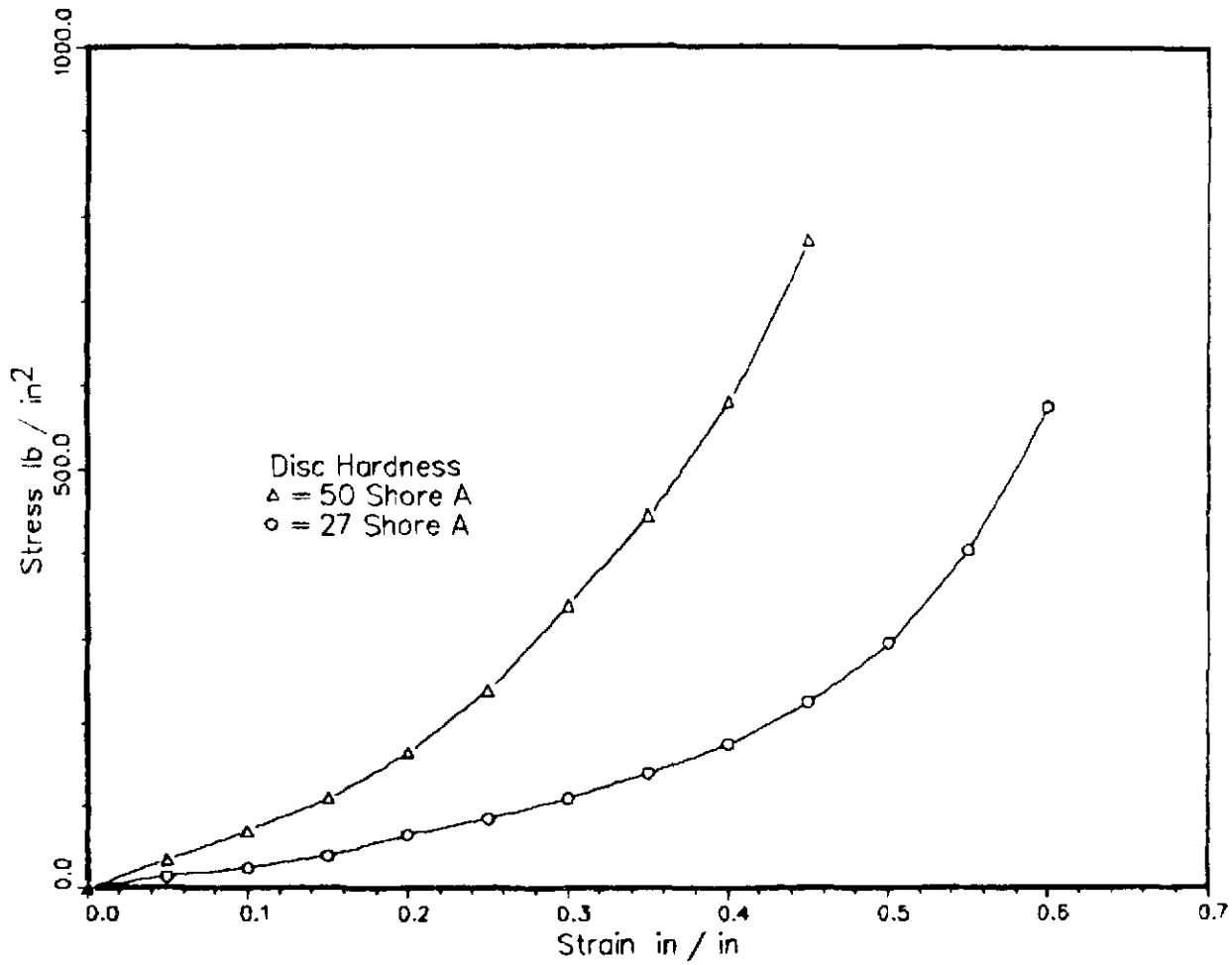


Figure 29. Stress vs. Strain - Unconfined Specimen.

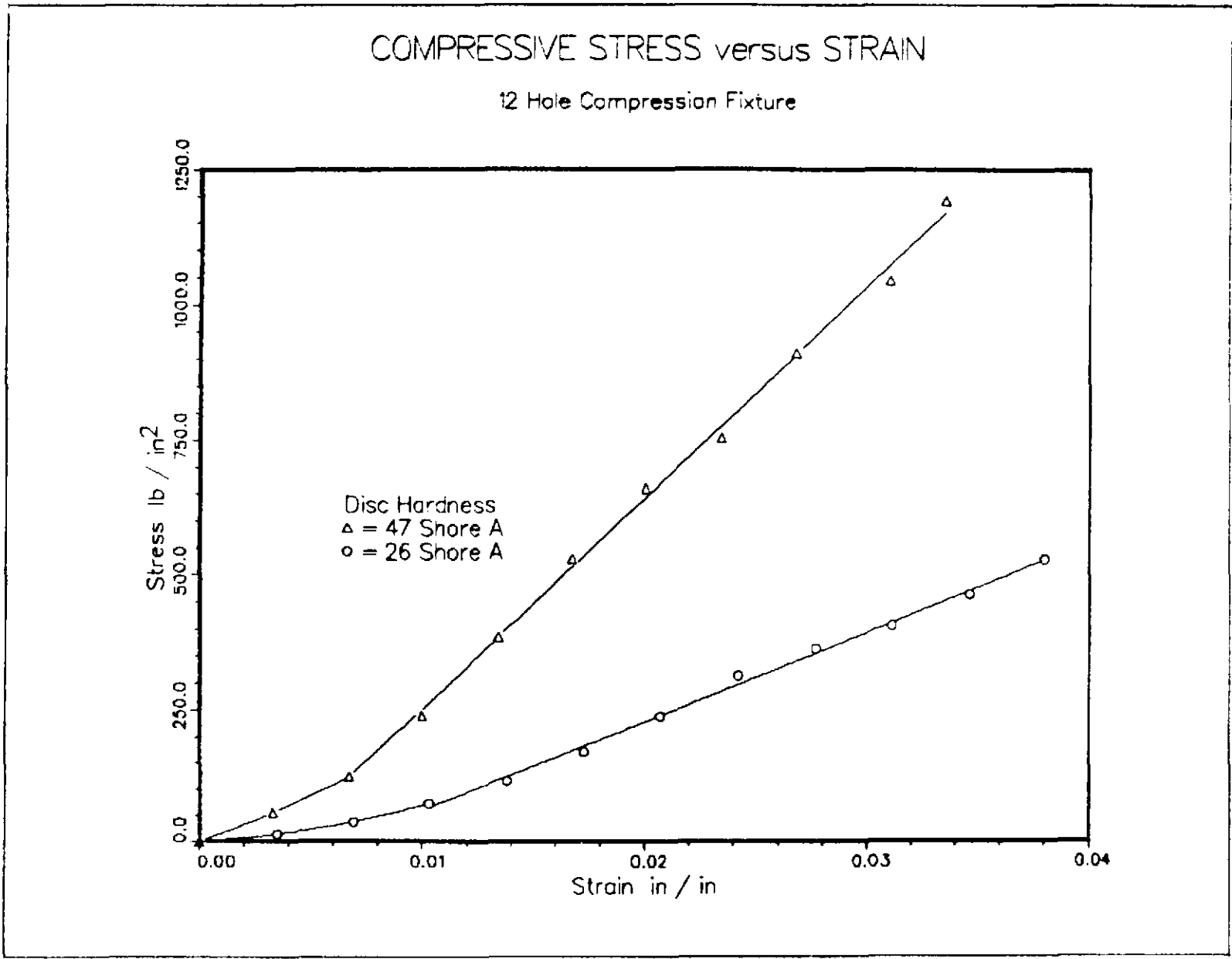


Figure 30. Stress vs. Strain - 12 Hole Fixture.

COMPRESSIVE STRESS versus STRAIN

ZERO Hole Compression Fixture

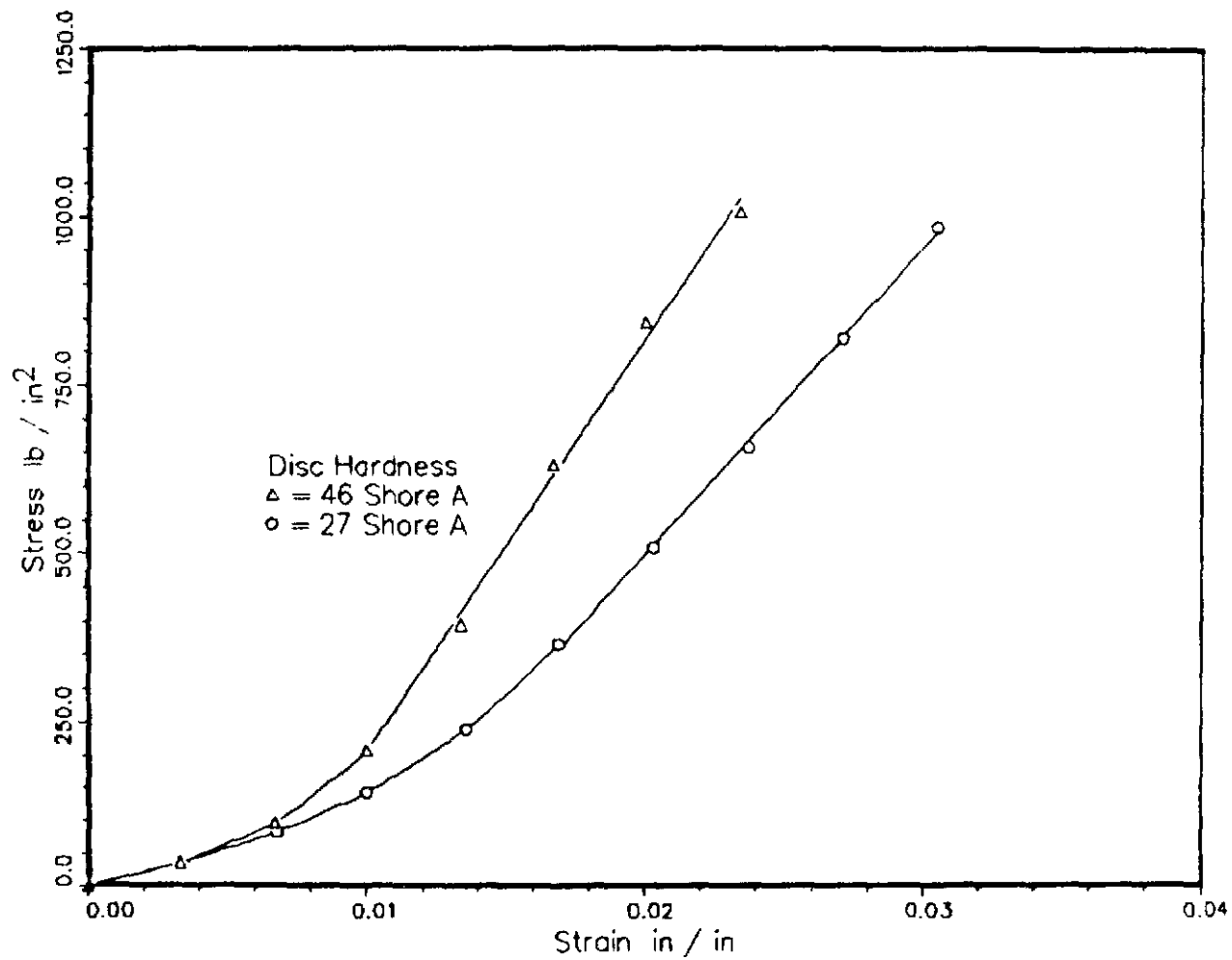


Figure 31. Stress vs. Strain - Zero Hole Fixture.

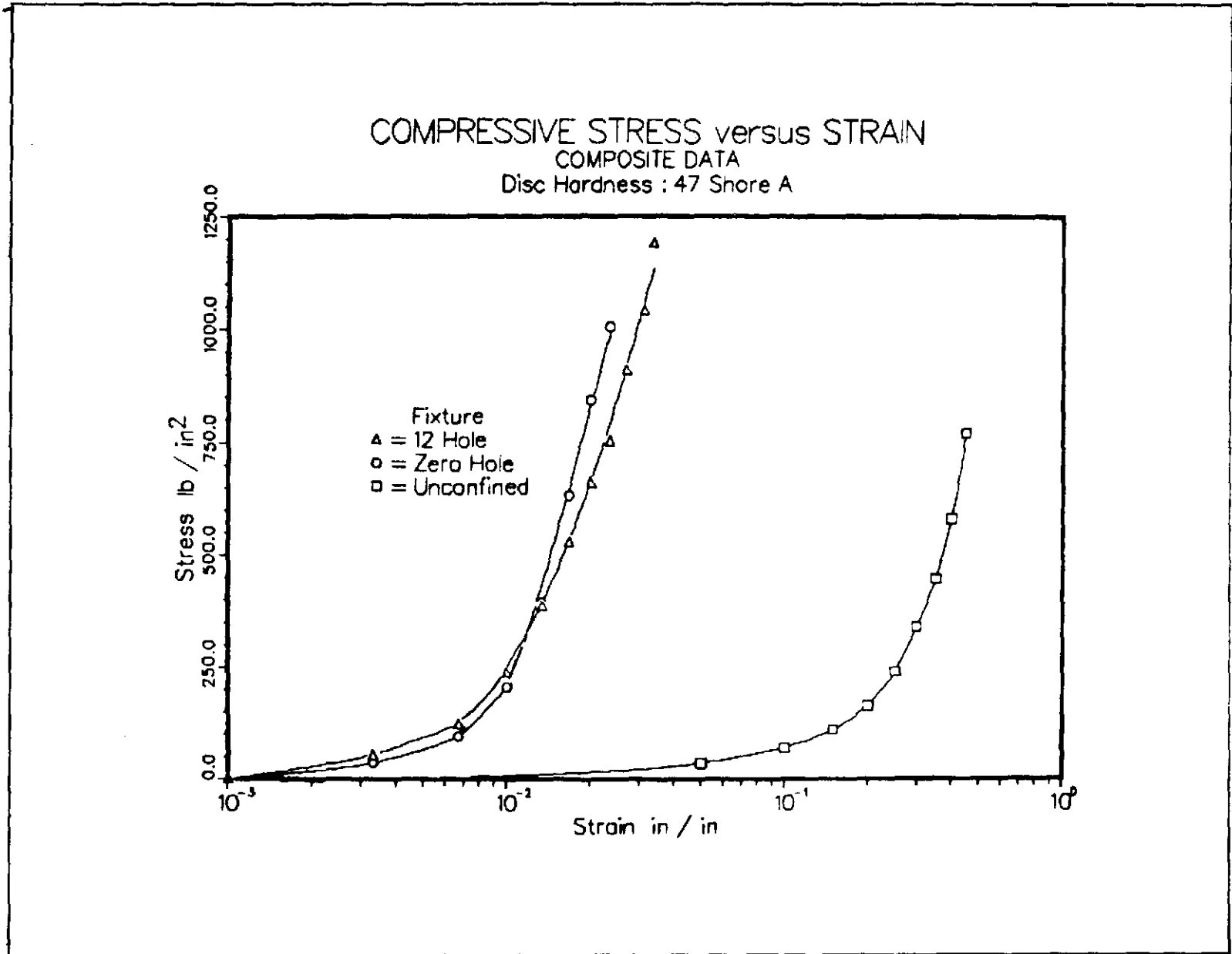


Figure 32. Stress vs. Strain - Composite Data.

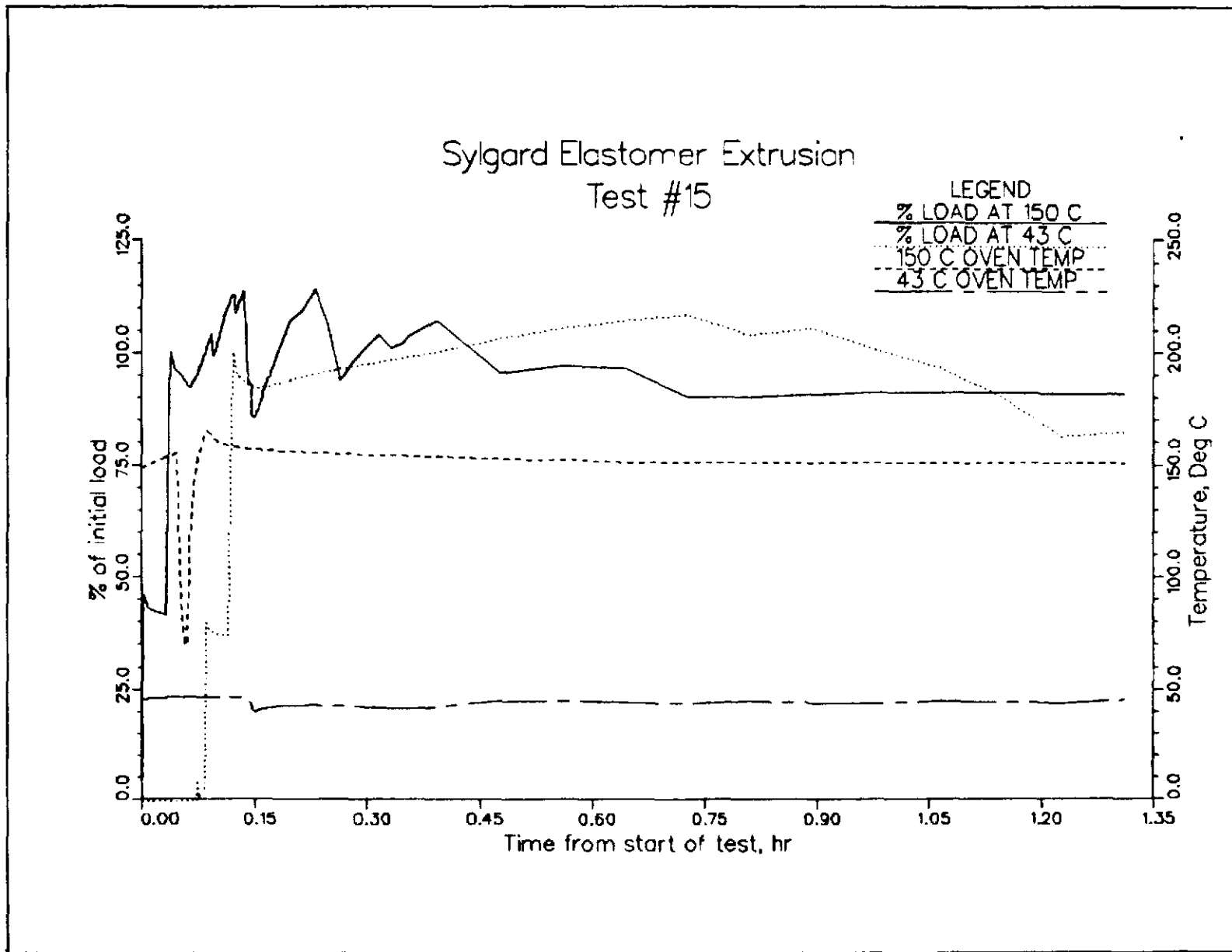


Figure 33. Elastomer Response - Steady State Temperatures.

specimen. This additional stress was sufficient to exceed the threshold resulting in evidences of spontaneous extrusion.

In Figure 34 we present the long term behavior of the sample maintained at 150°C. Plotted is compressive force as a function of elapsed time in days. Resolution is such that the "sawtooth" behavior noted in Figure 33 is lost. In this Figure, the solid curves and open triangles depict the observed stress decay. The dashed extrapolation is an extension of the straight line portion of the curve to zero time. We attribute the straight line decrease in compressive force to sample reduction resulting from material flow through the relief orifices. The initial decrease may be attributable to stress relaxation in the material with no reduction in material weight. This relaxation is assumed to occur after the initial extrusion observed in Figure 33.

Using the straight line portion of the curve we deduced a stress decay constant of 0.02/day. Using this stress decay constant, we estimate that the strain induced stress will decay to background levels (assumed to be 2.5% of the initial loading or 50 pounds) in approximately 150 days. In fact, we observed essentially background stress in the test specimen in 135 days--in good agreement with the estimated result.

In Figure 35 the long-term behavior of the specimen aged at 43°C is presented. As may be expected, the shape of the stress decay curve is similar to that for the 150°C case. We note an initial, rapid stress decay followed by a slowly decaying ("material flow") component. The initial stress relaxation component tracks well with that appearing in Figure 34. For this example, we estimate that the compressive force will decay to a background value in approximately 610 days (stress decay constant is .005 per day). This experiment was terminated after 187 days, and at that time, the residual compressive force was approximately 500 pounds. We estimate, on the basis of the calculated stress decay constant, an end force on the order of 410 pounds. Again, we note the experimental decay constant yields reasonable results.

In Figure 36 we present the aging data for the 3-hole/3-wire configuration. This configuration was aged under ambient (room temperature) conditions. The data obtained are consistent (see Figure 37) with the other long-term aging data--a two component force versus time history. Analysis of the data yields a decay constant (.0037 per day) that predicts a decay time of 825 days for the compressive force. The residual compressive force at the time of the test termination was estimated to be 660 pounds on the basis of the experimental decay constant. The measured compressive force at that time was 620 pounds. Of particular interest was the sensitivity of the

MATERIAL LOAD versus TEMPERATURE

Aging Temperature 150 Deg C

Disc Hardness : 42 Shore A

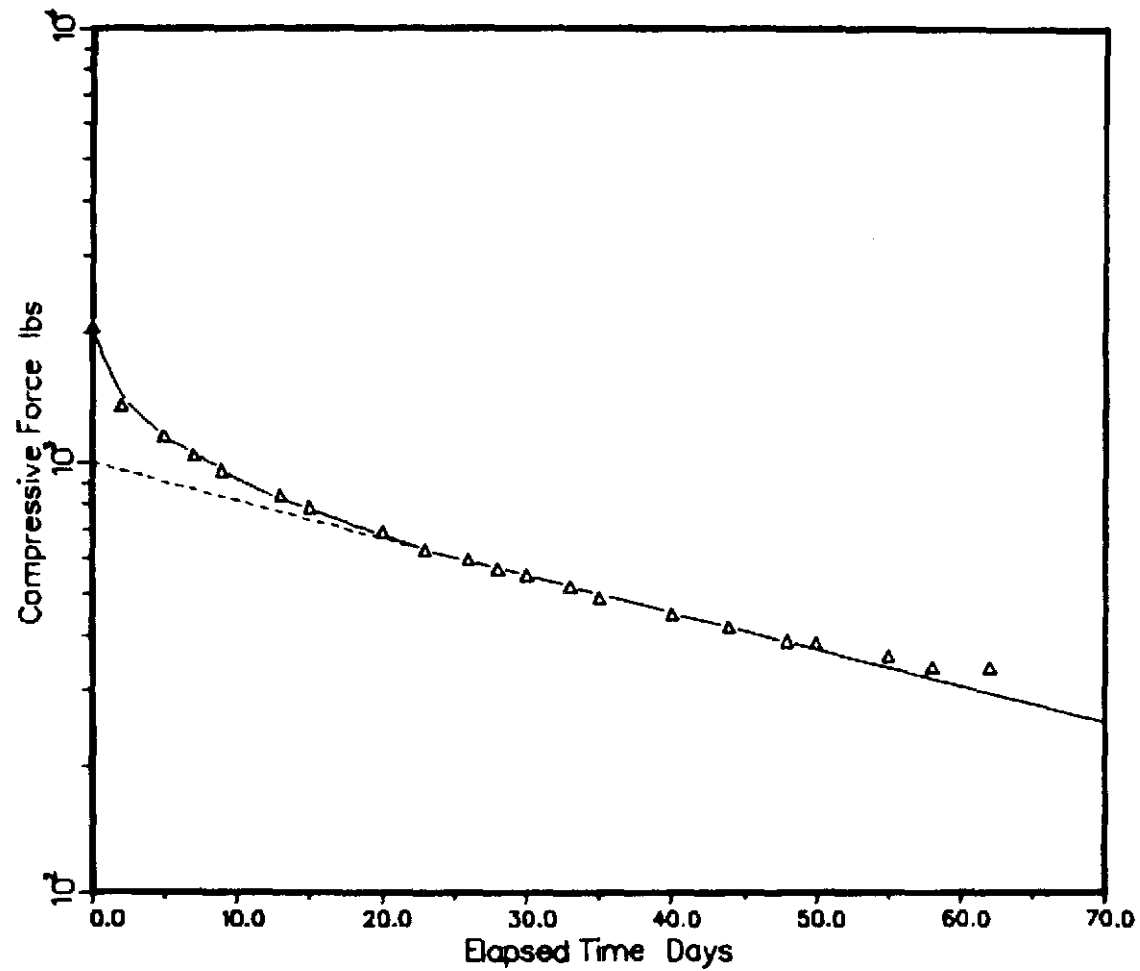


Figure 34. Elastomer Response - 150°C Aging Temperature.

MATERIAL LOAD versus TEMPERATURE

Aging Temperature 43 Deg C

Disc Hardness : 42 Shore A

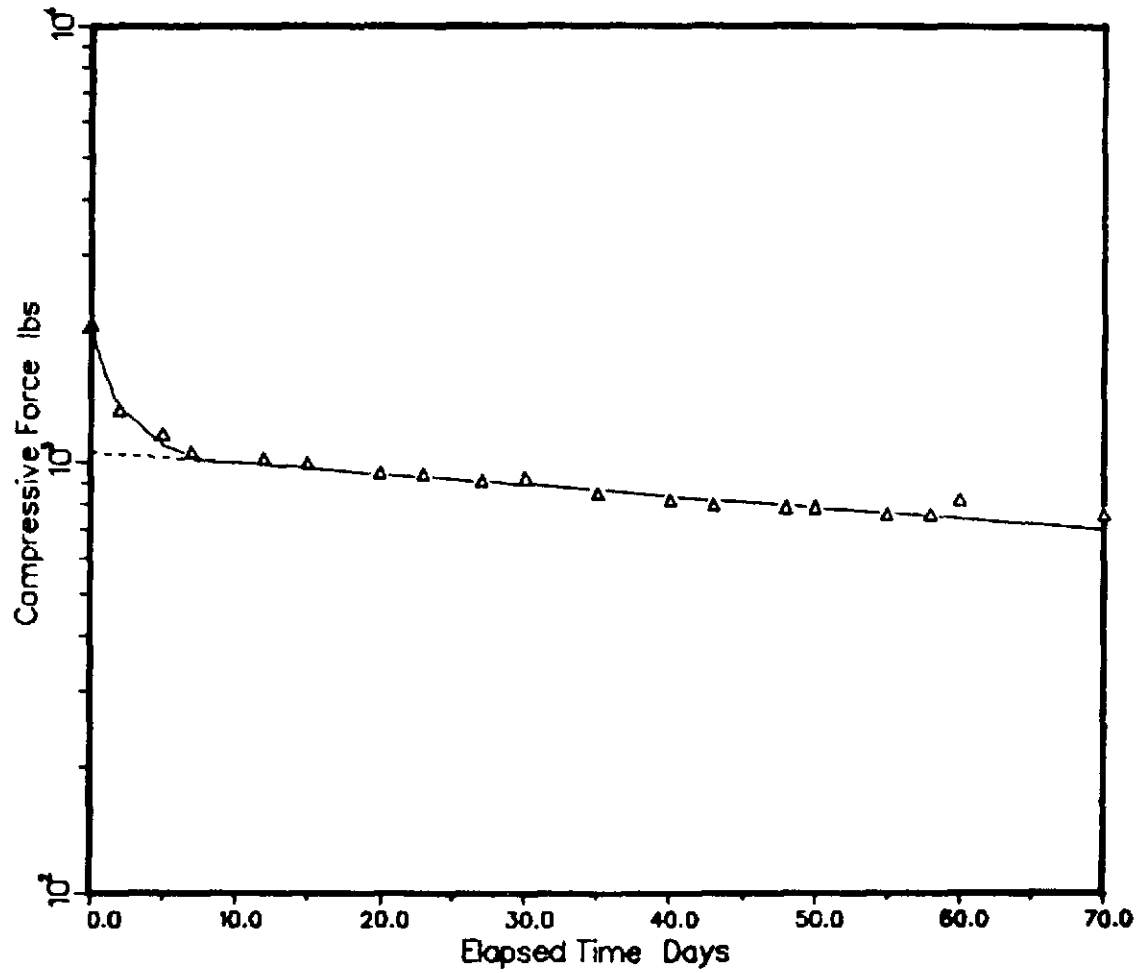
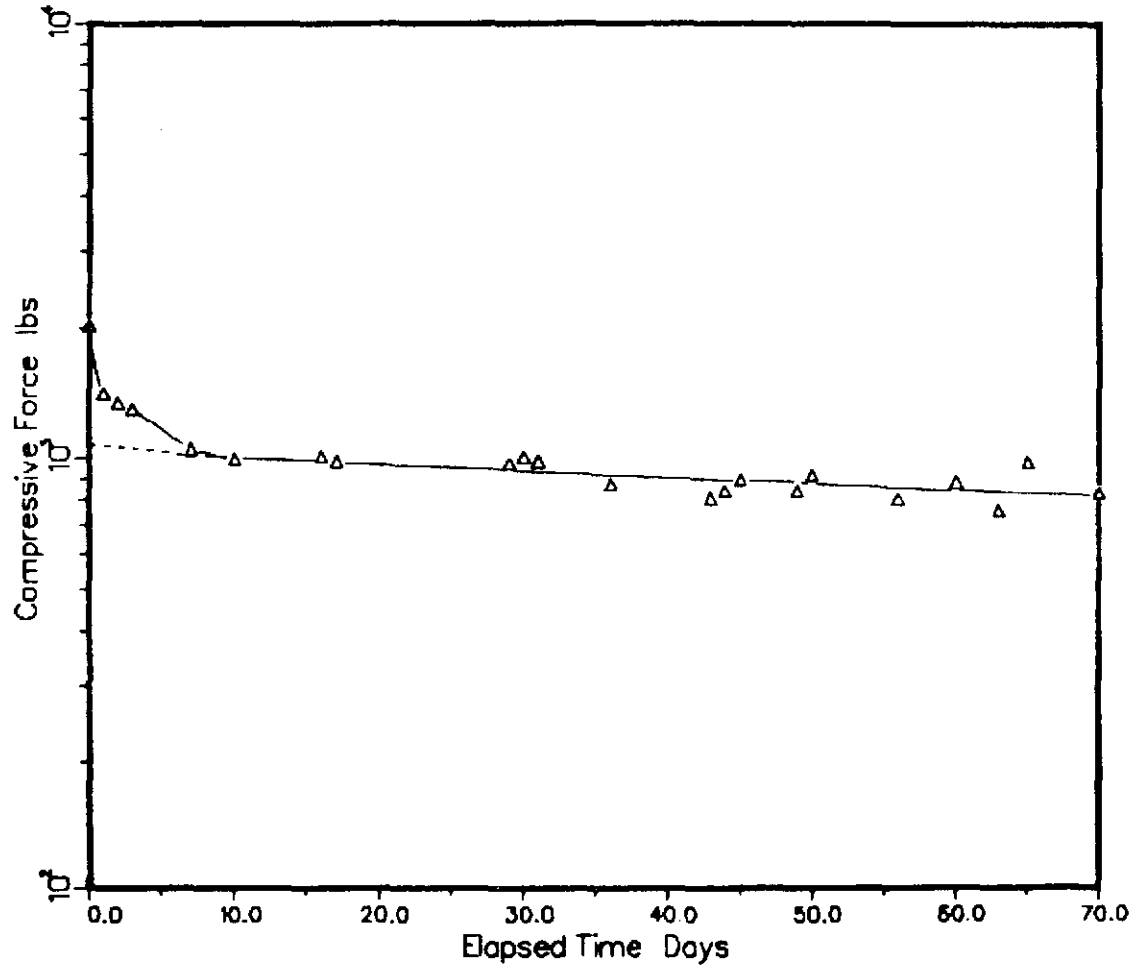


Figure 35. Elastomer Response - 43°C Aging Temperature.

MATERIAL LOAD versus TEMPERATURE

Aging Temperature - Ambient

Disc Hardness : 29 Shore A



- 50 -

Figure 36. Elastomer Response - Ambient Aging Temperature.

MATERIAL LOAD versus AGING TIME

COMPOSITE AGING DATA

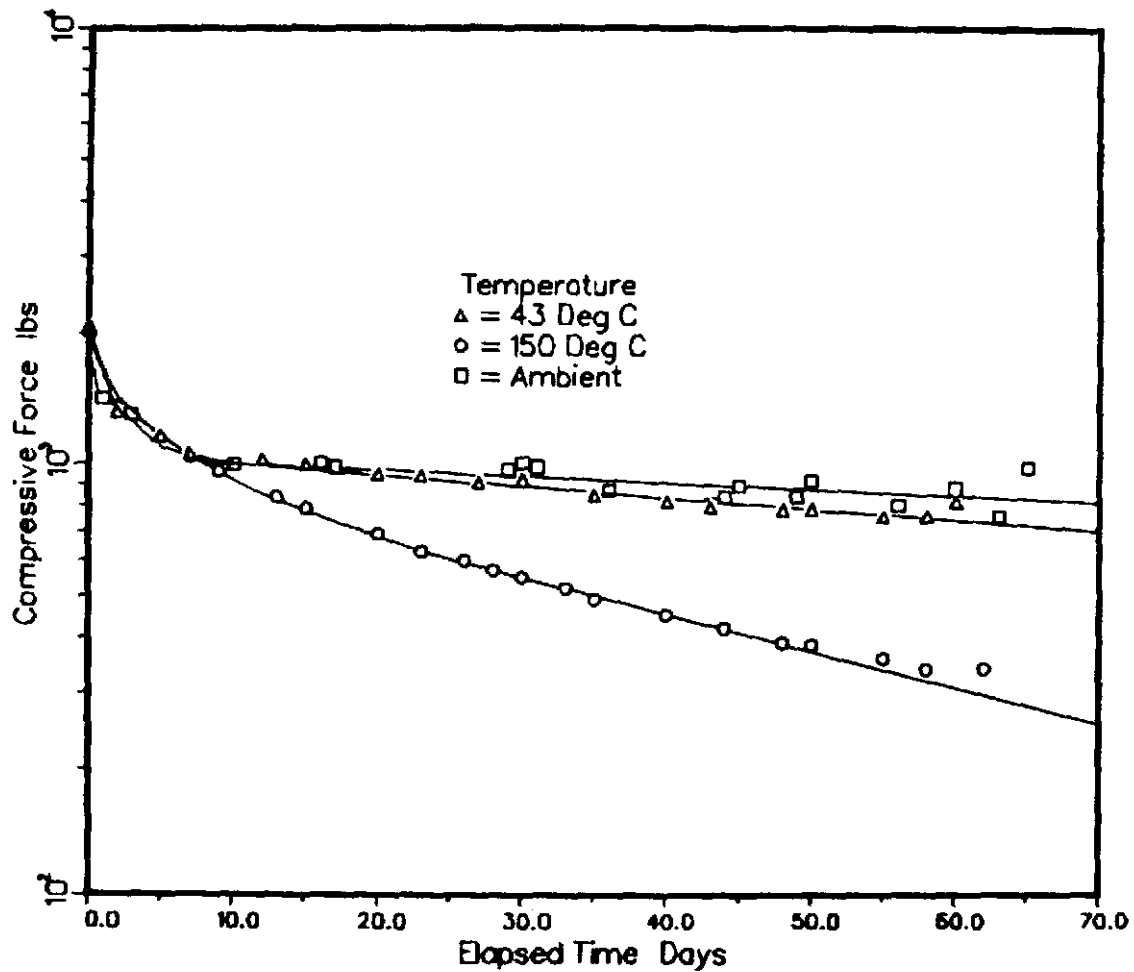


Figure 37. Elastomer Response - Composite Data.

applied compressive force to variations in the environment temperature as evidenced by the scatter of the data about the straight line decay approximation.

Following the steady state aging sequence, the three fixtures were subjected to a typical LOCA temperature profile simulated by means of a forced air oven. During this phase we again monitored compressive force, sample temperature, and oven temperature as a function of time. Accompanying each LOCA exposure was a control (loaded, to 2000 lbf, but unaged) sample. In the following figures we present representative data obtained during the LOCA simulations. In Figure 38 the stress-time history for the sample aged at 43°C in the 12-hole compressive fixture is presented. The 43°C data are represented by the triangles and the unaged data by the open circles. Superimposed on the stress-time profiles is the LOCA temperature-time profile. This stress-time profile for the aged disc has several interesting features. First, it should be pointed out that a residual compressive force was present at the test onset; the magnitude of this force was on the order of 500 pounds. Second, we note that the compressive force tracked with the temperature profile remarkably well. Peak temperature induced compressive force was on the order of 2500 pounds. At the termination of this experiment the compressive force approached zero as the temperature approached ambient. Note that the compressive force spanned the limits between 2500 pounds and zero. We also note that the stress-time history of the unaged disc tracks rather well with the aged disc data.

Data for the 3-hole/3-wire fixture are shown in Figure 39. In addition to the aged sample, we also included the results obtained with the unaged, control specimen. Initial compressive force on the aged sample (triangles) was approximately 2000 pounds (lbf), which decayed to a residual value of about 700 pounds (lbf) upon termination of the aging test and initial compressive force on the unaged sample (circles) was 2100 pounds (lbf). We observed that the unaged sample tracked the aged sample force-time history throughout the LOCA temperature profile. These observed force versus time plots were, however, on the order of two or three less than those observed during the "12-hole" exposure. This difference may be attributed to the difference in relief path configuration and/or difference in material hardness. Hardness of the discs used in the 12-hole configuration was about 47 Shore A and approximately 26 Shore A in the 3-hole/3-wire test. Since the total relief area available in the 12-hole fixture is a factor of four greater than that in the 3-hole configuration, we must conclude that material hardness was the dominant cause for the observed difference in material response. We note, also, during the 3-hole/3-wire exposure in the LOCA high temperature regime that a high compressive force could not be sustained.

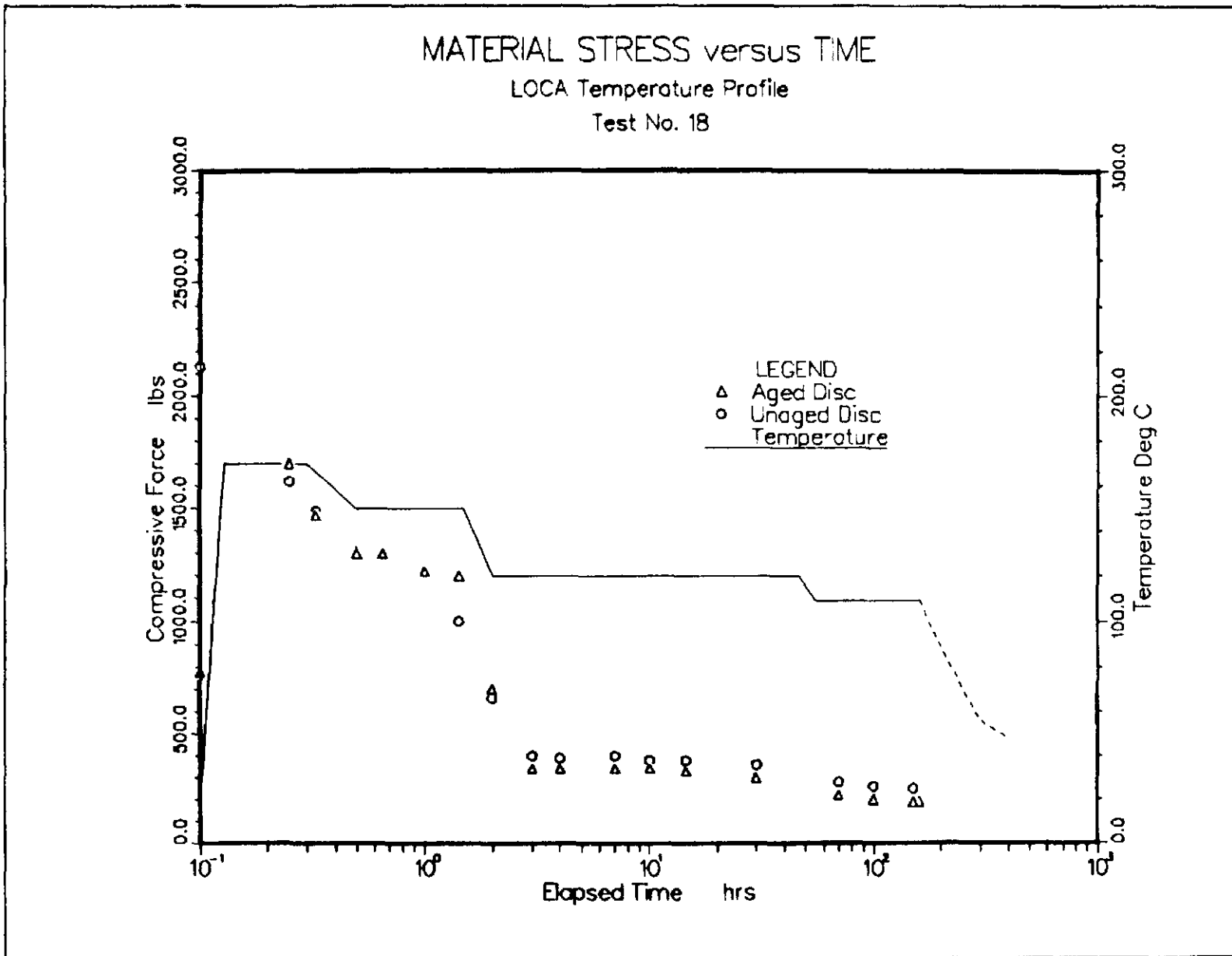


Figure 39. Elastomer Response - LOCA Temperature Profile.
Elastomer preaged at ambient temperature.

Finally, at the termination of the LOCA temperature profile both aged and unaged sample compressive forces decayed to background values. Evidence of damage to the insulated conductors is depicted in Figure 40. We note the similarity of damage between this test (Figure 40) and that observed during the D. G. O'Brien penetration test (Figure 2).

At the completion of the temperature exposures, all fixtures were disassembled and the discs weighed for total weight loss during the steady state and transient temperature exposures.

C. Specimen Weight Loss

We will demonstrate that the observed compressive force, as a function of time and temperature can be related to material loss which occurred during the steady state and transient temperature environments. To demonstrate this, we will analyze the data obtained with the three test specimens and compare results of these analyses to material loss based on pre and post exposure weights.

Specimens analyzed are listed in Table III.

TABLE III

Weight Loss Analysis

- A. Test 15 -- 12-Hole Fixture
150°C Steady State
LOCA Environment
- B. Test 15 -- 12-Hole Fixture
43°C Steady State
LOCA Environment
- C. Test 21 -- 12-hole Fixture
LOCA Environment

In Table III item A is analyzed first. Pertinent parameters for the specimen to be analyzed appear below:

Specimen height	(h_0)	=	1.26 cm
Specimen cross sectional area	(A)	=	7.61 cm ²
Initial weight	(M_0)	=	13.514gm
Final weight	(M_f)	=	12.041gm
Initial compressive force	(F_0)	=	2036 lb.
Final compressive force	(F_f)	=	0.0 lb.
Decay time to background	(t)	=	147d
Estimated decay coefficient	(λ)	=	0.020/d
Disc hardness	(H)	=	42 Shore A
Material density	(ρ)	=	1.38 gm/cm ³

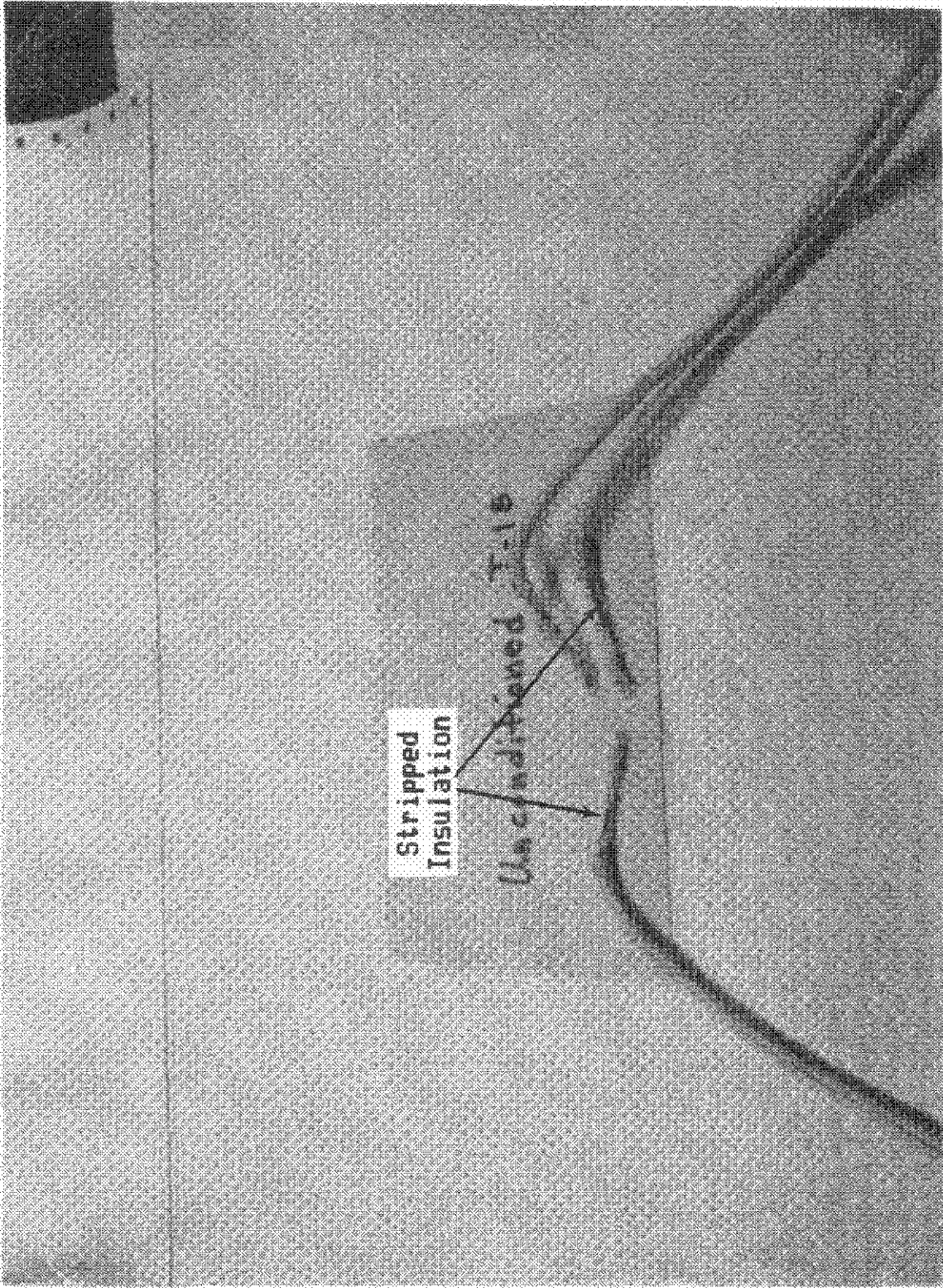


Figure 40. Effects of Extrusion on Cable Insulation-Disc Test.

The observed compressive force is the result of torque and temperature induced sample stress. Compressive force mitigation is then the result of material extrusion, stress relaxation, and material flow. Material response during the first hour or two into the steady state exposure was large. In Figure 33 this active response was plotted as percent of initial load as a function of elapsed time. The extrusion, characterized by the "sawtooth" variation in percentage load, is attributed to increased material loading resulting from temperature induced stress in the sample, followed by material loss and subsequent load reduction. The temperature increase is the result of heat flow from the warm environment, into the disc. Following the initial disturbance characterized by copious material flow, the specimen compressive load then decayed according to the stress-time profile given in Figure 34--a stress relaxation phase followed by stress decay resulting from material flow. From Figure 34 we note that the zero time compressive force extrapolates to a value of approximately 1000 lbs. force. Reference to the stress-strain data, Figure 30, and by extrapolating the stress-strain curves for the 12-hole fixture and 45 Shore A hardness material to zero stress in the elastic region, this 1000 lbs. stress is the result of a net strain of 0.0244 $\Delta L/L$. The strain equivalent resulting from temperature induced material expansion is:

$$\epsilon_T = \frac{h - h_0}{h_0} = \alpha T \quad \text{Where:}$$

α = temperature coefficient of expansion for the elastomer
 = $8 \times 10^{-4} \Delta h/h_0 / ^\circ\text{C}$, and

T = material temperature rise above ambient.

For the 150°C aging temperature (T = 125° above ambient), we estimate the temperature induced strain equivalent to be:

$$\epsilon_T = 8 \times 10^{-4} \times 125 = 0.1\Delta h/h_0$$

Total strain is the sum of that due to the disc compression and temperature induced dimensional change.

ϵ = torque induced strain + temperature induced strain equivalent

$$= 0.0244 + 0.10 \times \frac{\Delta h}{h} = 0.1244 \frac{\Delta h}{h_0}$$

For this specimen, the compressive force decayed to a background value during the steady state temperature sequence. Force

decay was the result of extrusion, flow, and stress relaxation. The first two processes resulted in specimen weight reduction whereas the third resulted in compressive force reduction without material flow.

For this sample total weight loss is estimated to be:

$$\begin{aligned} \Delta m &= \epsilon h_0 A \rho \\ &= .1244 \times 1.26 \times 7.61 \times 1.38 \\ &= 1.65 \text{ gm} \end{aligned}$$

The observed weight loss was:

$$\Delta M = M_0 - M_f = 13.514 - 12.041 = 1.47 \text{ gm}$$

Since the specimen remained confined in the test fixture until completion of the LOCA transient, it is necessary to estimate the magnitude of material loss during the temperature transient. Response of the elastomer during the LOCA excursion is presented in Figure 41 where elastomer load and percent of initial load are plotted as a function of elapsed time into the LOCA. From the plot we note that peak induced compressive force is on the order of 13% of the initial load or about 250 pounds force. We note, however, in Figure 33 that material extrusion is unlikely to occur, for this configuration, with compressive forces below 2000 pounds force. The oscillations in compressive load are completely dumped-out for loads on the order of 1500 pounds. In addition because of the short duration of this exposure, material loss due to flow is probably minimal. Thus total material loss occurred during the steady state exposure and we note that the observed and measured material losses are in reasonable agreement.

Next, analysis of the specimen aged at 43°C is considered. It should be noted at this point that the aging temperature chosen is as a reasonable approximation of the reactor plant ambient temperature. First, the pertinent specimen parameters are listed.

Specimen height	(h_0)	= 1.25 cm
Specimen cross sectional area	(A)	= 7.61 cm ²
Initial weight	(M_0)	= 13.419 gm
Final weight	(M_f)	= 12.557 gm
Initial compressive force	(F_0)	= 2061 lb.
Final compressive force*	(F_f)	= 556 lb.
Decay time*	(t)	= 187d
Estimated decay coefficient	(λ)	= .005/d
Disc hardness	(H)	= 42 Shore A

*At conclusion of the 43°C exposure.

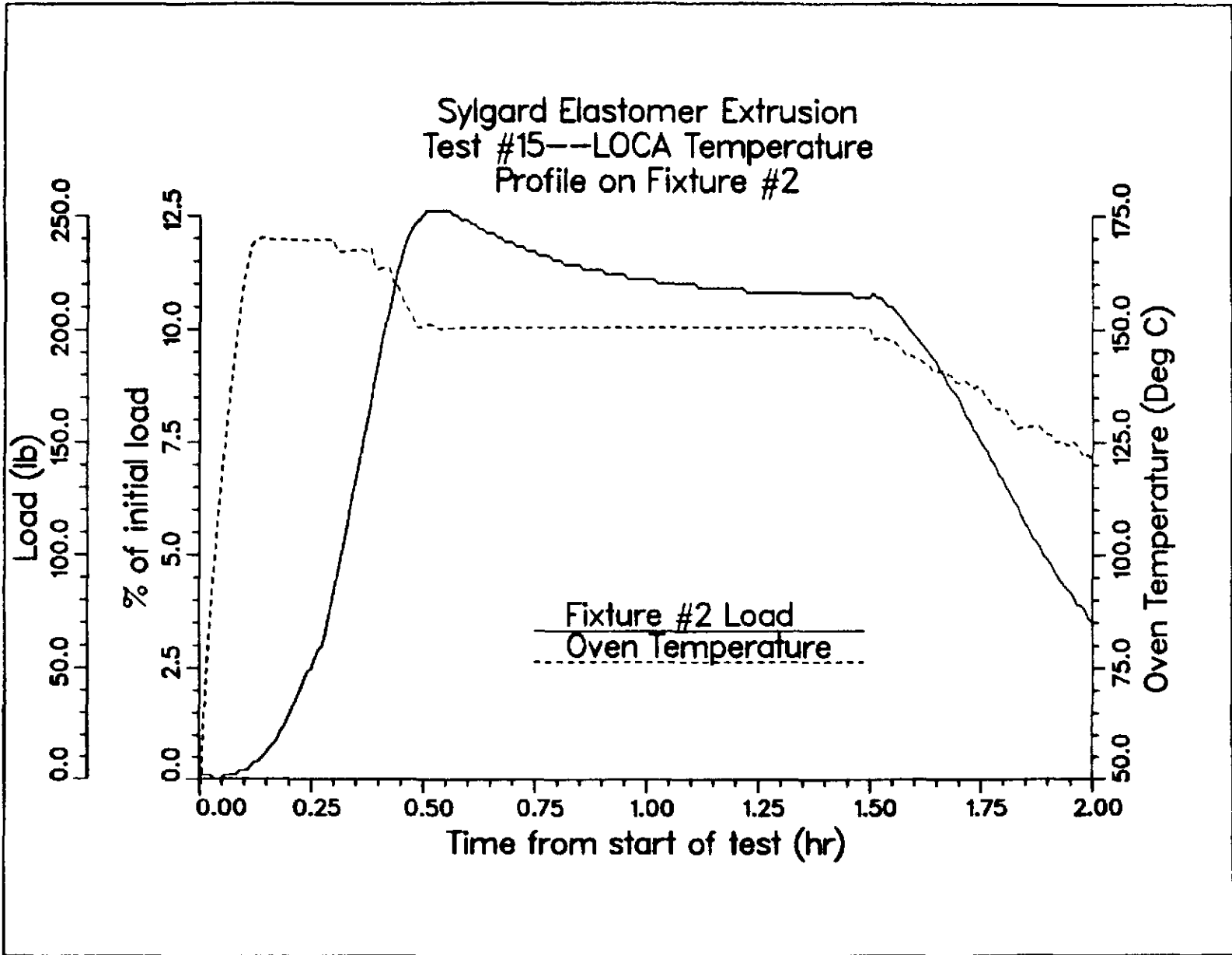


Figure 41. Elastomer Response - LOCA Temperature Profile.

Data analysis is analogous to that used for the 150°C exposure. We note, Figure 33, that the response of this specimen, at the onset of the steady state exposure, was much less than that observed during the 150°C exposure. None the less, evidence of extrusion was present during the early stages of the exposure. We estimate material loss during the steady state exposure as before (i.e., material loss is proportional to the initial and temperature induced strain equivalents). In this instance, however, a residual compressive force is present at the conclusion of the steady state exposure.

Based on the long-term stress decay, Figure 35, of this specimen, change in disc strain as a result of material flow may be estimated on the basis of initial (1050 lbs.) and final (480 lbs.) disc compressive forces and the stress-strain curve (Figure 30) for the 12-hole fixture. Converting the initial and final compressive forces to stresses we estimate the resulting strain equivalent change due to material flow to be 0.0103 $\Delta L/L$

Change in strain equivalent related to heat conduction into the sample from the 43°C environment yields:

$$\begin{aligned}\epsilon_T &= 8 \times 10^{-4} \times (43^\circ\text{C} - 20^\circ\text{C}) \\ &= 0.0184 \Delta L/L,\end{aligned}$$

and as before:

ϵ = torque induced strain + temperature induced strain equivalent.

$$= 0.0103 \frac{\Delta L}{L} + 0.0184 \frac{\Delta L}{L} = 0.0287 \frac{\Delta L}{L} = 0.0287 \frac{\Delta h}{h_0}.$$

$$\begin{aligned}\Delta M &= \epsilon h_0 A \rho \\ &= 0.0287 \times 1.25 \times 7.61 \times 1.38 = 0.377 \text{ gm.}\end{aligned}$$

The observed specimen weight loss is:

$$\Delta M = 13.419 - 12.557 = 0.862 \text{ gm.}$$

This result strongly suggests that additional material loss must have occurred during application of the LOCA temperature transient. From Figure 38 we note that onset of the temperature transient produced a dramatic elastomer response. Thermal expansion increased the compressive loading to approximately 2500 pounds force. We know, based on the data presented in Figure 33, that the onset of extrusion for this configuration occurs with compressive forces elevated above 2000 pounds force. In Figure 42 we have transformed the force versus time plot into one relating compressive force to material temperature. This

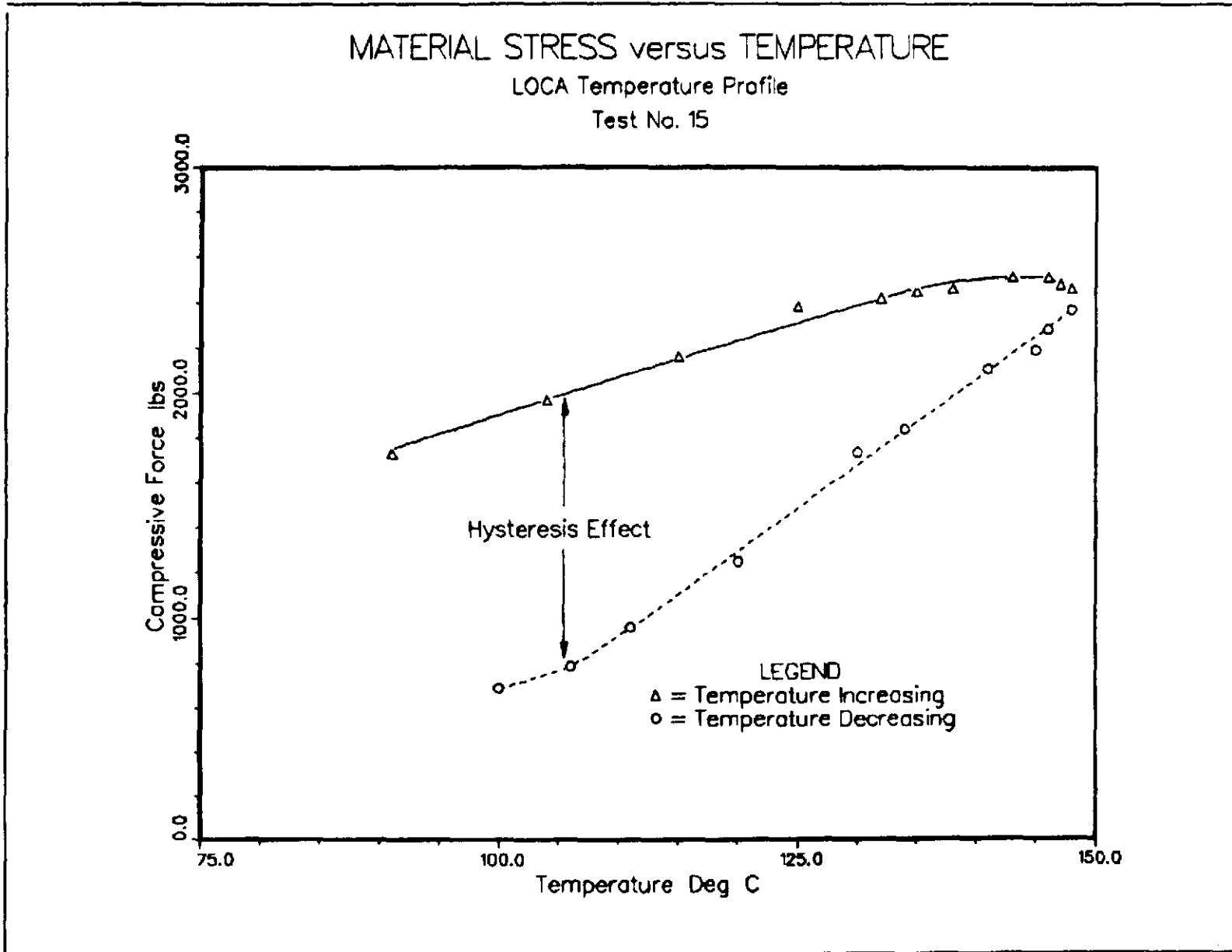


Figure 42. Elastomer Response - Force vs. Material Temperature.

transformed plot is another presentation of the buildup and decay of the compressive force transient presented in Figure 38. In Figure 42 the solid curve represents the loading as a function of increasing temperature and the dashed curve represents the compressive loading as the sample temperature begins to diminish. We note that a "hysteresis-like effect" is present in that the compressive force versus temperature profiles do not retrace on themselves. We attribute this hysteresis to material loss during the LOCA temperature excursion. By choosing a temperature at which the material exhibits elastic behavior with both increasing and decreasing temperature it becomes possible to estimate the material loss during the LOCA transient and evidenced by the observed hysteresis curve. If we assume the material is elastic at and below 110°C, we estimate (from Figure 42) a change in the compressive force of 1200 pounds. From Figure 30 we estimate that this compressive force differential is equivalent to a material strain of 0.031 $\Delta L/L$. By converting this strain equivalent into a volume change (loss) we estimate the material loss during the LOCA transient to be:

$$\Delta m = 0.41 \text{ gm}$$

This loss, coupled with that occurring during the steady state exposure, equates to an estimated total loss of

$$\Delta M = 0.377 + 0.41 = 0.79 \text{ gm estimated.}$$

This loss estimate agrees reasonably well with the measured value of:

$$\Delta M = 0.862 \text{ gm measured.}$$

Response of the unaged (12-hole fixture) control sample to the LOCA temperature transient is considered next. Parameters for this specimen are listed below.

Specimen height	(h_0)	=	1.25cm
Specimen cross sectional area	(A)	=	7.61cm ²
Initial weight	(M_0)	=	13.570gm
Final weight	(M_f)	=	12.669gm
Initial compressive force	(F_0)	=	2030 lb.
Disc hardness	(H)	=	46 Shore A

Exposure of the control sample to the LOCA transient resulted, as in the case of the last example, in heat flow into the sample and an increase in the sample compressive loading. As in the previous example, we transform this force-time plot into a force-temperature history. The results of this transformation are presented in Figure 43. The hysteresis effect is again present. We note that as the sample temperature increased the material response departed from elastic behavior in that the compressive loading remained constant with increasing sample temperature. Again, the solid curve indicates increasing

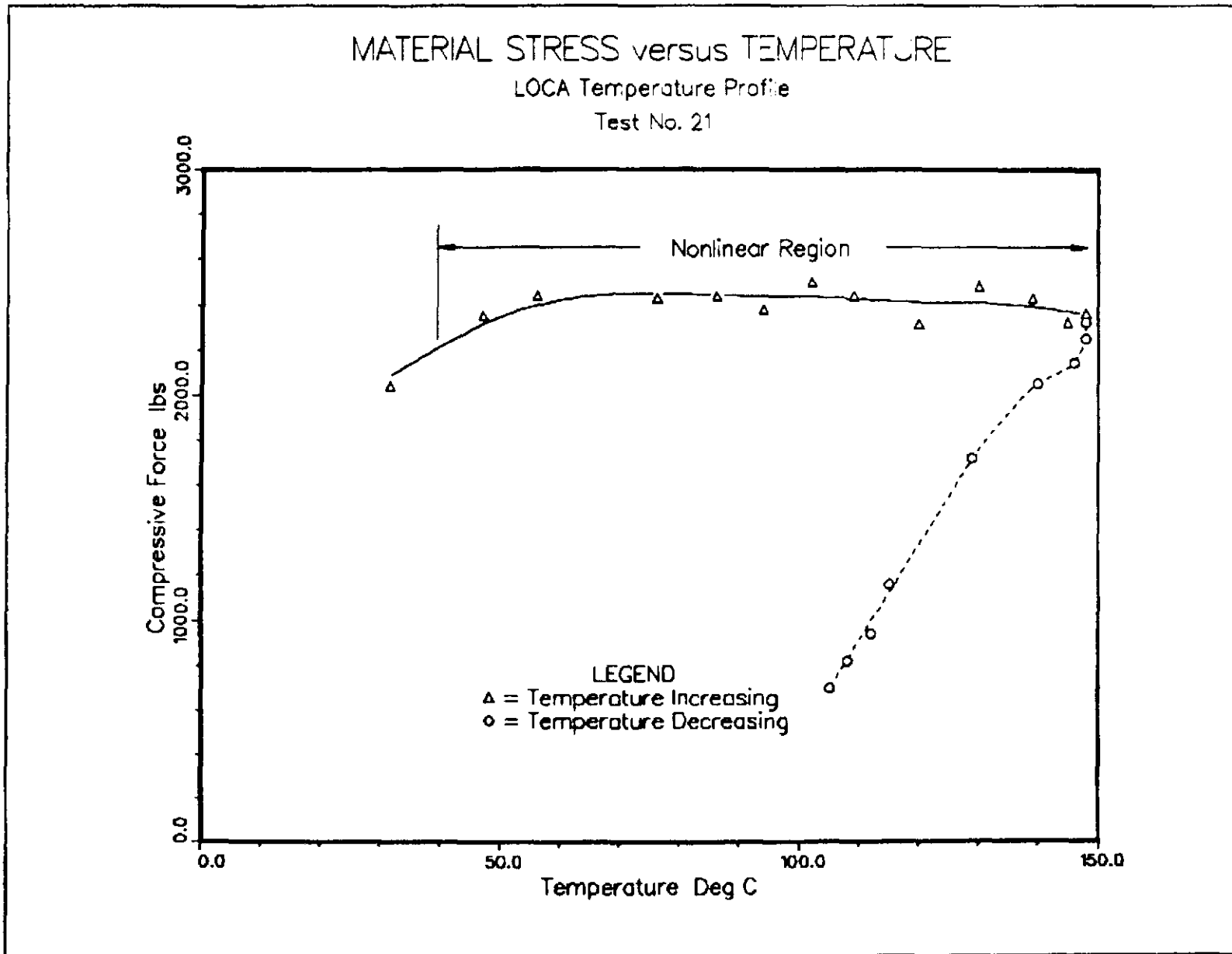


Figure 43. Elastomer Response - Force vs. Material Temperature.

temperature and the dashed curve indicates decreasing temperatures. We readily estimate specimen material loss on the basis of material response in the region of constant load as a function of increasing temperature. Assuming that material response is nonelastic in the temperature range of 50° to 140°C and that temperature induced volume compression is relieved through material extrusion, we estimate the material loss during the LOCA transient to be:

$$\epsilon_T = (8 \times 10^{-4} \Delta L/L^{\circ}C) \times (140 - 50)^{\circ}C$$

$$\epsilon_T = 0.072 \Delta L/L, \text{ with volume change of}$$

$$\Delta V = \epsilon_T h_0 A = 0.685 \text{ cm}^3.$$

and the material loss is calculated to be:

$$\Delta M = \rho \Delta V = 0.945 \text{ gm.}$$

Observed material loss was:

$$\Delta M = M_0 - M_f = 0.901 \text{ gm.}$$

The observed and estimated results are again in reasonable agreement. It is interesting to note that the total material loss in the last two examples was independent of the material aging history.

We next estimate material loss on the basis of flow during the steady state temperature exposure. Estimation of material loss in this phase will allow the estimation of a temperature dependent flow parameter for this particular material and set of compressive parameters. We analyze the data obtained at 150°C and 43°C with the 12-hole fixture. The flow parameter is based on observed compressive force decay as a function of elapsed time from the extrusion and stress relaxation transients. We assume that observed force decay is a result of material flow through the fixture orifices. Material flow is assumed to be directly related to the applied compressive forces as follows:

$$\frac{dv}{dt} = K P(t) \text{ where:}$$

$$\frac{dv}{dt} = \text{material flow rate (cm}^3/\text{sec)}$$

K = a parameter relating flow to applied force, and

P(t) = observed time dependent compressive force.

We know from observations that:

P(t) = P₀ exp(-λt) where:

P₀ = extrapolated initial compressive force as demonstrated in Figures 34 and 35, and

λ = force decay constant derived from the data given in Figures 34 and 35.

Based on the above assumptions, the reduction in specimen volume is:

$$v - v_0 = \left((KP_0)/\lambda \right) \times \left(1 - \exp(-\lambda t) \right).$$

Solving the above for K we obtain:

$$K = \lambda (v - v_0) / \left(P_0 (1 - \exp(-\lambda t)) \right)$$

Using the value of Δv (v - v₀)

derived from Figure 30 (i.e., 0.234 cm³)

the total material loss due to flow is:

$$\Delta M = (v - v_0) \times \rho = 0.323 \text{ gm.}$$

$$K = 9.8 \times 10^{-16} \text{ (cm}^3/\text{sec) / (dyne/cm}^2\text{)}.$$

Total material loss during the 150° steady state exposure was estimated to be 1.65 gm (measured = 1.47 gm) hence about 0.2 of the total estimated material loss was the result of flow.

Using these same methods it was estimated that the 43°C flow parameter is:

$$K = 1.46 \times 10^{-16} \text{ (cm}^3/\text{sec) / (dyne/cm}^2\text{)}$$

and material loss due to flow to be:

$$\Delta M = 0.147 \text{ gm.}$$

Material loss during the steady state exposure was estimated to be 0.396 gm. Fractional loss due to flow was then 0.371. We note that the flow parameters thus derived do not track with temperature for it is noted that the flow parameter increases by a factor of 6.7 as absolute temperature is increased by a factor of 1.3. Thus it is noted that flow will tend to become increasingly important with increasing temperature. In Figure 44 we present a flow parameter based on the two calculated values. Plotted is flow parameter as a function of material temperature.

V. CONCLUSIONS

We observed that response of the Sylgard-170 elastomer was rather insensitive to artificial (accelerated) thermal aging techniques. Attempts to characterize material degradation on the basis of a single parameter (Arrhenius technique) were not successful. Since observed degradation curves exhibited complex shape, it was assumed that the observed degradation was the result of multiple processes occurring during the aging phases. Similar behavior was observed by the material manufacturer (Dow-Corning). In light of this complex material response and small material degradation, it was concluded that the magnitude of the observed degradation did not allow estimation of either an activation energy or an accelerated material age. In terms of aging methodology, this implies the material is insensitive to accelerated aging environments. On the basis of these observations, it was decided that further material studies did not require aged samples; specifically, compressive studies did not require aged samples.

As a consequence, we completed our study on the elastomer with unaged samples. Initial compressive relief studies demonstrated that the elastomer response was sensitive to the applied compressive force and the degree of elastomer confinement. Initial stress-strain determinations of the material clearly demonstrated this. These determinations demonstrated that useful stress-strain data must be obtained under conditions similar to those used to obtain compressive relief data.

The compression relief data obtained here indicated that stress relief was complex. Depending on external conditions, relief was observed to consist of at least three mechanisms. In a single experiment we identified the three mechanisms occurring during the course of the investigation. Observed were the following:

1. Material extrusion - rapid loss of material accompanied by dramatic compressive force reduction, all occurring in times on the order of hours.

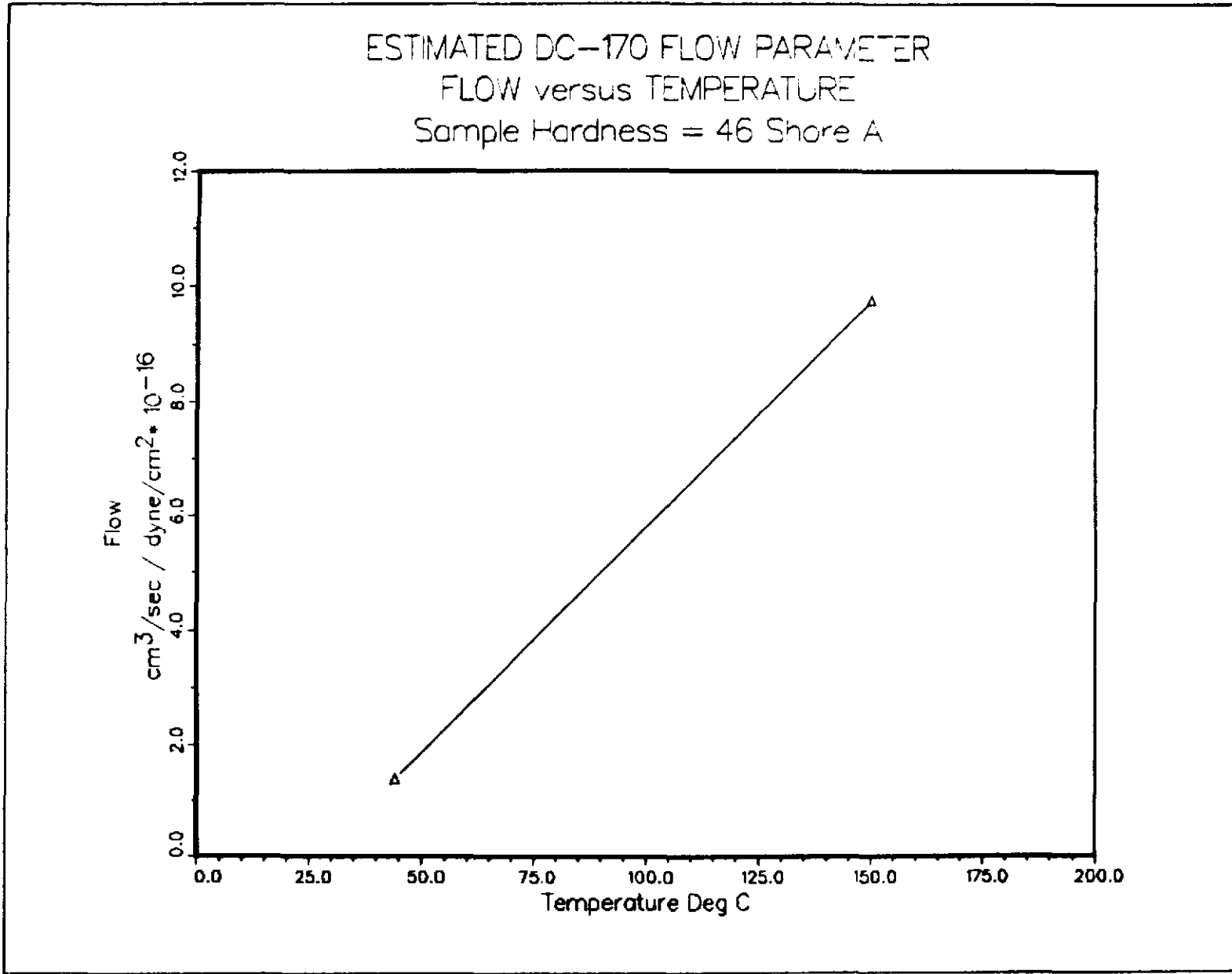


Figure 44. Flow Parameter vs. Temperature.

2. Stress relief - Apparent compressive force diminution at constant strain, occurring during time intervals on the order of days, and
3. Material flow - slow steady decrease in compressive force and material loss, over a time period on the order of hundred(s) of days.

The magnitudes of mechanisms 1 and 2 were estimated on the bases of compressive force - time/temperature data and verified by specimen weight loss.

We note that loss of material by extrusion was dependent on a compressive force threshold induced by applied strain and/or temperature induced strain equivalent. In Figure 45 a 3-hole/3-wire fixture is shown positioned in an aging oven just prior to aging. This assembly had been torqued to apply a 2000 pound compressive force to the elastomer material approximately 15 minutes prior to the photographic exposure. We note evidence of compressive force induced extrusion occurring around each of the three conductors. Evidence of temperature induced extrusion appear in Figure 46. This photograph was obtained at approximately 30 minutes into the aging sequence. At that time the oven temperature was 150°C and the elastomer temperature had attained 120°C. Temperature induced strain is indicated by the presence of copious quantities of extruded elastomer. The effect of elastomer extrusion on cable insulation is depicted in Figure 47. In the figure the elastomer has been sectioned to expose the conductors. We see that the elastomer flow has stripped insulation from the conductor and exposed the bare wire. Further evidence of extrusion damage to conductors is shown in Figure 48. Here the three conductors have been removed from the fixture for inspection. As may be noted, the damage is not uniform but is considerable for all three conductors. The damage observed during the test is similar to that observed during the D. G. O'Brien penetration test (Figures 1 and 2). This is not unexpected, however, since the test fixture/specimen was designed to simulate, to the extent practicable, the D. G. O'Brien penetration connector design. Use of the elastomer in other configurations and environments may not produce similar results, however, the designer should be aware that close confinement of the elastomer and that elevated temperature could produce damage in some components in proximity to the elastomer.

Although material extrusion sometimes competed, stress relief and material flow always occurred in all investigations. The data suggest that material flow is strongly temperature dependent with flow temperature correspondence being greater than one. Material flow was determined to be modest in comparison to extrusion, however, the data suggest that flow will continue until the compressive force diminishes to a background or near zero value.

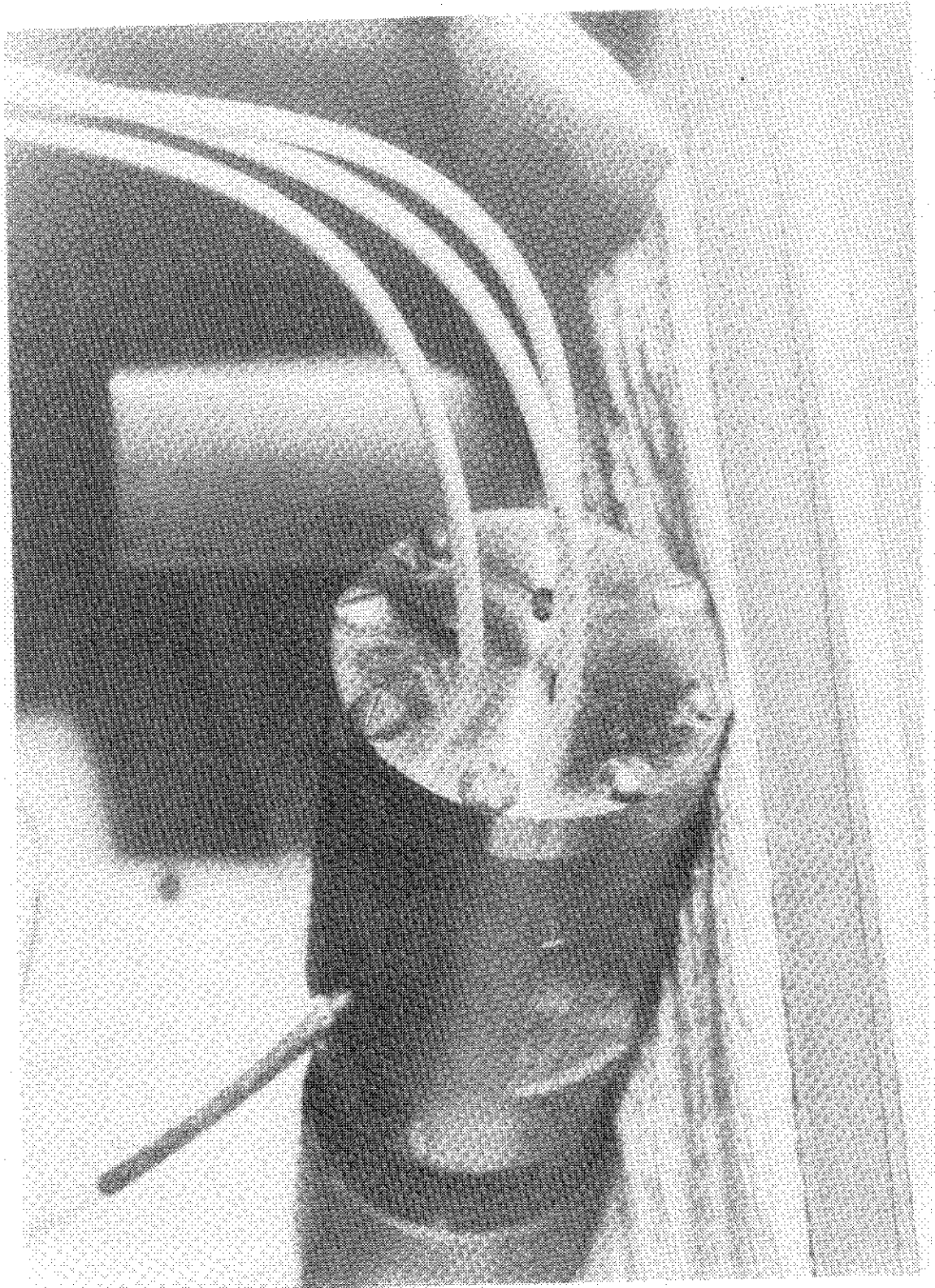


Figure 45. 3-Hole, 3-Wire Fixture in Aging Oven-Preexposure.

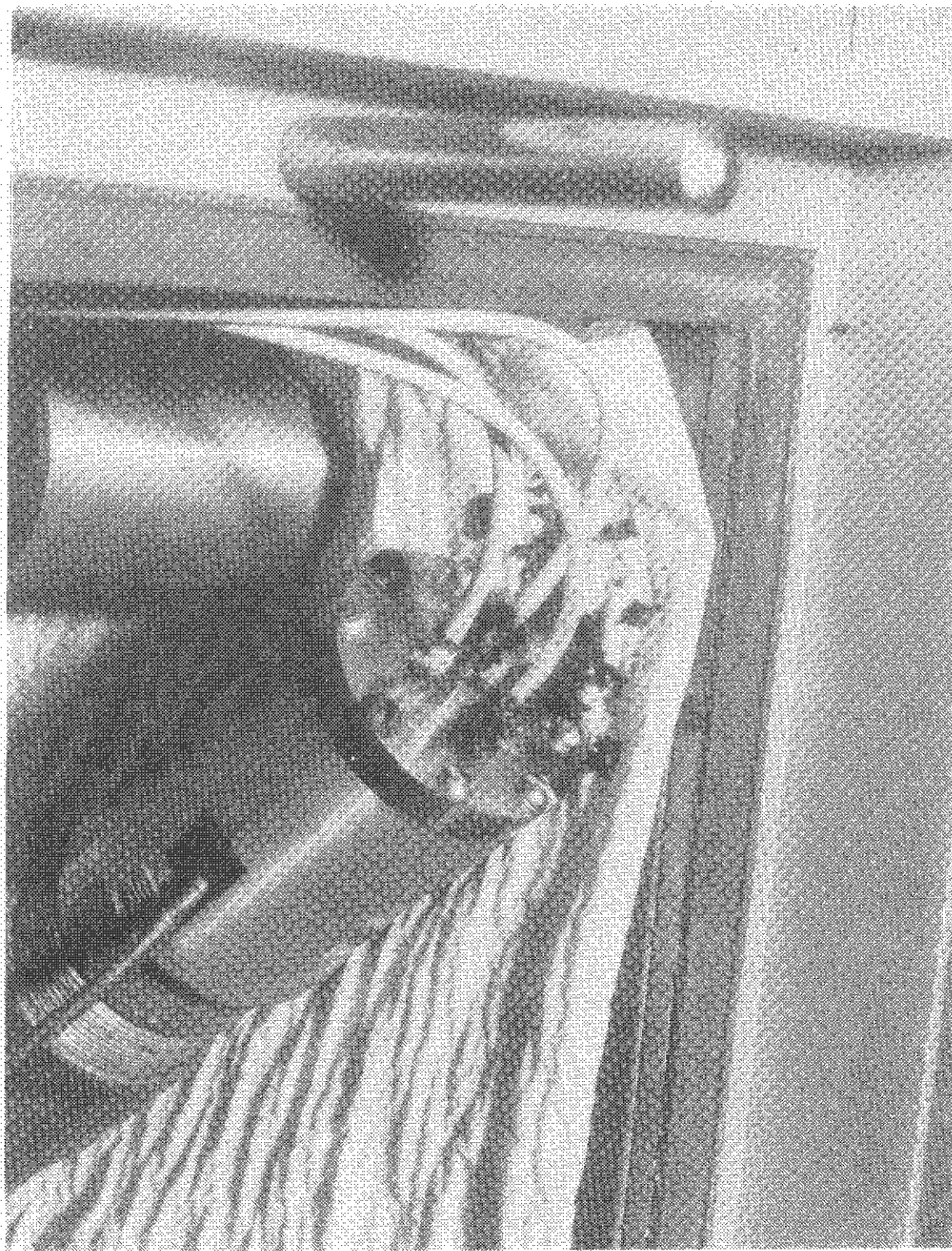


Figure 46. 3-Hole, 3-Wire Fixture in Aging Oyen-Midexposure.

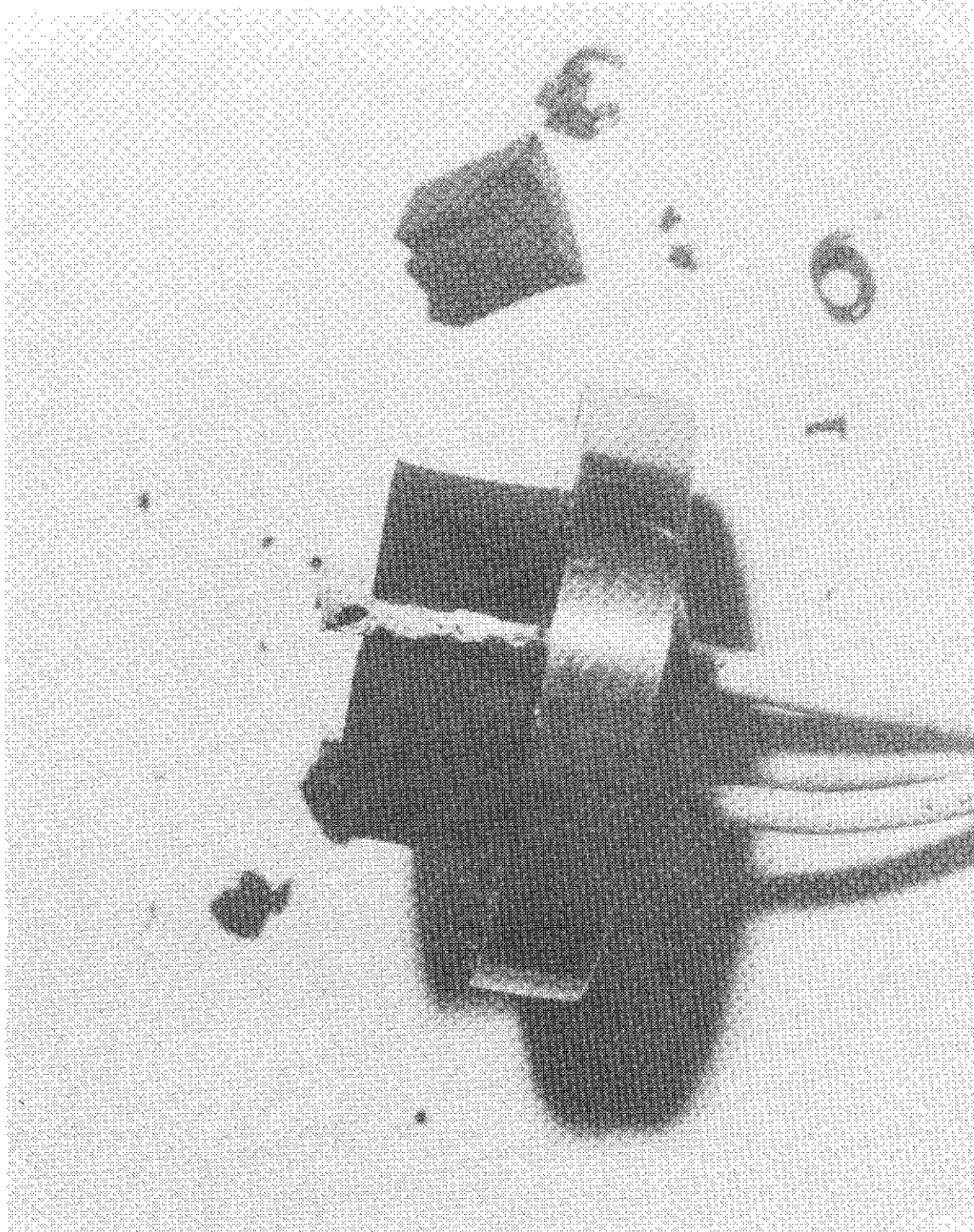


Figure 47. Sectioned Elastomer Showing Damaged Conductor.

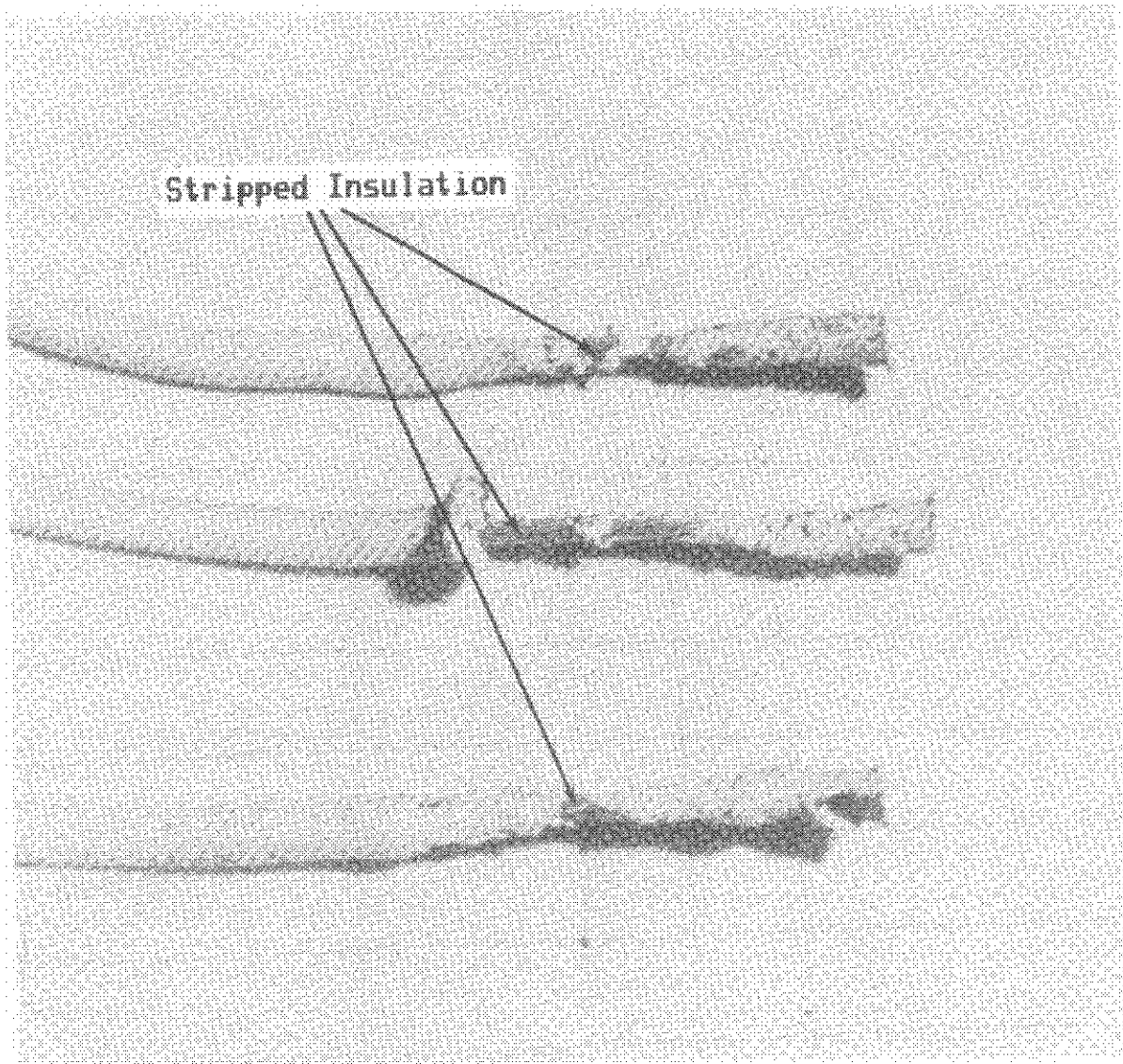


Figure 48. Damaged Conductor Specimens. (See Figure 2.)

The data obtained reveals the following points are applicable:

1. Behavior of the material under compression and/or at elevated temperatures is complex,
2. Depending on the application and temperature/compression, damage to interacting components may occur, and
3. Presence of a pressure relief path will probably eventually result in a reduction of the applied compressive force to background value.

In view of the above and the manufacturer's caution concerning close confinement applications, it is suggested that caution be used in applications of this material requiring the maintenance of a positive compressive force in the presence of any free surface. Since the force is likely to dissipate under these conditions, environmental seal applications may become vulnerable particularly in humid environments. Further, large compressive force requirements in non-steady state temperature environments such as a LOCA have been found to further degrade sealing capabilities. Again, depending on the configuration being considered, components may suffer damage, sealing integrity may be affected, and consequently circuit parameters may be altered.

REFERENCES

1. L. L. Bonzon, et al., "An Overview of Equipment Survivability Studies at Sandia National Laboratories," SAND83-0759C, Sandia National Laboratories, Presented at the International Meeting on Light-Water Reactor Severe Accident Evaluation Conference, Cambridge, MA, August 28 - September 1, 1983.
2. W. H. Buckalew, F. V. Thome, D. T. Furgal, "Equipment Qualification Research Tests of the Duke Power/D. G. O'Brien Type K Instrumentation Penetration Assembly," RS445/81/03, Sandia National Laboratories, March 1982. Limited Distribution: Obtain through W. Farmer, USNRC.
3. "Information About High Technology Materials: Sylgard® 170 A & B Silicone Elastomer," Dow Corning Corporation, 1980.
4. Excerpted portions of Dow Corning Corporation Report No. I-0340-13, attached to Appendix L of "Prototype Test Report Low Voltage and Instrumentation Electrical Penetrations," Report ER252, D. G. O'Brien Co., August 1977.
5. "Standard Test Methods for Rubber Properties In Compression," ASTM D575-83.

DISTRIBUTION:

U.S. Government Printing Office
Receiving Branch (Attn: NRC Stock)
8610 Cherry Lane
Laurel, MD 20707
375 copies for RV

Ansaldo Impianti
Centro Sperimentale del Boschetto
Corso F.M. Perrone, 118
16161 Genova
ITALY
Attn: C. Bozzolo

Ansaldo Impianti
Via Gabriele D'Annunzio, 113
16121 Genova
ITALY
Attn: S. Grifoni

ASEA-ATOM
Department KRD
Box 53
S-721 04
Vasteras
SWEDEN
Attn: A. Kjellberg

ASEA-ATOM
Department TQD
Box 53
S-721 04
Vasteras
SWEDEN
Attn: T. Granberg

ASEA KABEL AB
P.O. Box 42 108
S-126 12
Stockholm
SWEDEN
Attn: B. Dellby

Atomic Energy of Canada, Ltd.
Chalk River Nuclear Laboratories
Chalk River, Ontario KOJ 1J0
CANADA
Attn: G. F. Lynch

Atomic Energy of Canada, Ltd.
1600 Dorchester Boulevard West
Montreal, Quebec H3H 1P9
CANADA
Attn: S. Nish

Atomic Energy Research Establishment
Building 47, Division M.D.D.
Harwell, Oxfordshire
OX11 0RA,
ENGLAND
Attn: S. G. Burnay

Bhabha Atomic Research Centre
Health Physics Division
BARC
Bombay-85
INDIA
Attn: S. K. Mehta

British Nuclear Fuels Ltd.
Springfields Works
Salwick, Preston
Lancs
ENGLAND
Attn: W. G. Cunliff, Bldg 334

Brown Boveri Reaktor GMBH
Postfach 5143
D-6800 Mannheim 1
WEST GERMANY
Attn: R. Schemmel

Bundesanstalt fur Materialprufung
Unter den Eichen 87
D-1000 Berlin 45
WEST GERMANY
Attn: K. Wundrich

CEA/CEN-FAR
Departement de Surete Nucleaire
Service d'Analyse Fonctionnelle
B.P. 6
92260 Fontenay-aux-Roses
FRANCE
Attn: M. Le Meur
J. Henry

CERN
Laboratoire 1
CH-1211 Geneve 23
SWITZERLAND
Attn: H. Schonbacher

Canada Wire and Cable Limited
Power & Control Products Division
22 Commercial Road
Toronto, Ontario
CANADA M4G 1Z4
Attn: Z. S. Paniri

Centro Elettrotecnico
Sperimentale Italiano
Research and Development
Via Rubattino 54
20134 Milan,
ITALY
Attn: Carlo Masetti

Commissariat a l'Energie Atomique
ORIS/LABRA
BP N° 21
91190 Gif-Sur-Yvette
FRANCE
Attn: G. Gaussens
J. Chenion
F. Carlin

Commissariat a l'Energie Atomique
CEN Cadarache DRE/STRE
BP N° 1
13115 Saint Paul Lez Durance
FRANCE
Attn: J. Campan

Conductores Monterrey, S. A.
P.O. Box 2039
Monterrey, N. L.
MEXICO
Attn: P. G. Murga

Electricite de France
(S.E.P.T.E.N.)
12, 14 Ave. Dubrieroz
69628 Villeurbanne
Paris, FRANCE
Attn: H. Herouard
M. Hermant

Electricite de France
Direction des Etudes et Recherches
1, Avenue du General de Gaulle
92141 CLAMART CEDEX
FRANCE
Attn: J. Roubault
L. Deschamps

Electricite de France
Direction des Etudes et Recherches
Les Renardieres
Boite Postale n° 1
77250 MORET SUR LORING
FRANCE
Attn: Ph. Roussarie
V. Deglon
J. Ribot

EURATOM
Commission of European Communities
C.E.C. J.R.C.
21020 Ispra (Varese)
ITALY
Attn: G. Mancini

FRAMATOME
Tour Fiat - Cedex 16
92084 Paris La Defense
FRANCE
Attn: G. Chauvin
E. Raimondo

Furukawa Electric Co., Ltd.
Hiratsuka Wire Works
1-9 Higashi Yawata - 5 Chome
Hiratsuka, Kanagawa Pref
JAPAN 254
Attn: E. Oda

Gesellschaft fur Reaktorsicherheit (GRS) mbH
Glockengasse 2
D-5000 Koln 1
WEST GERMANY
Attn: Library

Health & Safety Executive
Thames House North
Milbank
London SW1P 4QJ
ENGLAND
Attn: W. W. Ascroft-Hutton

ITT Cannon Electric Canada
Four Cannon Court
Whitby, Ontario L1N 5V8
CANADA
Attn: B. D. Vallillee

Imatran Voima Oy
Electrotechn. Department
P.O. Box 138
SF-00101 Helsinki 10
FINLAND
Attn: B. Regnell
K. Koskinen

Institute of Radiation Protection
Department of Reactor Safety
P.O. Box 268
00101 Helsinki 10
FINLAND
Attn: L. Reiman

Instituto de Desarrollo y Diseno
Ingar - Santa Fe
Avellaneda 3657
C.C. 34B
3000 Santa Fe
REPUBLICA ARGENTINA
Attn: N. Labath

Japan Atomic Energy Research Institute
Takasaki Radiation Chemistry
Research Establishment
Watanuki-machi
Takasaki, Gunma-ken
JAPAN
Attn: N. Tamura
K. Yoshida
T. Seguchi

Japan Atomic Energy Research Institute
Tokai-Mura
Naka-Gun
Ibaraki-Ken
319-11
JAPAN
Attn: Y. Koizumi

Japan Atomic Energy Research Institute
Osaka Laboratory for Radiation Chemistry
25-1 Mii-Minami machi,
Neyagawa-shi
Osaka 572
JAPAN
Attn: Y. Nakase

Kalle Niederlassung der Hoechst AG
Postfach 3540
6200 Wiesbaden 1,
WEST GERMANY
Biebrich
Attn: Dr. H. Wilski

Kraftwerk Union AG
Department R361
Hammerbacherstrasse 12 + 14
D-8524 Erlangen
WEST GERMANY
Attn: I. Terry

Kraftwerk Union AG
Section R541
Postfach: 1240
D-8757 Karlstein
WEST GERMANY
Attn: W. Siegler

Kraftwerk Union AG
Hammerbacherstrasse 12 + 14
Postfach: 3220
D-8520 Erlangen
WEST GERMANY
Attn: W. Morell

Motor Columbus
Parkstrasse 27
CH-5401
Baden
SWITZERLAND
Attn: H. Fuchs

National Nuclear Corporation
Cambridge Road
Whetstone
Leicester LE8 3LH
ENGLAND
Attn: A. D. Hayward
J. V. Tindale

NOK AG Baden
Beznau Nuclear Power Plant
CH-5312 Doettingen
SWITZERLAND
Attn: O. Tatti

Norsk Kabelfabrik
3000 Drammen
NORWAY
Attn: C. T. Jacobsen

Nuclear Power Engineering Test Center
6-2, Toranomon, 3-Chome
Minato-ku
No. 2 Akiyana Building
Tokyo 105
JAPAN
Attn: K. Takumi

Ontario Hydro
700 University Avenue
Toronto, Ontario M5G 1X6
CANADA
Attn: R. Wong
B. Kukreti

Oy Stromberg Ab
Helsinki Works
Box 118
FI-00101 Helsinki 10
FINLAND
Attn: P. Paloniemi

Radiation Center of
Osaka Prefecture
Radiation Application-
Physics Division
Shinke-Cho, Sakai
Osaka, 593, JAPAN
Attn: S. Okamoto

Rappinl
ENEA-PEC
Via Arcoveggio 56/23
Bologna
ITALY
Attn: Ing. Ruggero

Rheinisch-Westfallscher
Technischer Überwachungs-Verein e.V.
Postfach 10 32 61
D-4300 Essen 1
WEST GERMANY
Attn: R. Sartori

Sydskraft
Southern Sweden Power Supply
21701 Malmo
SWEDEN
Attn: O. Grondalen

Technical University Munich
Institut für Radiochemie
D-8046 Garching
WEST GERMANY
Attn: Dr. H. Heusinger

UKAEA
Materials Development Division
Building 47
AERE Harwell
OXON OX11 0RA
ENGLAND
Attn: D. C. Phillips

United Kingdom Atomic Energy Authority
Safety & Reliability Directorate
Wigshaw Lane
Culcheth
Warrington WA3 4NE
ENGLAND
Attn: M. A. H. G. Alderson

Waseda University
Department of Electrical Engineering
4-1 Ohkubo-3, Shinjuku-ku
Tokyo
JAPAN
Attn: K. Yahagi

1200 J. P. VanDevender
1800 R. L. Schwoebel
1810 R. G. Kepler
1811 R. L. Clough
1812 L. A. Harrah
1812 K. T. Gillen
1813 J. G. Curro
2155 J. E. Gover
2155 O. M. Stuetzer
6200 V. L. Dugan
6300 R. W. Lynch
6400 A. W. Snyder
6410 J. W. Hickman
6417 D. D. Carlson
6420 J. V. Walker
6440 D. A. Dahlgren
6442 W. A. Von Rieseemann
6444 L. D. Buxton
6446 L. L. Bonzon (10)
6446 W. H. Buckalew
6446 L. D. Bustard
6446 J. W. Grossman
6446 E. H. Richards
6446 F. V. Thome
6446 F. J. Wyant (5)
6447 D. L. Berry
6447 P. R. Bennett
6449 K. D. Bergeron
6450 J. A. Reuscher
8024 M. A. Pound
3141 C. M. Ostrander (5)
3151 W. L. Garner

NRC FORM 336 (2-84) NRCM 1102 3201.3202	U.S. NUCLEAR REGULATORY COMMISSION	REPORT NUMBER (Assigned by TIDC, add Vol. No., if any)				
BIBLIOGRAPHIC DATA SHEET		NUREG/CR-4147 SAND85-0209				
SEE INSTRUCTIONS ON THE REVERSE		3 LEAVE BLANK				
2 TITLE AND SUBTITLE The Effect of Environmental Stress on Sylgard® 170 Silicone Elastomer		4 DATE REPORT COMPLETED				
5. AUTHOR(S) W. H. Buckalew and F. J. Wyant		<table border="1" style="width: 100%;"> <tr> <td style="text-align: center;">MONTH</td> <td style="text-align: center;">YEAR</td> </tr> <tr> <td style="text-align: center;">May</td> <td style="text-align: center;">1985</td> </tr> </table>	MONTH	YEAR	May	1985
MONTH	YEAR					
May	1985					
7. PERFORMING ORGANIZATION NAME AND MAILING ADDRESS (Include Zip Code)		6 DATE REPORT ISSUED				
Sandia National Laboratories Albuquerque, New Mexico 87185		<table border="1" style="width: 100%;"> <tr> <td style="text-align: center;">MONTH</td> <td style="text-align: center;">YEAR</td> </tr> <tr> <td style="text-align: center;">May</td> <td style="text-align: center;">1985</td> </tr> </table>	MONTH	YEAR	May	1985
MONTH	YEAR					
May	1985					
10 SPONSORING ORGANIZATION NAME AND MAILING ADDRESS (Include Zip Code) Electrical Engineering Branch Division of Engineering Technology Office of Nuclear Regulatory Research U.S. Nuclear Regulatory Commission Washington, DC 20555		8 PROJECT TASK WORK UNIT NUMBER				
12 SUPPLEMENTARY NOTES		9 FIN OR GRANT NUMBER FIN No. A-1051				
13 ABSTRACT (200 words or less)		11a TYPE OF REPORT				
<p>Dow Corning Sylgard® 170 Silicone Elastomer has been investigated to characterize its response to accelerated thermal aging, radiation exposure, and its behavior under applied compressive forces.</p> <p>Sylgard® 170 response to accelerated thermal aging suggests the material properties are not particularly age dependent. Radiation exposures, however, produce significant, monotonic changes in both elongation and hardness with increasing absorbed radiation dose.</p> <p>Elastomer response to an applied compressive force was strongly dependent on environment temperature and degree of material confinement. Variations in temperature produced large changes in compressive forces applied to confined samples. Attempts to mitigate force fluctuations by means of pressure relief paths resulted in total loss of the applied compressive force. Thus, seal applications employing this elastomer in Class 1E equipment required to function during or following an accident should consider the potential loss of compressive force from long-term aging and potential LOCA-temperature transient conditions.</p>		b PERIOD COVERED (Inclusive dates)				
14 DOCUMENT ANALYSIS - a KEYWORDS/DESCRIPTORS		15 AVAILABILITY STATEMENT				
b IDENTIFIERS/OPEN ENDED TERMS		Unlimited				
		16 SECURITY CLASSIFICATION				
		(This page)				
		U				
		(This report)				
		U				
		17 NUMBER OF PAGES				
		79				
		18 PRICE				